Développement de l'électronique et de la commande des actionneurs servo-électrohydrauliques (SEHA)

Ghiath Abdulmalek

université PARIS-SACLAY

Electronics and Control Development of Servo Electro-Hydraulic Actuators (SEHA)

Développement de l'électronique et de la commande des actionneurs servo-électrohydrauliques (SEHA)

Thèse de doctorat de l'université Paris-Saclay

École doctorale n° 580 : sciences et technologies de l'information et de la communication (STIC)
Spécialité de doctorat: Robotique
Graduate School : Sciences de l'Ingénierie et des Systèmes (SIS),
Référent : Université d'Evry Val d'Essonne

Thèse préparée dans l'unité de recherche **IBISC (Université Paris Saclay, Univ Evry)**, sous la direction de **Said MAMMAR, Professeur des Universités**, le co-encadrement de **Samer ALFAYAD, Professeur des Universités**, et de **Naima AITOUFROUKH-MAMMAR, Maître de Conférences**

Thèse soutenue à Paris-Saclay, le 11 décembre 2023 par,

Ghiath ABDULMALEK

Composition du Jury

Membres du jury avec voix délibérative

Fouzia BOUKOUR Directrice de recherche, Université Gustave Eiffel	Présidente du Jury
Iftikhar AHMAD Prof., National University of Sciences and Technology-Pakistan	Rapporteur
Faïz BEN AMAR Prof., Université Pierre et Marie Curie	Rapporteur
Barthélemy CAGNEAU Enseignant chercheur, Université de Versailles Saint-Quentin-en-Yvelines	Examinateur

Thèse de doctorat

NNT : 2023UPAST224

ÉCOLE DOCTORALE
Sciences et technologies de l'information et de la communication (STIC)

Titre : Développement de l'électronique et de la commande des actionneurs servo-électrohydrauliques (SEHA)

Mots clés : Système embarqué, Électronique, Robots humanoïdes, Électrohydraulique

Résumé :

Les robots humanoïdes incarnent un lien singulier entre l'ingénierie, la technologie et les aspirations humaines. Cependant, leur progression pose des défis complexes au-delà des aspects techniques, englobant des considérations fondamentales telles que les besoins énergétiques, les capacités de détection et les algorithmes de contrôle sophistiqués. Les actionneurs, véritable cœur de ces machines, jouent un rôle crucial en permettant des mouvements précis et en mimant la complexité des muscles et des articulations humaines. L'actuateur servo-électrohydraulique (SEHA), une proposition innovante de Samer ALFAYAD et al., représente un tournant majeur en générant de manière autonome de l'énergie hydraulique et en renforçant la sécurité des interactions humaines par la compensation de la force d'asservissement.

La mise en œuvre de SEHA nécessite une intégration de composants clés, conduisant à la création de la startup KALYSTA, soutenue par la SATT-Paris Saclay. Cette thèse explore la dimension électronique des actionneurs, cherchant à inaugurer une ère nouvelle de technologies d'actuation pour des robots plus performants et sécurisés. À travers SEHA et les innovations de KALYSTA, elle aspire à catalyser le développement de robots avancés pour diverses applications, ouvrant ainsi des perspectives prometteuses dans le domaine de la robotique humanoïde.

Title : Electronics and Control Development of Servo Electro-HydraulicActuators(SEHA)

Keywords : Embedded System, Electronics, Humanoid Robots, Electrohydraulics

Abstract :

Humanoid robots embody a unique connection between engineering, technology, and human aspirations. However, their advancement poses complex challenges beyond technical aspects, encompassing fundamental considerations such as energy requirements, detection capabilities, and sophisticated control algorithms. Actuators, the true core of these machines, play a crucial role in enabling precise movements and mimicking the complexity of human muscles and joints. The servo-electrohydraulic actuator (SEHA), an innovative proposal by Samer ALFAYAD et al., represents a significant breakthrough by autonomously generating hydraulic energy and enhancing the safety of human interactions through force feedback compensation.

Implementing SEHA requires the integration of key components, leading to the establishment of the startup KALYSTA, supported by SATT-Paris Saclay. This thesis explores the electronic dimension of actuators, aiming to usher in a new era of actuation technologies for more efficient and secure robots. Through SEHA and KALYSTA's innovations, it aspires to catalyze the development of advanced robots for various applications, promising exciting prospects in the field of humanoid robotics.

Maison du doctorat de l'Université Paris-Saclay
2ème étage aile ouest, Ecole normale supérieure Paris-Saclay
4 avenue des Sciences,
91190 Gif sur Yvette, France

Résumé

Les robots humanoïdes réalisent un pont remarquable entre l'ingénierie, la technologie et les aspirations humaines. Cependant. Leur développement présente une série de défis importants qui vont au-delà des simples obstacles techniques. Ces défis englobent des aspects fondamentaux, comme les exigences en matière de puissance et d'énergie ou les capacités de détection et de perception. Ils nécessitent également des algorithmes complexes de contrôle et de prise de décision. Ils font appel au domaine interdisciplinaire de l'interaction homme-robot.

A ce titre, les systèmes d'actionnement apparaissent comme des composants essentiels dans le paysage complexe des robots humanoïdes. Les actionneurs sont le cœeur de ces machines, car ils leur permettent d'effectuer des mouvements précis, fiables et efficaces. En outre, ils ont la responsabilité de reproduire les complexités et la flexibilité inhérentes à la musculature et aux articulations humaines. Relever le défi des actionneurs constitue une étape essentielle vers la réalisation de robots humanoïdes avancés capables de s'engager dans le monde, de manière naturelle et utile.

Pour répondre à ces objectifs multiples, Samer ALFAYAD et al. ont proposé une technologie d'actionnement révolutionnaire connue sous le nom d'actionneur servo-électrohydraulique (SEHA) (WO2020173933A1). SEHA introduit un changement de paradigme dans les systèmes d'actionnement grâce à des avantages très spécifiques. Il génère de manière autonome de l'énergie hydraulique à chaque articulation, optimisant ainsi l'utilisation de l'énergie. En outre, SEHA intègre une fonction de compensation de la force d'asservissement, ce qui renforce la sécurité des interactions humaines.

La mise en œuvre de SEHA nécessite une constellation de composants clés, notamment la couche EtherCAT pour une communication transparente, une instrumentation et des mesures précises pour un retour d'information en temps réel, un micrologiciel et un logiciel intégré en temps réel pour garantir l'efficacité et la réactivité. La conception de SEHA nécessite également une analyse complète du système pour l'optimisation des performances.

Le chemin pour concrétiser le potentiel de SEHA et des innovations connexes a abouti à la création de la startup KALYSTA, soutenue par un financement de la SATT-Paris Saclay. Dans une approche modulaire de ses produits, prochainement proposés à la vente, KALYSTA a introduit une suite de sous-produits, dont le Mini Groupe Hydraulique (MGH) pour la génération efficace d'énergie hydraulique, le Vérin Servo Instrumenté (SIC) pour les tests de la boucle de contrôle, et le Kit de Développement, une solution intégrée pour l'expérimentation de la technologie d'actionnement.

Cette thèse a pour objectif d'explorer la partie électronique des actionneurs, abordant les facettes complexes de leur développement, depuis les défis fondamentaux jusqu'aux technologies d'actionnement de pointe. À travers l'objectif de SEHA et les efforts de KALYSTA, elle cherche à ouvrir une nouvelle ère de technologies d'actionnement, permettant la création de systèmes robotiques plus efficaces et plus sûrs pour diverses applications.

La thèse comprend une introduction et sept chapitres principaux, chacun contribuant à la compréhension globale des robots humanoïdes et de la technologie d'actionnement. Le chapitre 2 passe en revue l'état actuel des connaissances dans le domaine. Le chapitre 3 se penche sur une étude biomédicale du muscle humain en lien avec lien avec l'actionnement mécatronique. Les chapitres 4 à 7 constituent le cœur des contributions pour le développement du système SEHA : retour sur ses principes de fonctionnement, sa simulation, sa commande, son électronique et un nouveau pilote dynamique. Le chapitre 7 est consacré à la présentation des résultats expérimentaux. Le dernier chapitre revient sur les réalisations et donne un aperçu des orientations et des recherches futures.

Abstract

Humanoid robots represent a remarkable intersection of engineering, technology, and human aspiration. However, their development presents a series of formidable challenges that extend beyond mere technical hurdles. These challenges encompass fundamental aspects, including power and energy requirements, sensing and perception capabilities, intricate control and decision-making algorithms, the nuanced domain of human-robot interaction, and the aesthetic complexities of design and fabrication.

Notably, actuation systems emerge as pivotal components within the complex landscape of humanoid robots. Actuators serve as the lifeblood of these machines, endowing them with the capability to perform precise, reliable, and efficient movements. Furthermore, they bear the responsibility of replicating the intricate complexities and flexibility inherent in human musculature and joints. Successfully overcoming the actuator challenge stands as a critical milestone toward the realization of advanced humanoid robots capable of engaging with the world in natural and useful ways.

To address these multifaceted objectives, Samer ALFAYAD et al. have introduced and patented a groundbreaking actuation technology known as the Servo Electro-Hydraulic Actuator (SEHA) (WO2020173933A1). SEHA introduces a paradigm shift in actuation systems with its distinctive advantages. It autonomously generates hydraulic energy at each joint, thereby optimizing energy utilization. Moreover, SEHA incorporates a servo force compensation feature, bolstering safety for human interactions.

The implementation of SEHA necessitates a constellation of key components, including the EtherCAT Slave for seamless communication, precise instrumentation and measurement for real-time feedback, real-time firmware and embedded software to ensure efficiency and responsiveness, and comprehensive system analysis for performance optimization.

The journey to realize the potential of SEHA and related innovations has culminated in the establishment of the startup KALYSTA, supported by funding from

SATT-Paris Saclay. KALYSTA's modular approach introduces a suite of sub-products, including the Mini Groupe Hydraulique (MGH) for efficient hydraulic energy generation, the Servo Instrumented Cylinder (SIC) for control loop testing, and the Development Kit, an integrated solution for experimentation with the actuation technology.

This thesis comprehensively explores humanoid robots, addressing the intricate challenges of their development, from foundational concepts to cutting-edge actuation technology. Through the lens of SEHA and the efforts of KALYSTA, it aims to usher in a new era of actuation technologies, enabling the creation of more efficient and secure robotic systems for a wide range of applications.

The SEHA system was studied, and an instrumentation system was proposed and implemented. An EtherCAT real-time protocol was established for communication, real-time feedback instruments, responsive firmware, and system analysis for performance optimization. The electronic and control board was optimized and industrialized, and electronic tests were conducted.

The thesis encompasses an introduction and seven chapters, each contributing uniquely to the comprehensive understanding of humanoid robots and actuation technology. Chapter 2 reviews the current state of knowledge in the field, while Chapter 3 delves into a biomedical study of human muscle. Chapters 4 through 7 dissect SEHA, including its working principles, simulation, control, electronics, and a novel dynamic driver. Chapter 8 culminates in presenting experimental results and offering insights into future directions and possibilities.

Contents

List of Figures

List of Tables

Acknowledgment

As I stand on the threshold of completing my thesis, I am filled with immense gratitude for the unwavering support of my loved ones, the expertise and mentorship of my supervisors, and the generous funding provided by the PAUSE program from Collège de France.

Reem, your unwavering encouragement has been my anchor throughout this journey; Hanin and Habiba, your infectious laughter has kept me motivated; and little Uways, your arrival added a special joy to this experience.

I sincerely thank my parents and brothers for their wisdom and camaraderie. To my friends, I cherish the gift of your friendship, which has enriched my learning experience and supported me.

The PAUSE program from the Collège de France has played a pivotal role in making my doctoral research possible. Their generous funding has enabled me to focus on my research, allowing me to pursue my passion for robotics and contribute to the advancement of this field. I am incredibly grateful for their support and the opportunity to continue my research at this prestigious institution.

Finally, my deepest thanks go to my supervisors, whose expertise and mentorship have shaped my research.

And always to the beloved homeland Syria.
With heartfelt appreciation,
Ghiath

Abbreviations and acronyms

Acronym	Full Form
AC	Alternating Current
ADC	Analog-to-Digital Converter
ARM	Advanced RISC Machine
ASIMO	Advanced Step in Innovative Mobility
ASD	Autism Spectrum Disorder
BLEEX	Berkeley Lower Extremity Exoskeleton
BEMF	Back-Electromotive Force
BiSS	Bidirectional/Serial/Synchronous
BLDC	Brushless Direct Current
CAN	Controller Area Network
CDC	Centers for Disease Control and Prevention
CHIMP	CMU Highly Intelligent Mobile Platform
CNS	Central Nervous System
CoM	Center of Mass
CPU	Central Processing Unit
DARPA	Defense Advanced Research Projects Agency
DC	Direct Current
Dev-Kit	Development Kit
EOS	End of the Stroke
EHA	Electro-hydraulic Actuators
EHSV	Electro-Hydraulic Servo Valve
EtherCAT	Ethernet for Control Automation Technology
FOC	Field-Oriented Control
FPGAs	Field Programmable Gate Arrays
IGBT	Insulated Gate Bipolar Transistor

Acronym	Full Form
IMU	Inertial Measurement Unit
IPROPI	Proportional Current Output
KASPAR	Kinesics and Synchronization in Personal Assistant Robotics
LIDAR	Light Detection and Ranging
LinACE	InAxis Linear Absolute Magnetic Shaft Encoder
LVDT	Linear Variable Differential Transformer
LVIT	Linear, Variable, Inductance, and Transducer
MGH	Mini Groupe Hydraulique
OP-AMP	Operational Amplifier
PAM	Pneumatic Artificial Muscle
PID	Proportional – Integral – Derivative
PI	Proportional – Integral
PMODE	Input Control Modes
PMSM	Permanent Magnet Synchronous Motors
PWM	Pulse Width Modulation
ROS	Robotic Operating System
RTOS	Real-Time Operating System
SEHA	Servo Electro-Hydraulic Actuator
SIC	Servo Instrumented Cylinder
SOS	Start of the Stroke
SPI	Serial Peripheral Interface
SSI	Serial Synchronous Interface
V	Valve
VHDL	VHSIC Hardware Description Language

Chapter 1

Introduction

Contents

1.1 Introduction

This chapter provides an overview of the motivation, objectives, and contributions of this thesis. The primary motivation for this project is to develop an actuation system for use in humanoid robots and portable assistive equipment. The second section of this chapter discusses the thesis objectives, which are to design, implement, and evaluate a novel actuation system. The final section of this chapter provides an outline of the thesis, which includes the chapters' contents and their relationships to each other.

1.2 Motivation

The human body's functionalities and physiology are still the most miraculous, efficient, and smart systems that humankind has known. Because of that, the dream of creating a machine that looks like a human, in intelligent and shaped aspects, has been the aim of humanity since the beginning of time. To have a humanoid robot, we need a mechanism of movement; then, we need to shape that mechanism and machine in a human body look. The central concept of creating an automated mechanical movement is to develop a system that can perform a specific task without the need for human intervention. This can be anything from a simple mechanism, such as a wind-up toy, to a complex system, such as a robotic arm used in manufacturing. Historically, Al-Jazari - a Muslim polymath and engineer who lived in the 12th century- was credited with being one of the first engineers to design and create automated mechanical machines. Al-Jazari's machines were complex and innovative and included devices such as automatic water clocks, musical fountains, and various automatons that could perform different tasks independently[1]. Figure 1.1 shows some automatic machines made by Al-

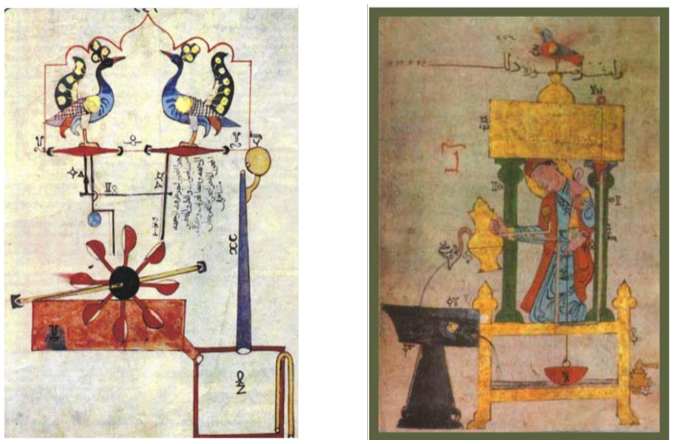

Figure 1.1 Automatic Water Clock(left) - Automatic Wudhu machine (right)[1]

jazari. The machine he called the Wudhu machine is just a basic humanoid robot that could automatically achieve one task to help people take a fresh shower[1]. Later, and during the High Renaissance in 1495, Leonardo da Vinci, the Italian

polymath, had several detailed drawings in his notebook of a mechanical knight who could stand, sit, turn, move his arms and head, and raise his visor[2]. Another attempt was made in 1738 by Around Jacques de Vaucanson, a French mechanical engineer, who made an android that played the flute, “le flûteur automate.”[3].

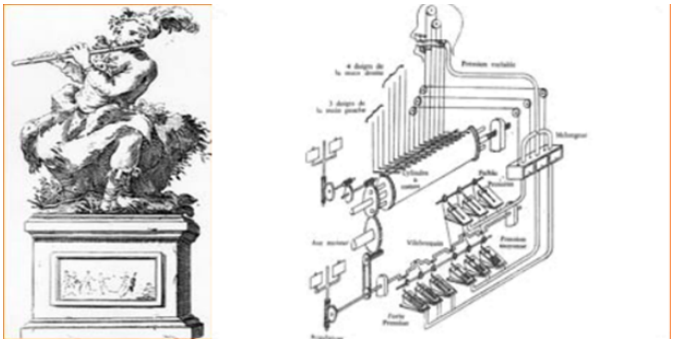

Figure 1.2 “le flûteur automate” Robot[3]

However, the word "Robot" was not crafted in the engineering and scientific domains; actually, it was derived from the word "robota" in 1920, which means subordinate labor in Slav languages – which was first introduced by the Czech playwright Karel Capek in his play "Rossum’s Universal Robots (R.U.R.)" [4]. As we can see, the first goal of building robot machines in history was for entertainment purposes like playing music. But, for now, robots are being developed and used for various critical applications, including disaster response and mitigation [5]. For example, robots can be used [6] ,[5] to locate and rescue people trapped in collapsed buildings after an earthquake, survey damage in a nuclear plant after a disaster, or help fight fires in areas too dangerous for firefighters. Some robots are also being used to monitor and respond to climate change by collecting data on temperature, weather patterns, and pollution levels. One good example of a humanoid robot designed for working in disaster scenarios is CHIMP (CMU Highly Intelligent Mobile Platform) [7]. It was developed by Carnegie Mellon University’s National Robotics Engineering Center in collaboration with the Defense Advanced Research Projects Agency (DARPA). CHIMP can carry heavy loads, such as debris or equipment, and can climb stairs and traverse rough terrain. It can also be remotely controlled. This allows operators to control the robot from a distance

safely[5]. Another essential aspect that humanoid robots are being developed for

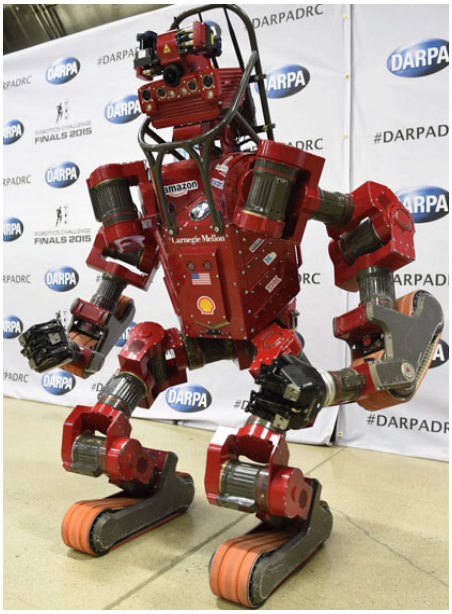

Figure 1.3 CHIMP, the CMU highly intelligent mobile platform, (Carnegie Mellon's National Robotics Engineering)[5]

is their potential to bring a range of social effects and benefits for example, assisting people with disabilities [8]. A good example of this application is KASPAR (Kinesics and Synchronization in Personal Assistant Robotics) humanoid robot -Figure 1.4 which was designed to interact with children with autism spectrum disorder (ASD) or other developmental disabilities. KASPAR was developed by the University of Hertfordshire's Adaptive Systems Research Group. It is designed to help children with ASD develop social skills, emotional understanding, and communication skills [9]. Overall, KASPAR is an exciting development in the field of robotics for healthcare and education, with the potential to help many children with ASD to develop important social and communication skills. Not only disaster relief and social and medical care are the reasons for the development of human robots, but there are also many other reasons and aspects, such as industrial and manufacturing, entertainment and leisure, and education and research.

Figure 1.4 Kaspar Robot plays with children

1.2.1 Humanoid Robots Challenges

Whatever the philosophy stands behind the development of humanoid robots, there are several other significant challenges that must be overcome in the development of humanoid robots [10] ,[11]. Here are a few examples

Power and Energy Humanoid robots require significant power and energy to operate, and finding efficient and sustainable ways to power them is a major challenge.

Sensing and perception To interact effectively with their environment, humanoid robots require sophisticated sensing and perception systems, including cameras, microphones, and other sensors. Designing these systems to sense and interpret the world around the robot accurately is a significant challenge.

Control and decision-making Humanoid robots require complex control and decision-making algorithms to coordinate their movements and perform tasks. Designing these algorithms to be both efficient and effective is a significant challenge.

Human-Robot Interaction Humanoid robots are designed to interact with humans in a lifelike and natural way, which requires sophisticated speech recog-

nition, natural language processing, and emotion recognition algorithms. Creating robots that can interact with humans intuitively and comfortably is a significant challenge.

Design and Fabrication Finally, the design and fabrication of humanoid robots is a significant challenge, requiring advanced materials, manufacturing processes, and specialized engineering expertise. Creating humanoid robots that are both functional and aesthetically pleasing is a significant challenge.

The development process is still a complex and challenging process that involves many technological, engineering, and design hurdles. However, of the many challenges that must be overcome, actuators are perhaps the most important. Actuators are the components that allow robots to move and perform tasks, and they must be precise, reliable, and efficient to ensure that the robot can function properly. In addition, because humanoid robots are designed to mimic human movement and behavior, actuators must be able to replicate the complexity and flexibility of human muscles and joints. Solving the actuator challenge is critical to developing advanced humanoid robots that can interact with the world in lifelike and useful ways.

1.3 Objective and Approach

To have efficient robotic devices that could achieve all the objectives listed above, Samer ALFAYAD et al. have proposed a novel actuation technology called Servo Electro-Hydraulic Actuator (SEHA) (WO2020173933A1). SEHA has several advantages over traditional actuation systems. First, SEHA creates hydraulic energy locally and independently at each joint. This allows for more efficient use of energy, as the required pressure is only delivered to the joints that need it. Second, SEHA provides a servo force compensation feature, which increases the safety of humans working around the robot or patients using the assistive device. In the case of an undesired shock, SEHA automatically reduces the delivered energy by decreasing the output cylinder's speed towards zero. To implement SEHA effectively, several

key components are required: EtherCAT Slave: This component serves as a communication interface, enabling seamless data exchange and coordination between the robot's various actuators and control systems. Instrumentation and Measurement: Accurate measurement and monitoring of the system's parameters are crucial for its optimal performance. Proper instrumentation allows real-time feedback and control, ensuring precise operation. Real-Time Firmware and Embedded Software: The actuation technology relies on real-time firmware and embedded software to achieve efficient and responsive control. These components facilitate quick decision-making and adaptability to changing conditions. System Analysis: A thorough understanding and analysis of the proposed SEHA as a system are essential for successful implementation. This involves evaluating its performance, identifying potential weaknesses, and optimizing its design. The project to commercialize SEHA and other related products is funded by the SATT-Paris Saclay, leading to the establishment of the startup KALYSTA in 2022. KALYSTA adopts a modular approach, offering three sub-products: i) MGH (Mini Groupe Hydraulique): A compact hydraulic unit designed to work in conjunction with the SEHA, contributing to the efficient generation and distribution of hydraulic energy. ii) SIC (Servo Instrumented Cylinder): This closed unit allows control loop testing under different load conditions. Equipped with embedded electronics and software, it facilitates easy manipulation of hydraulic mechanisms. iii) Development Kit: The kit combines the Mini Groupe Hydraulique (MGH) and Servo Instrumented Cylinder (SIC), providing a comprehensive solution for testing and experimentation with the actuation technology. Through KALYSTA's efforts, the SEHA and its associated sub-products are aimed at revolutionizing actuation technologies, enabling more efficient and safer robotic systems for various applications.

1.4 Thesis Outline

This thesis is structured as follows:

- Chapter 2 provides a state-of-the-art review of the current knowledge of humanoid robots, assistive devices, and actuators.

- Chapter 3 presents a bio-medical study of human muscle.
- Chapter 4 discusses the working principles of SEHA.
- Chapter 5 presents the simulation and control of SEHA using Matlab, Simulink, and Simescape.
- Chapter 6 describes the electronics and control layer of SEHA.
- Chapter 7 describes a new dynamic driver for SEHA.
- Chapter 8 presents the experimental results and discusses future work and perspectives.

Chapter 2

State of the Art

Contents

2.1 Introduction

Humanoid robots are equipped with actuation systems that enable them to move and interact with the environment, making them versatile and capable of performing various tasks. The actuation systems used in humanoid robots play a crucial role in determining their performance, agility, and overall capabilities. In this chapter, we introduce the most known humanoid robots and exoskeletons classified by the actuation technology they are built upon.

2.2 Humanoid Robots' Overview

Actuation systems are a critical component of robotics, as they are responsible for converting electrical or mechanical signals into motion or force. In other words, actuation systems enable robots to move and interact with their environment. Based on the kind of actuation technologies they employ to produce movement, humanoid robots can be categorized into three main categories.

1. Electrically actuated Humanoid Robots
2. Pneumatic-actuated Humanoid Robots
3. Hydraulic-Actuated Humanoid Robots

2.2.1 Electrically Actuated Humanoid Robots

Electrically actuated humanoid robots are robots that are designed to move and act like humans using electric actuators. These robots are often built with a network of motors, sensors, and controllers that enable them to perform a wide range of movements and actions, including walking, running, jumping, and even dancing.

ASIMO

We can consider the Japanese company Honda as a leading company in bipedal robot development. In 1986 Honda started its research on robots whose bipedal

walking was modeled after humans[4]. Figure 2.1 shows the history of Honda's robot from its first beginnings in 1986 with a very modest prototype E0 to the first version of ASIMO (Advanced Step in Innovative Mobility)shown in Figure 2, which was announced in 2000. Honda's engineers used the cameras and microphones as

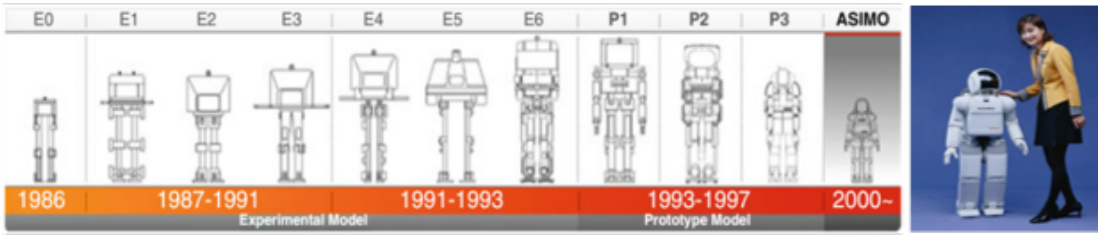

Figure 2.1 Honda's Humanoid Robot Development History[4]

head sensors for ASIMO, gyroscope, and accelerometer for the torso; for the foot, they used a six-axis force sensor; and for the hand, they used tactile sensors in the palms and force sensor on each finger. Concerning the actuator side in ASIMO, the robot is actuated using DC motors and brushless DC motors [12].

Digit

Figure 2.2-right, shows the humanoid robot Digit, released by Agility Robotics in collaboration with researchers from Oregon State University in 2019, as a second, more advanced version of their first bipedal platform called Cassie Figure 2.2 - left, released in 2016. Cassie is a dynamic walking robot that can traverse rough terrain and step over obstacles, but it doesn't like the humanoid robot. Digit comes with a humanoid robot design where Its legs are similar to Cassie's, but Digit is equipped with a torso full of sensors and a pair of arms used for balance, mobility, and manipulation [13]. Digit stands about 1.58 meters tall and weighs approximately 45 kg. It is designed to operate in a variety of environments and has advanced mobility capabilities that allow it to walk, climb stairs, and navigate over rough terrain. The robot is equipped with a suite of sensors, including LIDAR, cameras, and inertial measurement units, that allow it to perceive and interact with its environment [14]. One of Digit's key features is its advanced manipulation

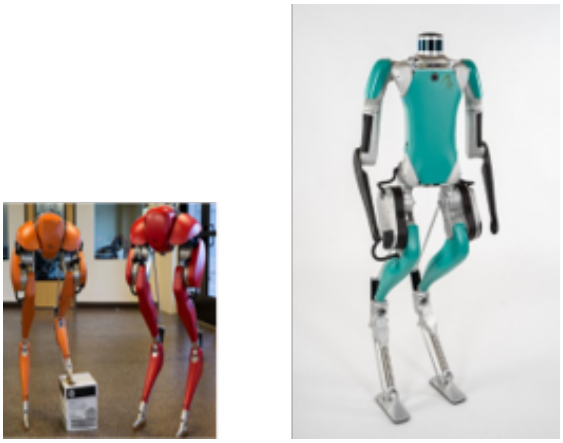

Figure 2.2 Cassie platform(Left) Digit Humanoid(Right) from Agility Robotics 2019[4]

capabilities. The robot has arms and hands that are capable of performing a wide range of tasks, including grasping objects, carrying packages, and opening doors. The hands are equipped with tactile force sensors that allow the robot to detect and respond to changes in the environment, making it particularly adept at tasks that require dexterity and precision. Digit uses electric actuators to control its joints and movements. The robot has a total of 20 actuated degrees of freedom, with each leg having 3 degrees of freedom (hip, knee, and ankle) and each arm having 2 degrees of freedom (shoulder and elbow). Each joint is actuated by a Maxon EC-90 brushless DC motor with custom-designed transmissions, which provide high torque and precise control. The motors are connected to harmonic drives, which allow for high gear ratios and low backlash. In addition to the electric actuators used in its joints, Digit also has several other actuators that control its mobility and manipulation capabilities. The robot's legs are equipped with a series of elastic actuators SEA, which provide compliance and shock absorption when walking and running.

Tesla Optimus

Recently, in 2022, Tesla revealed its humanoid robot Optimus. Up to now, there are not many academic details about Optimus, but according to the reveal show,

Optimus can walk, wave and dance on the stage without human assistance. Concerning the actuation, Tesla engineers used custom-made electric actuators[15]. Overall, the electric actuators used in Digit provide the robot with the power and precision required to perform a wide range of tasks, from walking and running to grasping and manipulating objects. However, electric actuation also has some lim-

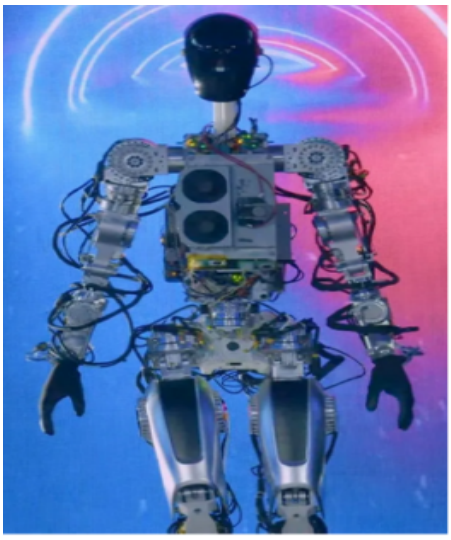

Figure 2.3 Tesla Optimus bot [17]

itations. For example, the electric motors used in humanoid robots can be heavy and bulky, limiting the robot's mobility and agility. Despite these limitations, electric actuation remains a popular choice for humanoid robots due to its flexibility and versatility. Ongoing research and development in this area aim to address the challenges associated with electric actuation and improve the performance and capabilities of humanoid robots.

2.2.2 Pneumatic Actuated Humanoid Robots

Pneumatic actuated robots are robots that use compressed air to power their actuators. One example of a pneumatic actuated robot is Lucy, a bipedal robot developed by the University of California, Berkeley. It uses pneumatic artificial muscles to emulate human muscles in contracting and extending. The pneumatic

technology was the least widespread because of the low bandwidth and high hysteresis of pneumatic actuation[16][17][18].

2.2.3 Hydraulic Actuated Humanoid Robots

It exits several humanoid robots using hydraulic systems such as DB and CB developed by SARCOS [19], but the most well-known is the ATLAS robot from Boston Dynamics. One of the most exciting advantages of hydraulic actuators is their power and the possibility to perform force control which comes with the price to pay, which is the pump's size. Moreover, installing a servo valve for each actuator in the robot increases the robot's total weight[20]. Another challenge in developing hydraulic-actuated humanoid robots is the tubes and the connectors integration, which may cause leakage problems.

Petman 2009

Petman is a full-size humanoid robot with 29 degrees of freedom. It can walk, squat, and even do push-ups. It was developed by Boston Dynamics for the U.S. Army to test chemical protective clothing[21]. Petman is a hydraulic actuated robot, but more information is needed about the sensors and instrumentation inside it.

Atlas DARPA 2013

After Petman, Boston Dynamics started developing Atlas for the DARPA challenge. Atlas DARPA came with twenty-eight hydraulic actuators, and as sensors, it came with LIDAR, stereo cameras, and dedicated electronics[21].

Atlas 2016

This version of Atlas is the most advanced one, and it was designed to operate outdoors and inside buildings. Atlas2016 can sense obstacles and negotiate rough

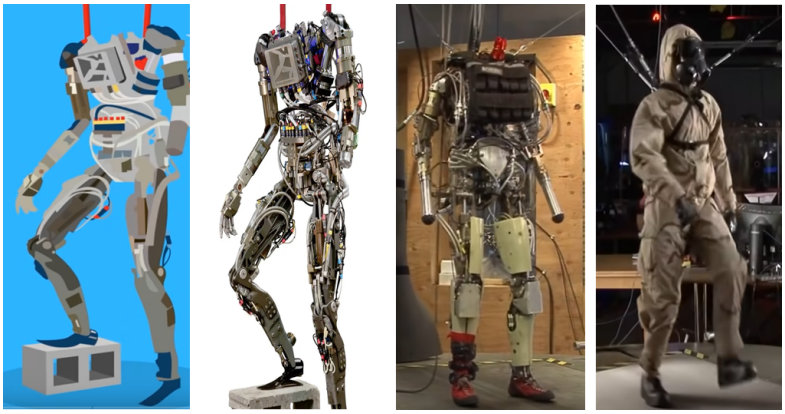

Figure 2.4 Petman 2009 the first humanoid Robot developed by Boston Dynamics

terrain autonomously or under teleoperation.(Figure 2.5 shows Atlas capabilities from 2016 to 2021) Like the previous versions, Atlas is hydraulically actuated with twenty-eight degrees of freedom, achieving a high strength-to-weight ratio and high smooth and dynamic movements[21]. Concerning the sensors, Atlas 2016 has the same sensors that existed in the Atlas DARPA.

Hydroid robot - University of Paris Saclay

As the name implies, HYDROïD is a hydraulic-actuated humanoid robot; the name comes from two words «HYDraulic» and «andROïD». HYDROïD (Figure 2.6)is still under development, but mainly it has 36 hydraulic DOFs (legs, arms, and torso), providing hybrid mechanisms with servo valves-based hydraulic actuation systems[18].

2.3 Exoskeletons Overview

As previously discussed, medicine greatly benefits from robotics, particularly in assisting individuals with specific disabilities. Among the vital technologies that can be of great help are exoskeletons. In this section, we will highlight two significant instances of exoskeletons: hydraulic and electric-actuated ones.

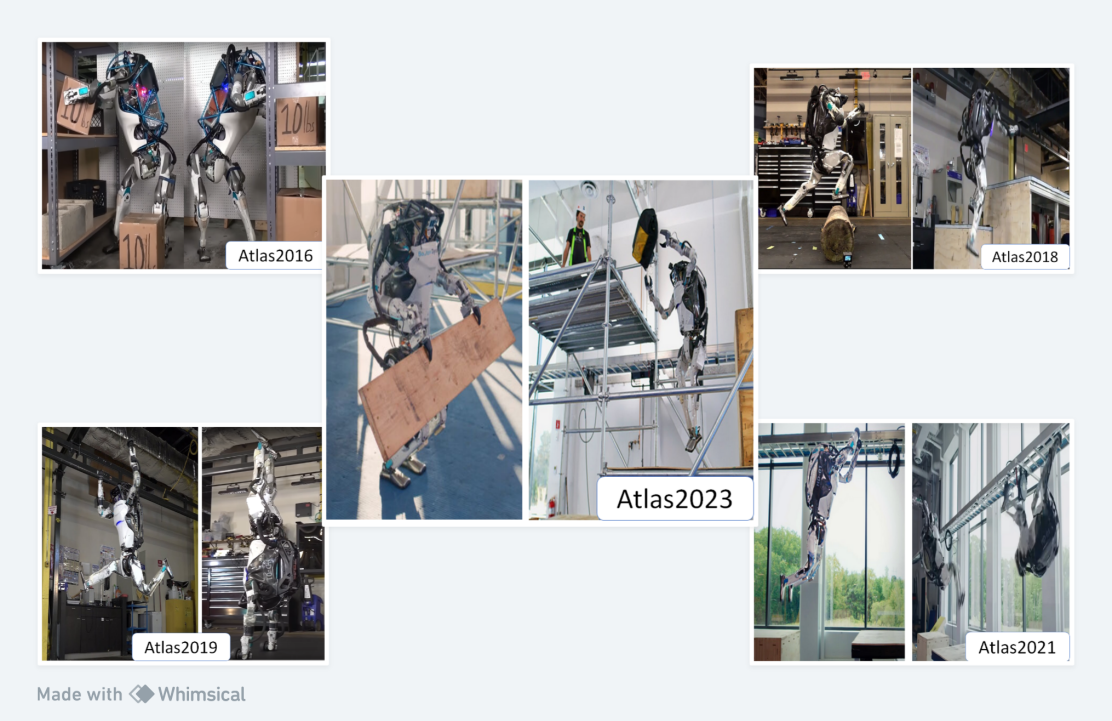

Figure 2.5 Development of Atlas - Evolution of Tasks and Movement

Figure 2.6 HYDROïD - Paris Saclay University

2.3.1 BLEEX

The Berkeley Lower Extremity Exoskeleton (BLEEX) is a powered exoskeleton that was developed by the University of California, Berkeley. It is designed to provide wearers with additional strength and endurance for carrying heavy loads[22]. The BLEEX has four hydraulically actuated joints: two at the hip, one at the knee, and one at the ankle. It is powered by a backpack-mounted battery pack that provides up to 8 hours of operation. The BLEEX can carry loads of up to 90.71 kilograms and can be used for various tasks, including military operations, search and rescue, and disaster relief [23]. The BLEEX is still under development, but it has the potential to revolutionize the way we carry heavy loads. It could make it easier for soldiers to carry their gear, for firefighters to rescue victims, and for people with disabilities to get around.

Figure 2.7 Bleex Exoskeleton

2.3.2 Mind-Walker

The University of Twente developed the Mind-Walker exoskeleton, shown in Fig 2.8, to help paraplegics regain the ability to stand and walk. The exoskeleton uses a serial elastic actuator to drive the abduction/adduction and flexion/extension of the hip joints and the flexion/extension of the knee, with four actuated joints at the hips and two at the knees [24]. Looking at the hardware, six low-level controllers

Figure 2.8 Mind-Walker Exoskeleton

built within the Mind-Walker exoskeleton are connected through EtherCAT. The sensor system consists of twin coil springs for torque estimation and encoders placed strategically on the motor to aid in commutation and velocity control. Each of the active and passive joints has an encoder, and the thighs and shafts each include a 9-axis Inertial Measurement Unit (IMU) that can estimate the center of mass (CoM) position and provide orientation data. The proportional control

method used by the exoskeleton replays modified joint trajectories recorded from a healthy person while using data from the IMU whenever displacement of the CoM is observed. Particularly near the conclusion of the swing phase, online changes are made to take the user's height and stride length into consideration [25].

2.4 Actuation Systems for Robotics and Portable Devices

2.4.1 Electric Actuation

As we have presented above, we can see that electrical actuation is typically the most used in most humanoid robots and exoskeletons(see figures 2.9.and 2.10) The principle of all-electric actuators is based on the electric motor used. Therefore, the force of actuation is generated by an electric current flowing through the wire of a coil in the presence of a magnetic Field. The electrical actuation is ideal for high-speed, low-force applications by nature. For low-speed/high-force applications, an additional complex mechanical system, mainly gearboxes, is recommended [18]. Electric actuation in humanoid robots has several advantages over other actuation

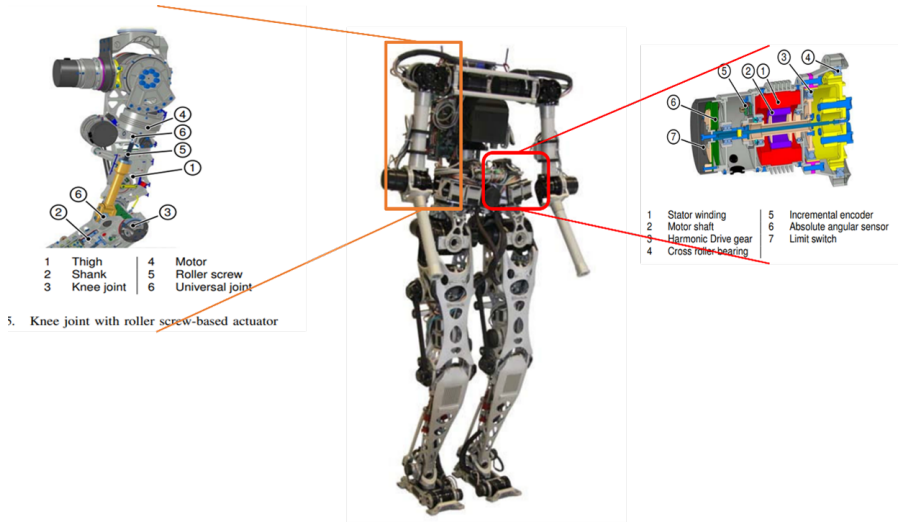

Figure 2.9 Electric Actuators in Lola Humanoid Robot

systems. It allows for precise control of movements and is relatively energy efficient.

Additionally, it can be used in a wide range of applications and environments. However, electric actuation also suffers from a low power-to-volume ratio, meaning that it takes up a lot of space for the amount of power it can generate. This can be a drawback in applications where space is limited, such as in robotics or medical devices. Figure 2.11 displays the power-to-weight ratios for various types

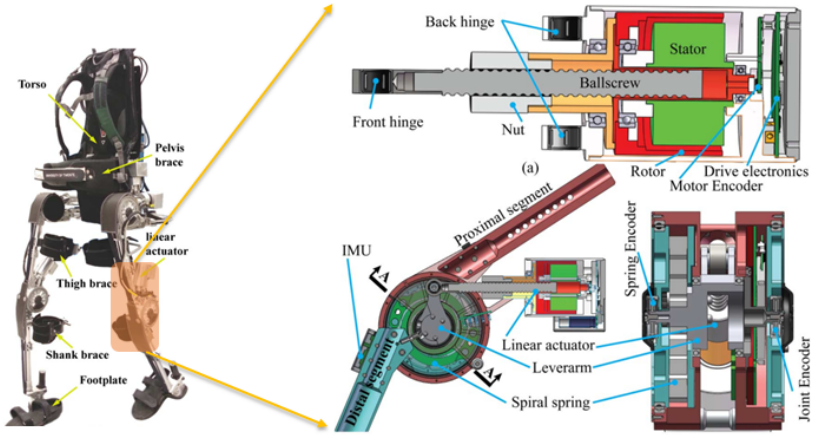

Figure 2.10 Electric Actuators in Mind Walker Exoskeleton

of actuators [26]. It is evident from the figure that DC actuators exhibit the lowest power-to-weight ratio in terms of watts per kilogram (W/kg) compared to their weight in kilograms (kg).

2.4.2 Pneumatic Actuation

Another possible actuation solution is represented by the pneumatic power, which can divide the actuators into two types, the conventional pneumatic actuators (linear pistons, rotary pistons, etc.) and the artificial muscles [23](Figure 2.12). Pneumatic actuation systems provide the best force-to-weight ratio because of the

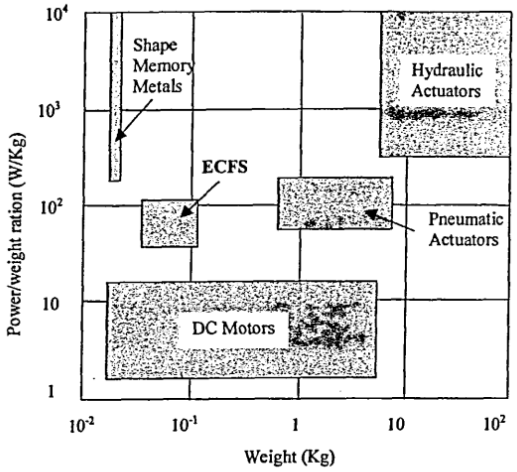

Fig. 1. Actuator comparison based on weight and output power-to-weight ratio.

Figure 2.11 Actuator Comparison based on weight and output power-to-weight ratio [26]

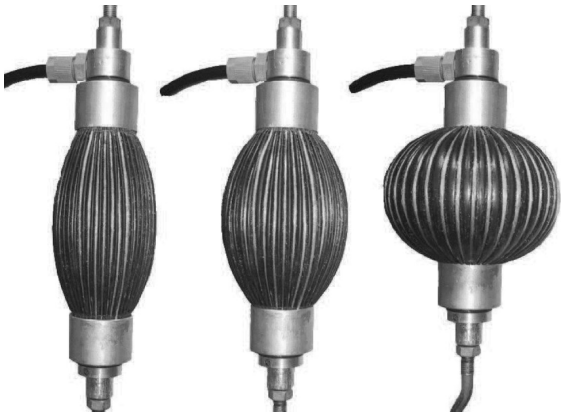

Figure 2.12 Pneumatic Artificial Muscle

use of compressed air as a medium to transmit the energy. But and unfortunately, the high compressibility of the air is a source of two main disadvantages :

1. The bandwidth of the pneumatic actuation system is limited and around 20Hz [18].

2. The compressibility of the air permits the storage of high amounts of energy in the compressed air. Therefore, in case of external leakage or accidental damage, the air containers become very dangerous for the human operator and the ambient environment [18].

2.4.3 Pneumatic-Electric Hybrid Actuation

In order to overcome the weak points of the pneumatic actuator, the concept of a hybrid pneumatic-electric actuator is born to combine the advantages of both electric and penumatic, one example of using this technology in humanoid robots is the humanoid robot arm developed by Shotaro Mori et al [27], shown in Figure 2.13 The pneumatic component of a hybrid actuator is typically used to provide high

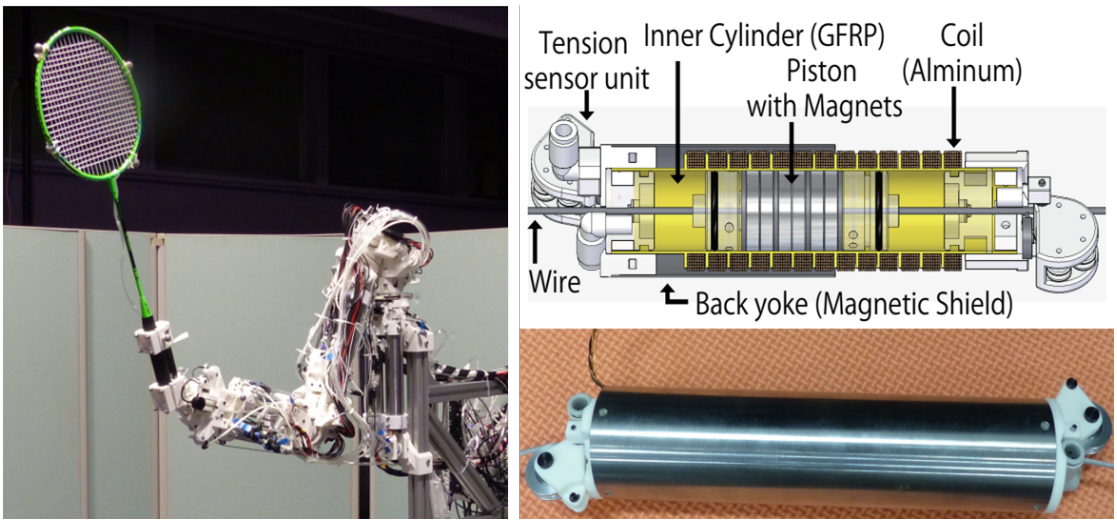

Figure 2.13 Left: Shotaro Mori et al., Pneumatic Electric Actuated Humanoid Robot Arm, Right: Hybrid Pneumatic-Electric Actuator Structure [27]

force, while the electric component is used to provide high speed and accuracy. However, the pneumatic component is also the limiting factor in terms of force capability. This is because the pneumatic component is limited by the pressure of the compressed air, which can only be increased to a certain point before it becomes impractical or dangerous. As a result, pneumatic-electric hybrid actuators are not suitable for applications that require high forces.

2.4.4 Hydraulic Actuation

Hydraulic actuation is known for its high power-to-weight and power-to-volume ratios (Figure 2.14). This is due to the low compressibility of hydraulic oil, which makes the actuator stiffer and leads to faster response times and higher natural frequencies. Hydraulic actuation is also relatively quiet and self-lubricating, which means that it requires less maintenance. However, there are some drawbacks

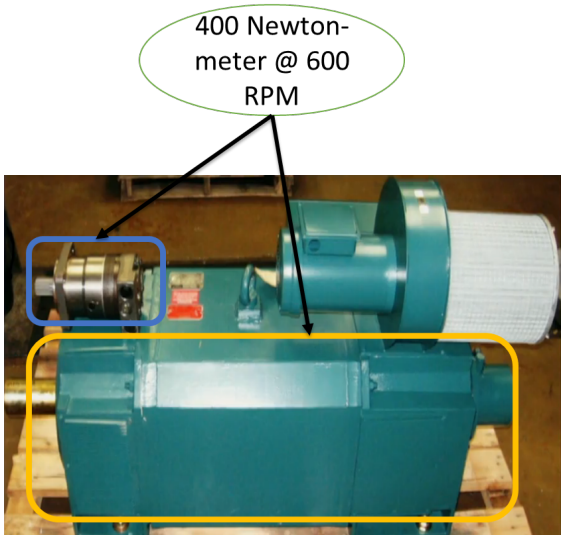

Figure 2.14 Hydraulic Motor and Electric Motor Torque to Volume Comparison

to hydraulic actuation. Hydraulic control systems can be more expensive and complex to implement and maintain than other actuation methods. This is because they require specialized components, such as pumps, valves, and hydraulic fluid. Additionally, the complexity of hydraulic systems can make their control more

challenging, requiring expertise in hydraulic engineering and precise calibration to achieve the desired performance.

2.4.5 Electro-Hydraulic Actuation - EHA

Electro-hydraulic actuators (EHA) are hybrid actuation technology that combines hydraulics' power with the electronics' controllability. They are self-contained, meaning that they have a single energy input source: an electric motor that drives a pump. The pump's flow drives an integrated actuator, which provides the generated force to the attached mechanism.

Product	Motor Type	Pump Type
IEHA-AlFayad et al	BLDC	Radial piston-Variable displacement
EHA-KAWASAKI	DC	Axial piston-Variable displacement
EHA Nakamura et al	–	Gear Pump
EHA-Parker	DC	Geroter-Fixed Displacement
EHA-Track Warner	DC	Gear pump
SEHA-Kalysta	BLDC	Axial piston-Variable displacement

Table 2.1 Electro-Hydraulic Actuators State of the Art [28],[29] ,[30]

The development of EHAs, especially those constrained by geometry or weight, faces multiple challenges. These challenges include:

1. Achieving hydraulic and electronic integration in a compact and lightweight volume.
2. Developing miniature components.
3. Preserve the system's functionality.

Despite these challenges, EHAs offer several advantages over traditional hydraulic actuators. These advantages include increased efficiency, improved controllability, reduced noise and vibration, and increased safety.

As a result, EHAs are becoming increasingly popular in a variety of applications, including aerospace, defense, and industrial automation.

2.5 Discussion

In conclusion, the electro-hydraulic actuator stands out as the superior choice when compared to hydraulic, pneumatic, and electric actuators. Its unique combination of advantages makes it a highly efficient, reliable, and versatile solution.(2.15 shows the comparison between the main actuation technologies that we discussed above)

Feature	Pneumatic	Electric	Hydraulic	Pneumatic Electric	Electro-Hydraulic
Force	+	++	+++	++	+++
Response time	-	++	+	+	++
Controlability	- -	++	+	+	++
Power to weight	+	+++	+++	++	+++
Power to volume	+	++	+++	++	+++
Cost	-	++	- -	+	++
Noise	-	++	+	+	++
Energy efficiency	+	++	-	+	+
Safety	++	++	+	++	++

Figure 2.15 Comparison Between Actuation Technologies [23]

Firstly, the electro-hydraulic actuator combines the benefits of both hydraulic and electric systems. It harnesses the power and precision of hydraulic fluid for force transmission while incorporating electric control and automation capabilities. This integration results in enhanced controllability and responsiveness, allowing for smooth and accurate motion, hence more dynamic robots.

Secondly, compared to hydraulic actuators, electro-hydraulic systems eliminate the need for bulky and expensive hydraulic power units and extensive piping. They offer a more compact and lightweight design, leading to reduced installation and maintenance costs. Moreover, the elimination of hydraulic fluid also eliminates concerns related to fluid leaks, contamination, and environmental hazards.

Thirdly, when compared to pneumatic actuators, electro-hydraulic systems provide significantly higher force output. Lastly, compared to electric actuators, electro-hydraulic systems deliver higher power density, enabling them to handle more demanding tasks easily. This characteristic makes them particularly advantageous in situations where high force, fast response, and precise control are paramount.

2.5.1 SEHA Actuator Final Objective

Since SEHA proposes a new actuation system for robotics and assistive devices, we aim to occupy its proper placement among other actuation systems.

In Figure 2.16, the main types of actuators are depicted. Where the X-axis represents the strain ϵ, which is calculated as the displacement (x) divided by the reference length (l). On the other hand, the Y-axis represents the stress σ, which is obtained by dividing the applied force (F) by the cross-sectional area (A) [31]. Notably, electro-moving coils exhibit high strain values but relatively low strength. In contrast, hydraulic actuation enables the attainment of both high strains and stresses. However, hydraulic actuation comes with high costs and involves complex operational expenses.

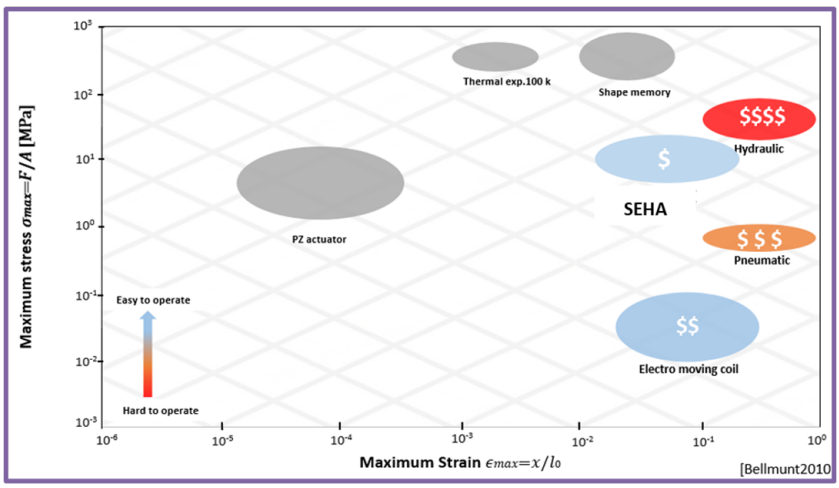

Figure 2.16 SEHA in Actuators' Market [23]

In recent years, there has been a growing trend toward the development of hybrid actuators, which aim to leverage the advantages of different actuation types while mitigating their drawbacks. To address this objective, Khatib et al. introduced a hybrid electro-pneumatic actuator [32]. This actuator combines the benefits of electric and pneumatic actuation to cater to robot applications that prioritize human-friendly interactions.

Similarly, several electrohydraulic actuators have been developed [28],[29], [33], [34], where an electric motor is coupled with a hydraulic pump to drive an output cylinder through a specially designed hydraulic circuit. The objective of electro-hydraulic actuation technology is to offer comparable force capabilities to conventional hydraulic cylinders while maintaining the cost-effectiveness and operational simplicity associated with conventional electrical actuation.

As a result, these hybrid actuators have the potential for diverse applications in sectors such as marine, aerospace, automotive, and industrial fields. Their unique combination of characteristics makes them suitable for a wide range of scenarios that require both robust force capabilities and efficient operation.

Our Contribution

Although electro-hydraulic actuation has been shown to improve the performance of humanoids and assistive devices, it still has some questions to be addressed, such as:

1. How the electronics and control system could integrate with mechanic solutions and approaches to deal with the risk of leakage (Alfayad *et al,* Seliman *et al*, and Kardo *et al* [35][23]).

2. How can the complexity of control of SEHA be addressed?

   (a) SEHA are more difficult to control than other types of actuators because of their nonlinear dynamics and the challenges involved in identifying their behavior.

   (b) How can we develop better control algorithms for SEHA?

   (c) How can we improve the identification of the behavior of SEHA?

3. How can efficient electronics and sensory integration be achieved for SEHA?

   (a) How can we design more efficient electronics for SEHA?

   (b) How can we integrate sensors and instrumentation more robustly for SEHA?

4. How can the ability of SEHA to be a communication slave be improved?

   (a) The control of SEHA within humanoid robots and assistive devices often involves a centralized computer, potentially restricting their capacity for independent action.

   (b) How can we design SEHA that are more capable of independent action when needed and how is that related to safety?

   (c) How can we improve the communication between SEHA and a centralized computer?

This thesis addresses these challenges and questions trying to suggest some approaches for the better development of a Servo Electro-Hydraulic Actuator (SEHA) Figure 2.17 provides an overview of the three key mechatronic development stages necessary for SEHA to be prepared for robotic applications. These stages encompass 1) Mechanical, 2) Electronics, and 3) ROS (Robotic Operating System). The electronics level is elaborated upon in more detail in this thesis, as it constitutes the primary focus of our contribution, and we will delve into these concepts in the upcoming chapters.

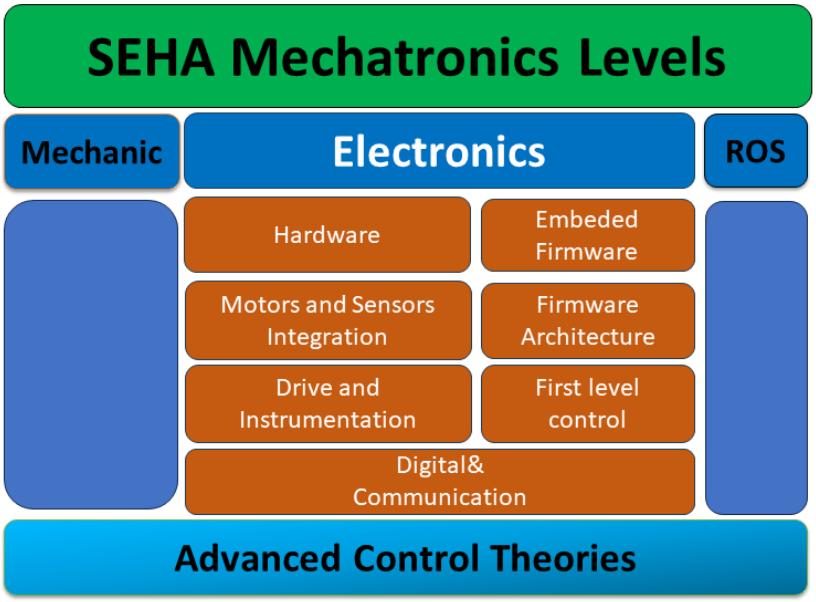

Figure 2.17 SEHA Mechatronic Layers

Chapter 3

Biomedical Study of Human Muscle

Contents

3.1 Introduction

Most robotic systems, aiming to imitate complex movements seen in living systems, rely heavily on artificial muscles. Practical implementation necessitates an ideal blend of actuation parameters, such as strain, stress, energy density, and robust mechanical strength. Because of such a fact, the best way to develop better actuation systems for robots and assistive devices is to understand the mechanism of the human muscles. To do that, we need to investigate the human muscular, nervous, and neuromuscular systems. Studying the intelligence underlying muscle movement is crucial for comprehending the dynamics of human body motion. At the heart of this comprehension lies the interaction between the nervous and muscular systems, which is the fundamental key to unlocking such understanding. Since the muscular system is very complicated and has a strong connection with the nerve systems we will take the walking mechanism as an example.

3.1.1 Walking Mechanism

The walking mechanism in humans is the process of moving the legs in a coordinated way to propel the body forward. It is a complex process that involves the coordinated effort of the skeletal system, muscular system, and nervous system. The skeletal system provides the bones and joints that support the body and allow it to move. The muscular system provides the muscles that power the movements of the body. The nervous system controls the muscles and coordinates their movements. The walking mechanism can be divided into two phases: the stance phase

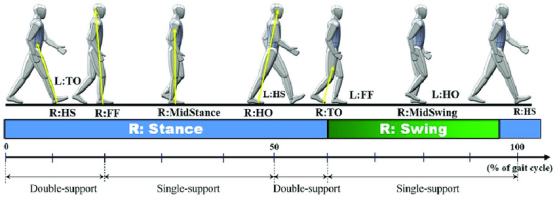

Figure 3.1 Human Walking Mechanism

and the swing phase (Figure 3.1).

- The stance phase is the time when one foot is on the ground. During this phase, the body weight is supported by the stance leg. The muscles of the stance leg contract to keep the body upright and to absorb the impact of the foot hitting the ground.
- The swing phase is the time when the foot is off the ground. During this phase, the body weight is supported by the other leg. The muscles of the swing leg contract to move the foot forward [36].

The walking mechanism is controlled by the central nervous system (CNS). The CNS sends signals to the muscles of the legs, telling them when to contract and relax. The CNS also receives feedback from the muscles and joints, which helps it coordinate the movements of the legs [37].

3.2 Human Muscular System

The muscular system is composed of three main types of muscles: skeletal muscle, smooth muscle, and cardiac muscle.

3.2.1 Skeletal muscle

Skeletal muscle is the most abundant type of muscle in the human body, accounting for 30-40% of a person's total body mass. It is controlled by the peripheral portion of the central nervous system (CNS), making it under conscious or voluntary control. The basic unit is the muscle fiber, which contains multiple nuclei. These muscle fibers are striated, exhibiting transverse streaks, and each functions independently of neighboring muscle fibers [38].

3.2.2 Smooth Muscle

While the skeletal muscles are responsible for skeletal movement, smooth muscle is distributed in the walls of hollow internal organs such as blood vessels, the

gastrointestinal tract, the bladder, and the uterus. The autonomic nervous system regulates it and cannot be consciously controlled, acting involuntarily. The non-striated (smooth) muscle cell has a spindle shape with a central nucleus. Smooth muscle contracts slowly and rhythmically.

3.2.3 Cardiac Muscle

As the name implies, cardiac muscle is located in the heart, precisely in the walls of the heart, and is also controlled by the autonomic nervous system. Similar to smooth muscle, cardiac muscle cells have a central nucleus, but they are also striated like skeletal muscle. The shape of cardiac muscle cells is rectangular. The contraction of cardiac muscle is involuntary, powerful, and rhythmic[39][40].

3.2.4 Muscle Mechanical Properties

Now and after introducing the main types of muscles we will explore the mechanical properties of muscles that govern how they respond to forces and displacements. These properties are important for understanding how muscles work and how they can be used to generate movement (Figure3.2). The four main mechanical properties of muscles are:

- Excitability: The ability of muscles to respond to stimuli. Muscles are stimulated by nerve impulses, which cause them to contract.
- Contractility: The ability of muscles to shorten their length. This is the property that allows muscles to generate force.
- Extensibility: The ability of muscles to be stretched. This is important for allowing muscles to move freely through their range of motion.
- Elasticity: The ability of muscles to return to their original length after being stretched. This property is important for preventing muscles from overstretching

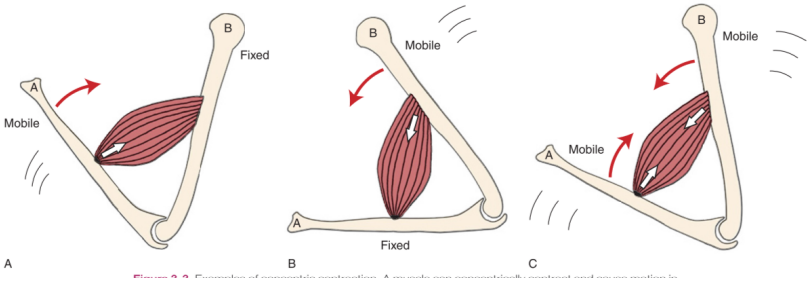

Figure 3.2 Examples of muscle different movements. A muscle can concentrically contract and cause motion in one of three ways. By naming the muscle's attachments A and B, we can describe these three scenarios. In A, bone A moves toward bone B. In B, bone B moves toward bone A. And in C, both bones A and B move toward each other [41].

In addition to these four main properties, muscles also have other mechanical properties, such as:

- Stiffness: The resistance of a muscle to being stretched.
- Velocity: The speed at which a muscle contracts.
- Power: The rate at which a muscle does work.

The mechanical properties of muscles are affected by several factors, including the type of muscle fiber, the muscle's length, and the muscle's temperature [42]. The mechanical properties of muscles are important for understanding how muscles work and how they can be used to generate movement.

3.2.5 How the Muscle Works ?

To get a comprehensive understanding of the working mechanism of the muscle, we will study the intricate mechanism that defines muscle contraction, which takes place at a microscopic level and is referred to as the "sliding filament mechanism."

A muscle consists of thousands of individual muscle cells, known as muscle fibers. Within a muscle, these fibers are grouped together into bundles termed

"fascicles." Additionally, a muscle contains multiple layers of fibrous fascia, sharing a similar structure but designated differently based on their location. Specifically, the endomysium envelops each individual muscle fiber, the perimysium encircles each fascicle, and the epimysium encompasses the entire muscle (as depicted in Figure 3.3). Importantly, these fibrous layers extend beyond each end of the muscle to form the fibrous tissue attachments linking the muscle to the bone or adjacent soft tissue. If this attachment has a cord-like shape, it is commonly called a "tendon," while if it is broad and flat, it is referred to as an "aponeurosis." Notably, the primary function of the tendon or aponeurosis is to transmit the pulling force generated by the muscle belly to its attachment point . It's worth noting that although we often describe a muscle's tendon (or aponeurosis) as a separate structure, it is essential to grasp that the tendon is an extension of the fibrous fascia, which is an integral part of the muscle's overall structure (Figure 3.3 B). Due to this structural interconnectedness, some texts refer to muscles as "muscle-tendon" or "myofascial units"[41]. A closer examination of an individual muscle fiber reveals its composition with structures known as "myofibrils." Myofibrils run longitudinally within the muscle fiber and are constructed from filaments (as shown in Figure 3.3). These filaments are organized into units termed "sarcomeres," with the term "sarcomere" literally signifying a "unit of muscle." To gain a profound understanding of how a muscle operates, one must comprehend the functioning of a sarcomere. Sarcomeres comprise thin and thick filaments.

The thin filaments, consisting of actin, are situated on both sides of the sarcomere and attach to the Z-lines, which mark the sarcomere's boundaries. In contrast, the thick filament comprises myosin and is positioned in the center, featuring projections known as "heads." When a stimulus is sent from the nervous system to the muscle, binding sites on the actin filaments are exposed, allowing the myosin heads to attach to them, forming what are called "cross-bridges." Subsequently, the myosin heads endeavor to bend inward toward the center of the sarcomere, generating a pulling force on the actin filaments. If this pulling force is sufficiently robust, it leads to the actin filaments being pulled toward the center of the sarcomere, facilitating their movement along the myosin filament, thereby giving rise to

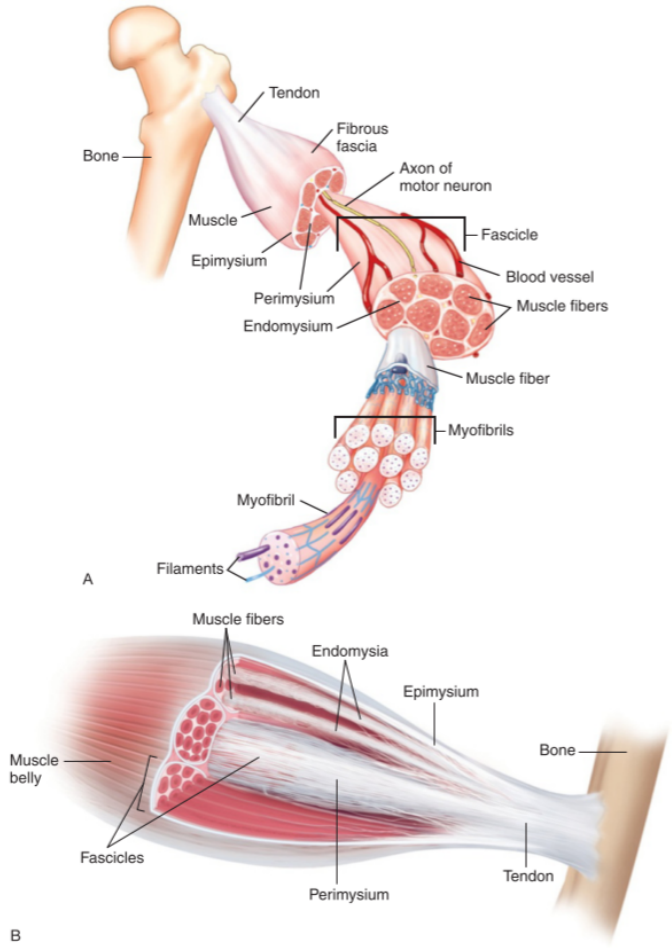

Figure 3.3 Cross sections of a muscle. A, A muscle is composed of fascicles, which are bundles of fibers. The fibers themselves are filled with myofibrils, which are composed of filaments. Fibrous fascial sheaths called endomysia, perimysia, and epimysium surround the fibers, fascicles, and entire muscle, respectively. B, The fascia of a muscle is integral to its structure [41] .

the term "sliding filament mechanism." This action causes the Z-lines to be drawn closer to the center, resulting in the shortening of the sarcomere (Figure 3.4). It is important to recognize that whatever transpires in one sarcomere mirrors the activities occurring in all the sarcomeres of all the myofibrils within the muscle fiber. By extrapolating this concept, it becomes evident that if all the sarcomeres in a myofibril contract, the myofibril itself will undergo shortening. If all the myofibrils within a muscle fiber shorten, the muscle fiber itself will contract. Should a sufficient number of muscle fibers undergo shortening, the muscle as a whole will contract, consequently pulling one or both of its attachments toward the center, thereby facilitating bodily motion. This elucidates how a concentric contraction unfolds. When we mention that a muscle's contraction generates a pulling force directed toward its center, this force is the cumulative result of the bending forces exerted by all the myosin heads. If the summation of these forces surpasses the resistance to shortening, it prompts the actin filaments to be drawn toward the center of the sarcomere, giving rise to a concentric contraction. Conversely, if the collective forces of the myosin heads are insufficient to overcome the resistance to shortening, the actin filaments will be pulled away from the sarcomere's center, leading to an eccentric contraction. When the forces generated by the myosin heads equate to the resistance force, the actin filaments remain stationary, resulting in an isometric contraction. Therefore, the crux of muscle contraction lies in the creation of cross-bridges by the myosin heads, which subsequently pull on the actin filaments.

3.3 Human Nervous System

The nervous system is undeniably the defining characteristic that makes humans human. It serves as the central component responsible for perceiving, interpreting, reacting, and generating consciousness. Its crucial function lies in the transmission of signals from the brain to the rest of the body and vice versa, encompassing internal organs. Through these intricate signals, the nervous system governs critical functions, including movement, respiration, vision, cognition, and a myriad of

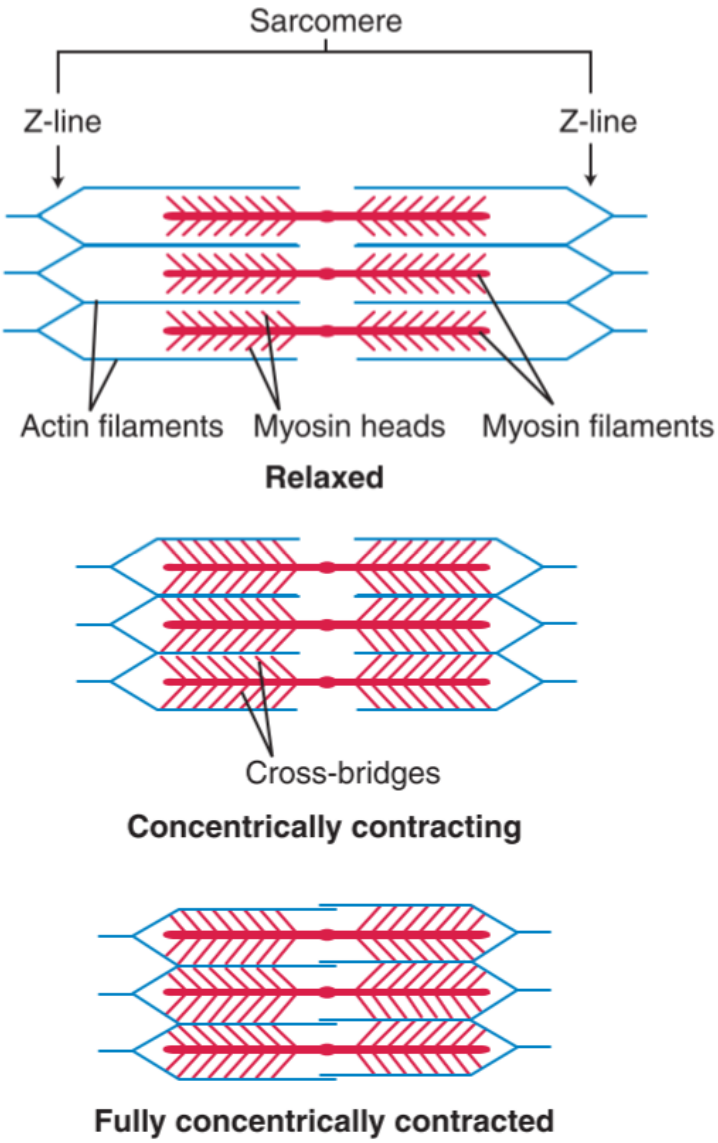

Figure 3.4 A sarcomere is composed of actin and myosin filaments. When the nervous system orders a muscle fiber to contract, myosin heads attach to actin filaments, attempting to pull them in toward the center of the sarcomere. If the pulling force is strong enough, the actin filaments will move and the sarcomere will shorten[41].

other essential processes. The nervous system (Figure 3.5) comprises two primary components :

1. The central nervous system CNS which includes mainly the brain and spinal cord.

2. The peripheral nervous system, which represents the nerves branching off from the spinal cord and reaching throughout the body.

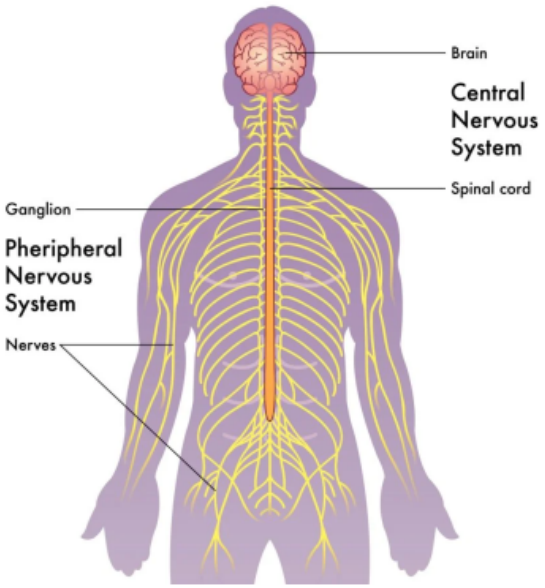

Figure 3.5 Human Nervous System

3.3.1 Nerve Cells-Neurons

Both central and peripheral nervous systems are made of nerve cells or neurons, as they are called most often (see Figure 3.6). The shape of neurons varies depending on their location and function within the body. However, all neurons share common features, such as dendrites, which are finger-like projections, and an elongated fiber called an axon. The structural components of a neuron, as illustrated in Figure 3.6, consist of three main regions. Firstly, the dendrites perform the functions of

receiving, integrating, and processing input from neighboring neurons. Secondly, the soma or cell body receives signals, processes the integrated information received from the dendrites, and serves as the site for genetic and metabolic activities. Lastly, the axon is responsible for transmitting an output signal to specific targets.

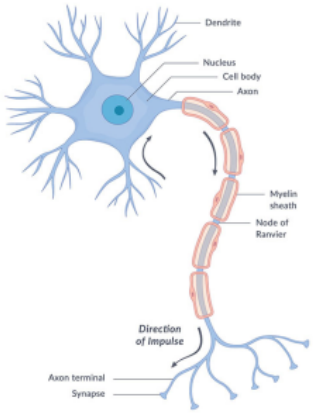

Figure 3.6 Nerve Cell

Sensory Neurons

Sensory neurons (Figure 3.7) are specialized cells in the nervous system that respond to sensory stimuli from the surrounding environment. For instance, when you come into contact with a hot surface using your fingertips, it is the sensory neurons that become activated and generate signals to communicate this information to the rest of the nervous system. Sensory neurons can be activated by various types of inputs, either physical or chemical, corresponding to our five senses. Physical inputs encompass sound, touch, heat, and light, while chemical inputs arise from taste or smell, which the neurons then transmit to the brain. The majority of sensory neurons are classified as pseudo-unipolar, indicating that they possess a single axon that splits into two branches.

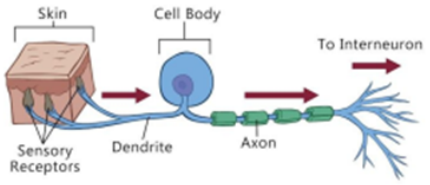

Figure 3.7 Sensory Neuron

Motor Neurons

The motor neurons (Figure 3.8) establish connections with muscles, glands, and organs throughout the body, and they are the basic components of the central nervous system. These neurons carry signals from the spinal cord to both skeletal and smooth muscles (such as those present in the stomach), thereby directly governing all muscle movements in our body. Notably, there exist two distinct types of motor neurons: lower motor neurons, which travel from the spinal cord to the muscles, and upper motor neurons, which communicate between the brain and the spinal cord. Motor neurons exhibit the most common structural configuration observed in nerve cells, known as multipolar. This means that they possess one axon and multiple dendrites. A third type of neuron serves as the connecting link between

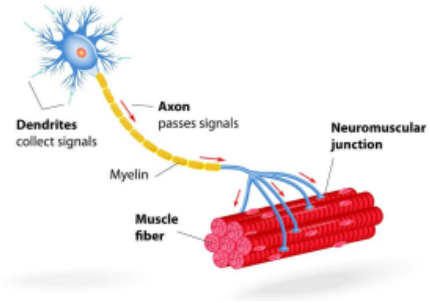

Figure 3.8 Motor Neuron

spinal motor and sensory neurons; we call these neurons the interneurons. The main function of these neurons is not only to facilitate the transmission of signals between sensory. and motor neurons but also to engage in communication with one another, creating intricate circuits of different complexity.

3.4 Neuromuscular System

After providing a comprehensive study of the human muscular and nervous systems, we need to go closer to understanding muscle movement and action; here is where the neuromuscular comes in. 1- The human nervous system also transmits and processes signals that are effectively digital by nature. 2- Digital signals in robotics are transmitted along parallel lines, but in the nervous system, the information is transmitted along a serial line in which the value is encoded in terms of the frequency of electrical impulses called action potentials. To provide an explanation of muscle control, we will employ a bottom-up approach, tracing the control signal from an individual muscle fiber to the brain. Muscles are composed of bundles of individual fibers. Within the muscle, there are groups of tens or hundreds of muscle fibers, which are distributed somewhat randomly. These groups are regulated by a singular neuron situated in the spinal cord known as an motoneuron. A motor unit is formed by the combination of a group of muscle fibers and the corresponding -motoneuron that controls them [43]. The soma and dendrites of the motoneurons are exclusively found within the spinal cord, while the axons exit the spinal cord in clusters called nerves. The individual axons are often referred to as nerve fibers. These nerve fibers split from the primary nerve trunk at different points in the body and follow specific pathways to reach the muscles they govern. As each axon enters the muscle, it branches out and forms a synapse, known as a neuromuscular junction, with a single muscle fiber. Therefore, each muscle fiber is regulated by a solitary axon, namely an motoneuron. The motoneurons receive inputs from numerous other neurons, including peripheral sensory neurons, some of which are excitatory and others that are inhibitory.

3.5 Voluntary and Involuntary Movements

Voluntary and involuntary movements are the two main types of movements in humans. Voluntary movements are those that are consciously controlled by the brain, while involuntary movements are those that are not under conscious control.

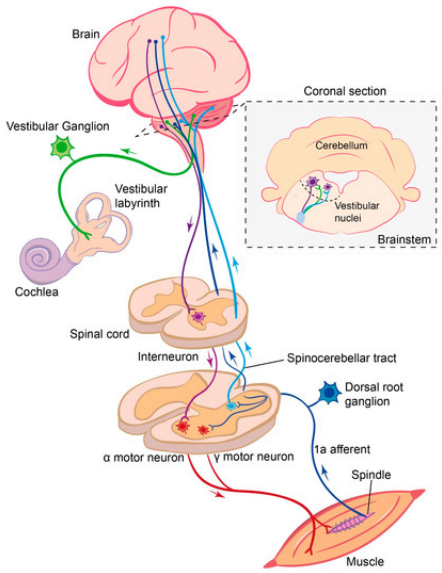

Figure 3.9 Summary of the somatosensory and vestibular sensory pathways and their integration into the brain and spinal cord[37]

Voluntary movements are initiated by the motor cortex in the brain. The motor cortex sends signals to the spinal cord, which then sends signals to the muscles. The muscles contract and cause the movement to occur. Voluntary movements are typically slow and precise. They are used for tasks such as walking, talking, and eating. Involuntary movements are not consciously controlled by the brain. They are caused by a variety of factors, including reflexes, muscle spasms, and neurological disorders. Some examples of involuntary movements include:

- Reflexes: Reflexes are involuntary movements that are triggered by a stimulus. For example, the knee-jerk reflex is triggered by tapping the tendon below the kneecap.
- Muscle spasms: Muscle spasms are involuntary contractions of a muscle. They can be caused by fatigue, stress, or injury.
- Neurological disorders: There are several neurological disorders that can cause involuntary movements. These disorders include Parkinson's disease, Huntington's disease, and Tourette syndrome [44].

Involuntary movements can be a sign of a medical problem. If you are experiencing involuntary movements, it is important to see a doctor to determine the cause. Here is a table summarizing the key differences between voluntary and involuntary movements:

Aspect	Voluntary movements	Involuntary movements
Control	Consciously controlled	Not consciously controlled
Speed	Slow and precise	Fast and jerky
Purpose	Used for tasks such as walking, talking, and eating	Caused by a variety of factors, including reflexes, muscle spasms, and neurological disorders
Examples	Walking, talking, eating	Knee-jerk reflex, muscle spasms, Parkinson's disease, Huntington's disease, Tourette syndrome

Figure 3.10 Voluntary and Involuntary movements

3.6 Study Conclusion

In conclusion, the study of muscle mechanics, specifically the "sliding filament mechanism," reveals the astonishing complexity of muscle function. From the hierarchical organization of muscle fibers to the intricate interplay between actin and myosin filaments within sarcomeres, we gain insights into the fundamental principles governing muscle contraction. While achieving a complete replication of the human muscle system's structure and versatility remains a formidable challenge, we are trying through the development of SEHA to give some features to our Actuation system that may mimic the human muscle systems. This knowledge has paved the way for groundbreaking for such developments and for better integration of SEHA actuator in robotic devices. While the full replication of nature's

masterpiece may elude us, the pursuit of this endeavor continues to inspire innovation and unlock new frontiers in robotics. In the next chapters, we will introduce the SEHA System to introduce the electronics and control integration, which will feature the SEHA some muscle properties.

Chapter 4

Servo Electro-Hydraulic Actuator System SEHA

Contents

4.1 Introduction

We introduced in the previous chapters the general features of SEHA; in this chapter, we will dive into the internal components of the SEHA system. Generally, we can describe the electro-hydraulic actuator as a type of actuator that converts electrical signals into hydraulic pressure to control the position or movement of a

mechanical system. It consists mainly of an electric motor, a hydraulic pump, and a hydraulic cylinder or piston - Figure.4.1

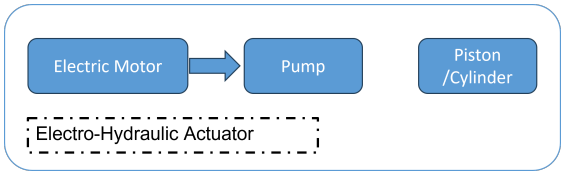

Figure 4.1 Electro-Hydraulic Actuator Main Components

The electric motor drives the hydraulic pump, which pressurizes hydraulic fluid and sends it to the hydraulic cylinder or piston. The position or movement of the cylinder or piston is controlled by varying the amount of hydraulic fluid sent to it. This is achieved by adjusting the electrical input to the electric motor, which controls the speed and direction of the hydraulic pump.

To improve the performance of the robot and meet various requirements, particularly those related to safety, availability, and reliability, the development of actuators with additional functionalities has been undertaken. Consequently, the main aspect of this research focuses on replacing the single hydraulic power unit that supplies the active joints with multiple power units and integrated actuators. This approach ensures that the required pressure is delivered precisely at the joint, thereby enhancing overall system efficiency. The resulting actuator is a hybrid solution known as the Servo Electro-Hydraulic Actuator (SEHA). The SEHA incorporates a power generation module, an integrated hydraulic cylinder, hydraulic circuit blocks, an internal hydraulic feedback mechanism for safe operation, necessary sensors for appropriate control, and electronic cards to establish a self-contained and efficient unit (Figure 4.2). The Servo Electro-Hydraulic Actuator offers the following features:

- Improved power-to-weight and power-to-volume ratios.
- Increased availability, resulting in reduced maintenance frequency.
- Enhanced safety, particularly in human-robot interaction applications, such as assistive devices.

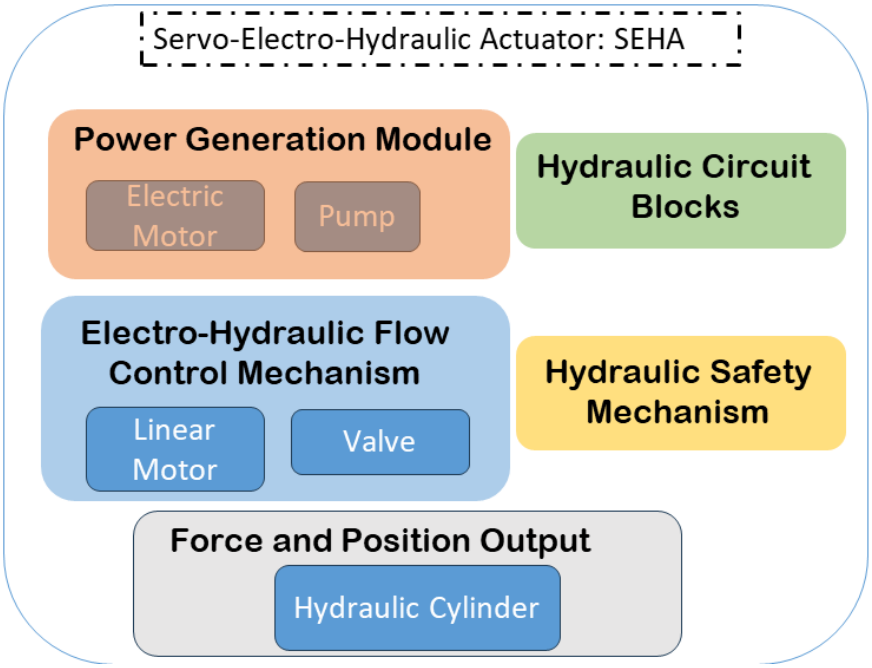

Figure 4.2 SEHA Main Block Diagram

- Greater portability and autonomy.
- Enhanced joint movement characteristics that mimic human-like motion.
- Real-Time Slave Communication
- Real-Time Local Controller Availability

4.2 SEHA System Analysis

4.2.1 SEHA 's Principle

Figure 4.3 shows the hydraulic circuit of SEHA, where we can see the swash-plate mechanism that helps to control the flow, and other hydraulic components, as we will explain later in this chapter. Figure 4.4 illustrates the functional principle of SEHA, the actuator employs an electric motor that is mechanically connected to a pump. The flow direction and quantity of the hydraulic cylinder's movement are

determined by the generated flow. This flow, which drives the hydraulic cylinder, can be adjusted by either controlling the motor's speed or utilizing a servo speed control unit that affects the pump's variable displacement mechanism.

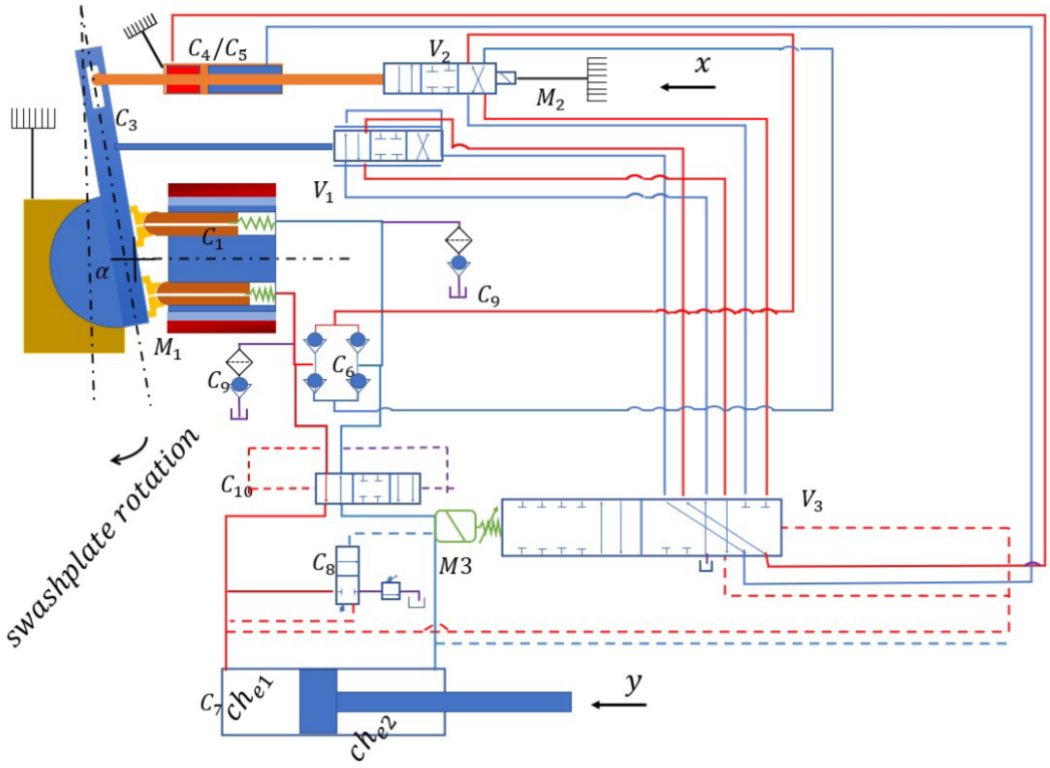

Figure 4.3 SEHA Hydraulic Circuit Principle[23]

By utilizing the electric motor to drive the hydraulic cylinder, the system avoids the need for additional directional valves that contribute to friction-related losses. Furthermore, adopting a hydraulic circuit without directional valves ensures that the actuator can be back-driven, thus enhancing safety. However, this approach has a drawback: it does not guarantee instant flow generation due to the gradual increase in rotational speed. Additionally, changing the actuator's driving direction requires a dead speed zone for the electric motor [45].

To overcome these limitations, it is concluded that SEHA operates more effectively by varying the displacement of the pump. A linear motor actuates a

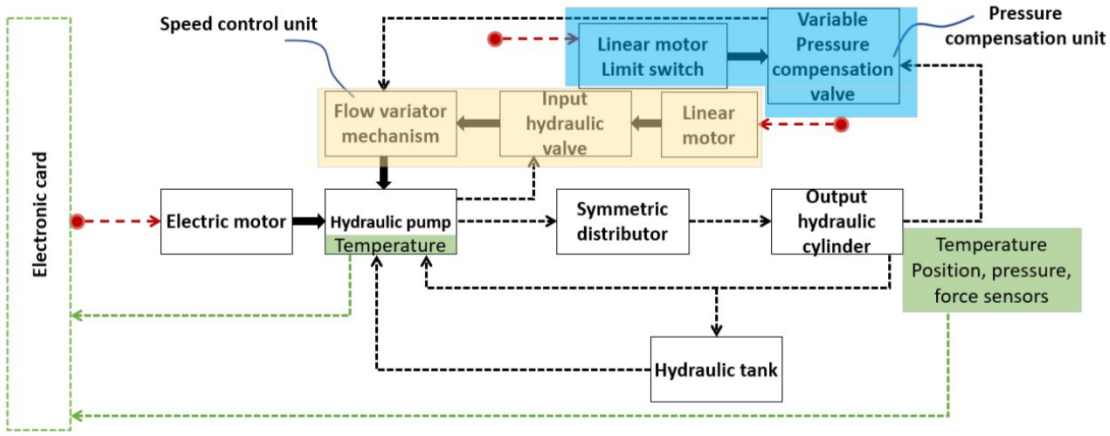

Figure 4.4 SEHA Functional Diagram

hydraulic valve, serving as the system's input, which mechanically influences a flow modulation mechanism responsible for controlling the pump's displacement. In scenarios where there is a pressure increase in the circuit, the hydraulic feedback of the actuator engages a developed servo force compensation valve to decrease the pump's flow and alleviate the system.

To facilitate a comprehensive understanding of SEHA, its development is divided into separate units based on their respective functions, and this technique is called a modular design strategy. In many different disciplines and industries, modular design has several advantages. First off, it offers more scalability and flexibility. A system or product can be divided into modular parts, making it simpler to add, delete, or replace certain modules without affecting the entire system. This adaptability enables effective customization, upkeep, and upgrades, which saves time and resources.

The modular structure also encourages uniformity. Companies can optimize their production processes and cut costs by creating standardized modules that are simple to connect to various systems. Additionally, standardization promotes interoperability by making it simple to swap out or combine compatible modules, which improves compatibility and cooperation between various systems or devices.

This breakdown allows for a detailed exploration of each unit's role and con-

tribution to the overall operation of the actuator.

4.2.2 Main Hydraulic Group System

The hydraulic pump is a crucial component in hydraulic systems, serving several key functions, such as flow generation, power transmission, pressure generation, and speed and direction control. The development of the main hydraulic system requires high integration and a lightweight design to align with the desired features of the SEHA. Generally, the hydraulic pump consists of two main components, the driver motor, and the pump mechanism which has been studied by Maya et al. and Kardofaki et al.

Electric Motor for the Pump

The primary role of an electric motor is to power the pump mechanism. However, as previously mentioned, the motor should have a compact size and seamless integration with the mechanical system. Additionally, it should be easy to control and require minimal maintenance. Numerous motor technologies exist, each with its own set of advantages and drawbacks.

Although induction motors offer the advantage of not requiring a commutation mechanism and find application in a diverse range of industries, their drawback lies in their large size. This size limitation makes them unsuitable for SEHA's primary objective and specific application [46]. Another interesting and widely used technology is the direct current motor DC. DC motors are known for their compact size and are capable of delivering a broad range of power, making them suitable for various applications ranging from light to heavy-duty. However, DC motors face a disadvantage due to their commutation mechanism that involves brushes [47]. This design characteristic necessitates frequent maintenance and can contribute to a higher failure rate in pump systems. A third very common technology in robotics applications nowadays is the BLDC motor. BLDC motors are common in robotics due to their prominent characteristics, which include the following key features:

1. High Efficiency: BLDC motors offer high efficiency compared to other motor types, resulting in improved energy utilization and longer battery life. This efficiency is especially crucial in robotics, where maximizing the runtime is essential for extended operation and increased productivity [48].

2. Precise Control: BLDC motors provide precise speed and position control, enabling accurate and repeatable movements in robotic systems. This level of control allows robots to perform intricate tasks with precision, enhancing their overall performance and productivity.

3. Compact Size and Lightweight: BLDC motors are typically compact and lightweight, making them well-suited for robotic applications. Their small size allows for easier integration into the mechanical structure of robots, allowing for more efficient use of space and enabling the design of smaller and more agile robots.

4. High Torque and Power Density: BLDC motors offer high torque and power density, allowing robots to generate significant force even with compact motor sizes. This characteristic is beneficial for tasks that require lifting, manipulation, or overcoming resistance, enabling robots to perform demanding tasks effectively [49].

5. Low Maintenance: BLDC motors have a brushless design, eliminating the need for regular brush replacement and reducing maintenance requirements. This feature is particularly advantageous in robotics, where minimizing downtime for maintenance is crucial for continuous operation and productivity [49].

6. Reliability and Durability: BLDC motors are known for their robust construction and durability. They can withstand rigorous operating conditions, shocks, and vibrations commonly encountered in robotic applications, ensuring reliable performance over extended periods.

7. Noise Reduction: BLDC motors operate with reduced noise levels compared to brushed motors, making them suitable for applications that require low

acoustic emissions. This feature is especially important in robotics used in environments where noise reduction is essential, such as healthcare settings or residential areas [49].

Overall, the high efficiency, precise control, compact size, high torque, low maintenance, reliability, and noise reduction characteristics of BLDC motors make them a preferred choice in robotics. On the hydraulic side, there are many types

Criteria	AC Induction Motor	BLDC Permanent Magnet Motor	DC Motor
Principle of Operation	Electromagnetic Induction	Permanent Magnets	Electromagnetic Field
Commutation	None	Electronic Commutation	Mechanical Commutation
Efficiency	Moderate to High	High	Moderate to High
Speed Control	Limited range	Wide range	Wide range
Starting Torque	Good	High	High
Maintenance	Low	Low	Moderate to High
Cost	Moderate to High	Moderate to High	Low to Moderate
Size and Weight	Relatively Large	Compact	Compact
Application Range	Wide range	Moderate to High	Wide range
Range of Power	Low to High	Low to Medium	Low to High
Driver Complexity	Moderate	Moderate	Simple

Figure 4.5 Comparison between Different Motor Technologies

of pumps, but the most common in robotics applications are radial piston pump, axial piston pump, and Vane pump [50][51][52][53]. Vane pumps exhibit the lowest power-to-weight ratio among the three pump types due to their limited pressure capacity [53]. Conversely, piston pumps demonstrate higher efficiencies and superior power-to-weight ratios [52]. Axial piston pumps outperform both vane and radial pumps, with efficiencies reaching 98%, operating effectively within a wide pressure range of 140 to 800 bars [53]. Moreover, while increasing flow in radial pumps necessitates an enlargement of the cylinder block diameter, axial piston pumps can achieve increased flow by extending their length. This characteristic

holds great significance as it allows for better alignment with the human body shape, particularly when the pumps need to fit within a specified volume in a robot or assistive device. For these reasons and the motor comparison above, a BLDC motor paired with an axial piston pump will be employed in the development of the Main Hydraulic Group [23]. (Figure 4.6 shows the BLDC motor integration with the pump) Another important issue to discuss after choosing the

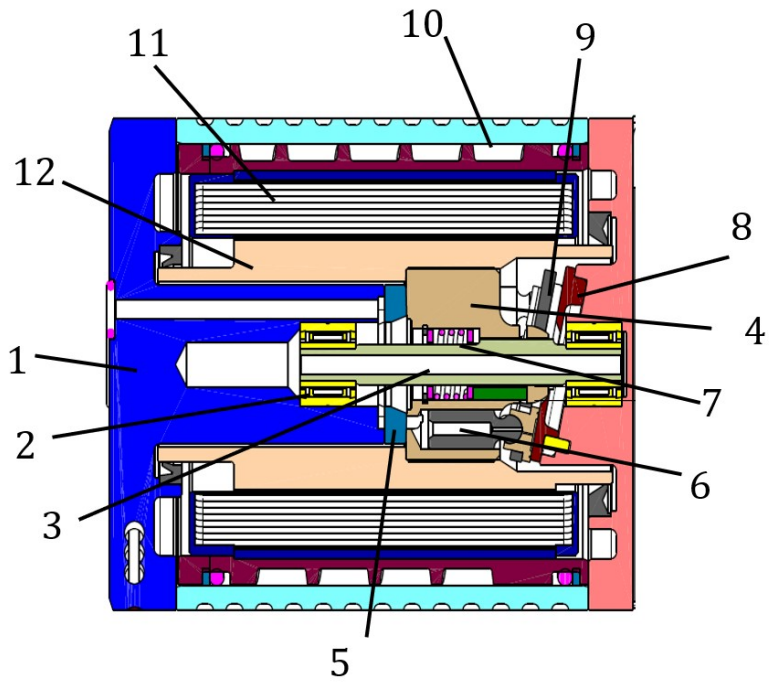

Figure 4.6 Main Hydraulic Group assembly; 1- MGH's body; 2- Bearing; 3- shaft; 4- Cylinder block; 5- valve plate; 6-piston; 7-spring; 8- swashplate; 9- retainer ring; 10- Oil jacket; 11- stator; 12- rotor

motor technology is the nominal values for the voltage and the current where the nominal power has been chosen by the mechanic developer to be 1500W, still the nominal current and voltage need to be considered. When it comes to compact design, both high voltage low current motors and high current low voltage motors have their advantages and disadvantages. High voltage low current motors have the advantage of being more efficient in terms of power transmission. Since power is equal to the product of voltage and current, high voltage low current motors can transmit the same amount of power with lower current levels. This

leads to reduced resistive losses and allows for smaller wire sizes, resulting in a more compact motor design. Additionally, high-voltage low-current motors tend to have higher insulation resistance, which can reduce the risk of electrical faults and increase the overall reliability of the motor. Because of these reasons, we chose a high-voltage low-current BLDC motor (325VDC, 5ADC). In upcoming chapters we will introduce the driver solutions for this motor.

4.2.3 Servo Speed Control Unit

The speed of a SEHA output cylinder can be controlled in two ways: by varying the motor's rotational speed or by changing the displacement. The first method, used by Nakamura et al., has the advantage of high back-drivability and fewer components, but it does not generate instantaneous power as the speed increases. The second method, which uses a mechanism to act on the swashplate, requires more components but allows for the achievement of displacement variation [30][33][23].

Valve

A directional valve with mechanical feedback is shown in Figure 4.7. The valve V2 has a linear motor M2 that creates an offset. The external body of the valve is mechanically fixed to a servo-hydraulic cylinder C4/C5. This cylinder moves the swashplate's actuation shaft until the opening of valve V2 is closed. The opening of the valve V2 determines the linear movement of the actuation shaft, which in turn defines the rotational angle of the swashplate. The mechanical part is studied and optimized by Kardofaki et al.. and Maya et al. [23], and here in this section, we are optimizing the choice of the proper electric motor that would be fully integrated with the mechanical design and has the best dynamic design.

Linear Motor

We conducted a comprehensive review study comparing the performance of three distinct linear electric motor actuators: voice coil, DC linear motor, and BLDC

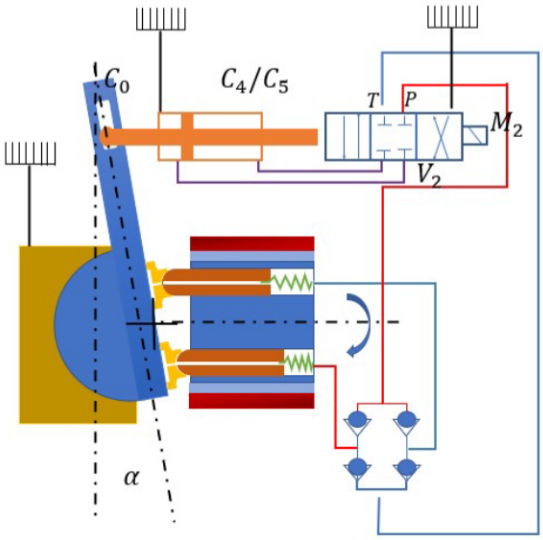

Figure 4.7 Speed Control of the pump

linear motor (Table 4.1). Our analysis sheds light on their respective strengths and weaknesses, offering valuable insights for various applications [54] [55].

To ensure SEHA's optimal dynamism while working within size constraints for integrating electric components into the mechanical and hydraulic structure, we opted for the integration of voice coil technology.

4.2.4 Servo Force Compensation Unit

Devices such as assistive devices, humanoids operating in unstructured environments, industrial robots, and systems utilizing actuators like SEHA are susceptible to unexpected additional loads. These loads can directly impact the safety of patients, individuals near the robots, or the materials' integrity. To mitigate these risks, implementing a safety unit becomes crucial, and there are several methods to achieve this:

- Virtual impedance control: By employing virtual impedance control techniques, the system can dynamically adjust its response to external forces, providing a level of protection against unexpected loads.

Feature	Voice coil linear motor	BLDC linear motor	DC linear motor
Construction	A voice coil linear motor consists of a permanent magnet and a coil that is wrapped around a moving armature.	A BLDC linear motor consists of a permanent magnet, a stator with windings, and a moving armature.	A DC linear motor consists of a permanent magnet and a coil that is wrapped around a moving armature, but it uses a DC power supply instead of an AC power supply.
Drive type	Direct drive	Geared drive	Direct drive
Speed	High speed	Medium speed	Low speed
Force	Low force	High force	Medium force
Accuracy	High accuracy	Medium accuracy	Low accuracy
Efficiency	Low efficiency	High efficiency	Medium efficiency
Cost	Low cost	High cost	Medium cost
Size	Small	Medium	Large
Electronic driver complexity	Simple	Complex	Simple

Table 4.1 Linear Motor Technologies

- Load cell with closed-loop control: Integrating a load cell into the system allows for continuous monitoring of the applied forces. Closed-loop control algorithms can then regulate the actuator's behavior based on the measured load, ensuring a safer and more controlled operation.

- Incorporating a compliant element: Introducing a compliant element between the actuator and the load can absorb and distribute the additional forces, reducing the risk of damage or injury. This compliant element acts as a buffer, absorbing impacts and preventing direct transmission of excessive forces.

- Development of a hydraulic valve: Another approach involves designing a hydraulic valve that directly influences the swashplate's angle. By adjusting the swashplate, the valve can regulate and maintain pressure below a predetermined threshold, safeguarding the system from excessive pressure surges.

These safety measures aim to protect the circuit, personnel, and materials involved in the operation of such devices, ensuring a safer and more reliable performance in various applications.

4.3 Conclusion

In this chapter, we explore its internal components, which include an electric motor, hydraulic pump, and hydraulic cylinder. These components work together to convert electrical signals into hydraulic pressure for precise control of mechanical systems.

Our research focuses on enhancing robot performance and safety by replacing a single hydraulic power unit with multiple integrated actuators, resulting in the Servo Electro-Hydraulic Actuator (SEHA). SEHA offers improved power-to-weight and power-to-volume ratios, increased availability, enhanced safety, portability, and lifelike joint movements, making it ideal for various applications.

We adopt a modular design strategy for SEHA, promoting scalability, flexibility, and compatibility. The main hydraulic group system features a high-voltage, low-current BLDC motor and an axial piston pump for optimal performance.

The servo speed control unit allows for precise speed adjustment through a directional valve with mechanical feedback and a linear motor. Additionally, a servo force compensation unit ensures safety by handling unexpected loads effectively.

We will study the model and detailed simulation of SEHA's electronic components in the upcoming chapters.

Chapter 5

SEHA Simulation and Control

Contents

5.1 Introduction

Integrating electro-mechanical and hydraulic elements in SEHA makes it a complex and multifaceted system, offering unprecedented capabilities. However, their complexity makes them difficult to model accurately. The presence of non-linearities further complicates the modeling process, making it a formidable task. To understand the dynamic behavior and performance characteristics of such a complex system, simulation is an invaluable tool. It allows us to explore the complexities of the physical world in a controlled and virtual environment, shedding light on the

intricate interplay of components and how they respond to different conditions. In the case of SEHA, we will use the simulation to unravel its intricate behavior, visualize the dynamic interactions of mechanical and hydraulic components, and uncover the subtleties of nonlinear effects that govern their operation.

5.2 SEHA Mathematical Model

The mathematical model that describes our system is very complex. Extensive research by Maya et al. has proven that the relationship between the input variable (x) and the output variable (y) is nonlinear [23]. This complexity means that we need to use advanced analytical techniques and a deep understanding of the system to describe and predict its behavior accurately.

Table 5.1 Nomenclature

Symbol	Description	Unit
x	Offset created by V2	m
y	Linear movement of the C7	m
α	Swash-plate rotation angle	rad
ω	Rotational speed of the pump	rad/s
Q	Pump's flow	m^3/s
T_e	Electromagnetic torque produced by the motor	N·m
T_l	Load torque	N·m
P	Number of pole pairs in the motor	
k_t	Motor's torque constant	N·m/A
I	Current in the motor windings	A
θ_r	Rotor's electrical angle	rad
e_a, e_b, e_c	Back electromotive force generated by the motor	V
k_b	Back electromotive force constant	V/(rad/s)
ω_r	Rotor's angular velocity	rad/s
V_p	Voltage applied to one phase of the motor	V
i_a, i_b, i_c	Stator Currents	A
R	Phase resistance	Ohms (Ω)
L	Phase inductance	Henrys (H)
M	Mutual inductance	Henrys (H)

The input x is then a function of the output movement of the hydraulic cylin-

der y, its derivatives, the pump's rotational speed and its derivatives, SEHA's geometrical parameters, and oil characteristics.

$$x = f(y, \dot{y}, \ddot{y}, \dddot{y}, y^{(4)}, y^{(5)}, y^{(6)}, \omega, \dot{\omega}, \ddot{\omega}, \dddot{\omega})$$

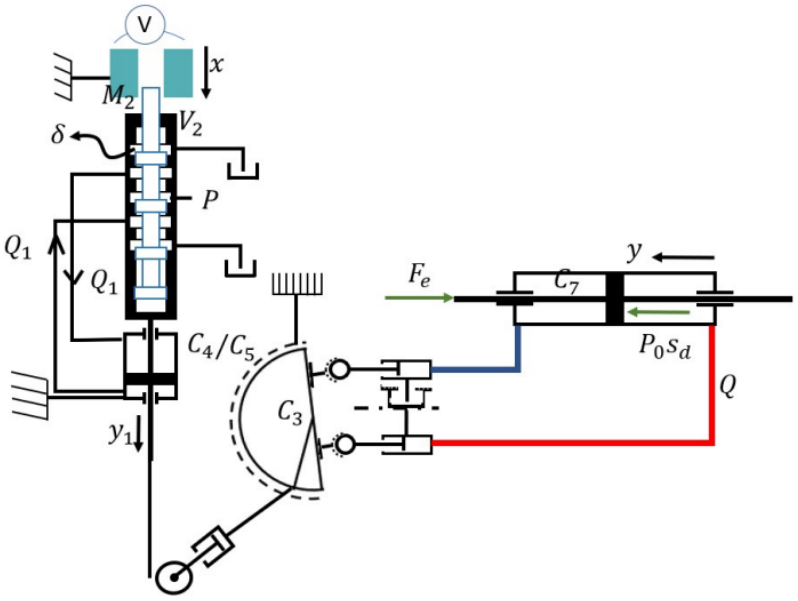

Figure 5.1 SEHA Output Cylinder

5.3 SEHA Mechanical and Hydraulic Simulation

Figure 5.2 shows the simulation platform that was developed by Maya et al, it consists mainly of four blocks labeled from one to four:

1. Hydraulic pump: we consider the input for this block to be the motor velocity Ω (we will simulate the BLDC motor with its driver later in this chapter) and the output is the hydraulic flow Q.

2. Speed control unit: which consists mainly of a valve that will be actuated by a voice coil linear motor, in this platform we assume the input for this block is the linear shift x (the voice coil motor is not simulated in this model)

3. Output Cylinder with the load, where the input for this block is the flow and the output is piston position and velocity.

4. visualization and scaling block

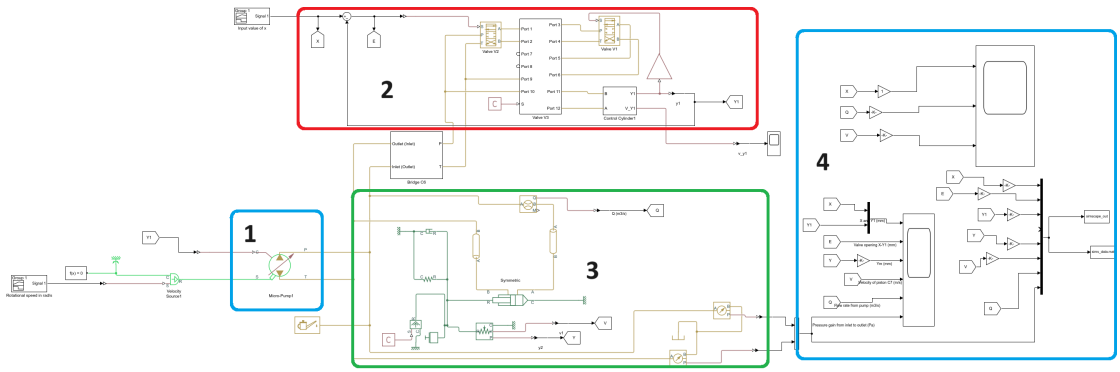

Figure 5.2 SEHA System Simulation in Simulink

Using the simulation platform (figure 5.2), Maya et al. [23] has studied the response time for SEHA with different loads and different pump speeds, we can conclude this study in Figures 5.3,5.4, and 5.5. We found that the response time of the hydraulic system decreases as the pump's rotational speed increases. The system performs best at lower loads, where the response time is 25% faster with a 150 kg load than with an 850 kg load. The effect of the output cylinder characteristics on the response time is more significant at higher loads.

In other words, the system reacts faster when the pump spins faster, and the load is lighter. The output cylinder characteristics have a greater impact on the response time when the load is heavier.

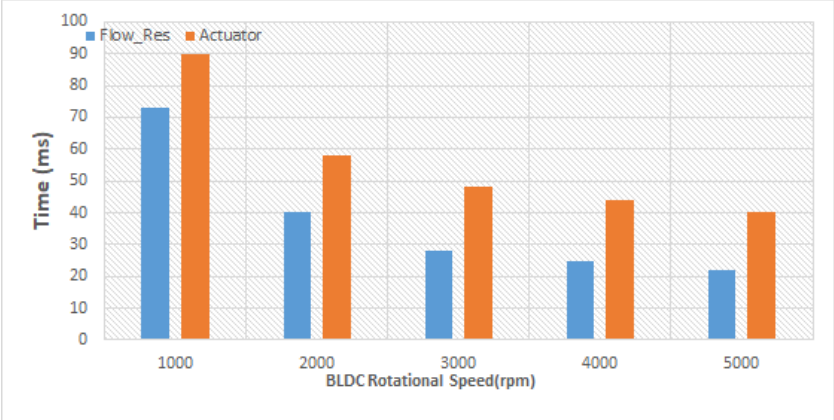

Figure 5.3 Flow and Position Response Time for 1.5kN of Load

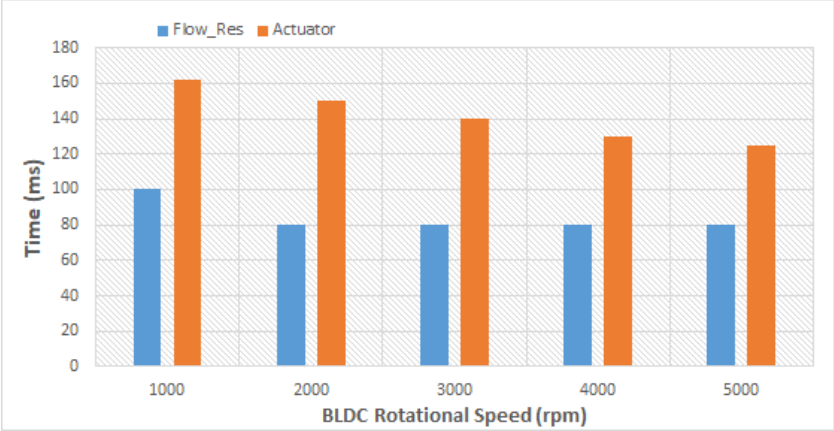

Figure 5.4 Flow and Position Response Time for 5kN of Load

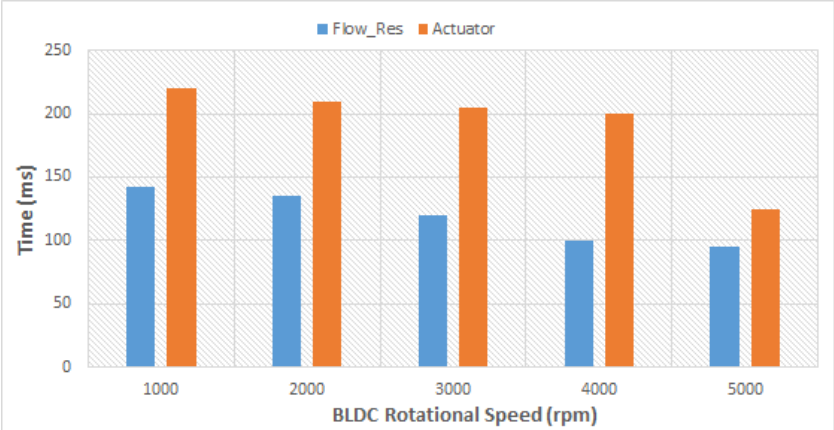

Figure 5.5 Flow and Position Response Time for 8.5kN of Load

5.4 SEHA Electric Motors Simulation

5.4.1 BLDC Motor Simulation and Control

The components of a BLDC motor include the rotor, which is the moving part housing permanent magnets for magnetic field generation, and the stator, which remains stationary and contains wire coils that, when energized, create a magnetic field. Hall effect sensors or an encoder detect the rotor's position, providing essential feedback for accurate control. The controller, known as drive electronics, manages the timing and amplitude of current applied to the stator windings, ensuring precise rotation of the rotor. The working principle involves electronic commutation, utilizing feedback from sensors to determine which stator windings to energize. When energized, the stator windings generate a magnetic field that interacts with the rotor's permanent magnets, causing rotation. Continuous adjustments in winding currents by the controller maintain the rotor's motion and allow for precise speed and direction control, achieved by modifying current timing and amplitude. The dynamic model of the BLDC motor is described in equations 5.1 and 5.4

$$v_a = Ri_a + L\frac{di_a}{dt} + M\frac{di_b}{dt} + M\frac{di_c}{dt} + e_a \tag{5.1}$$

$$v_b = Ri_b + M\frac{di_a}{dt} + L\frac{di_b}{dt} + M\frac{di_c}{dt} + e_b \tag{5.2}$$

$$v_c = Ri_c + M\frac{di_a}{dt} + M\frac{di_b}{dt} + L\frac{di_c}{dt} + e_c \tag{5.3}$$

$$T_e = k_t \cdot I_a \tag{5.4}$$

$$J \cdot \omega_r = T_e - T_l \tag{5.5}$$

Instead of manually implementing the electrical and mechanical equations to simulate the BLDC motor and its driver, we used the BLDC motor components available in the Simscape Electrical library within Simulink, as shown in Figure 5.6. To estimate the response time for the BLDC motor with the driver, we built

a simulation platform in Simulink MATLAB (Figure 5.6). The platform consists

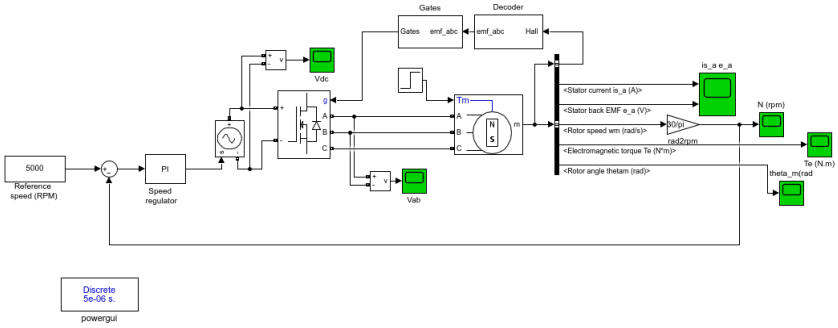

Figure 5.6 MGH-BLDC motor Speed Control with Power Driver

basically of the BLDC motor and the six bridge power driver, all in velocity closed-loop control. For the MGH design, we are using a custom-made BLDC motor with the following motor parameters:

$$P = 1500\,\text{Watt} \tag{5.6}$$

$$R = \frac{R_m}{2} = 2\Omega \tag{5.7}$$

$$M = L_m = 13\,\text{mH} = 13 \times 10^{-3}\,\text{H} \tag{5.8}$$

$$L = \frac{L_m}{2} = 6.5\,\text{mH} = 6.5 \times 10^{-3}\,\text{H} \tag{5.9}$$

$$L_s = L - M = -6.5 \times 10^{-3}\,\text{H} \tag{5.10}$$

$$J = 0.5\,\text{kg} \cdot \text{cm}^2 = 5 \times 10^{-5}\,\text{kg} \cdot \text{m}^2 \tag{5.11}$$

$$k_b = 50.4\,\text{V}_{\text{peak}}/\text{krpm} = 0.68\frac{\text{Vrms}}{\text{rad/s}} \tag{5.12}$$

Using these parameters in the simulation platform, we simulate the motor speed control with an IGBT power driver with no load and a full load. Figure 5.7 shows the step response for the motor-driver system in the extreme two cases 1- free running no-load 2- full load.

1. Free Running (No Load): here, we find that the settling time for the system is $t_{set} = 4.01ms$.

2. Full Load PI Controller: using the PI controller in the full load condition, we did not have a stable steady-state velocity value; instead, we have an oscillating steady state as shown in Figure 5.7 and to have an acceptable settling time, we had to return the PI controller with $t_{set} = 3.46ms$.

3. Full Load PID Controller: we decided to explore the introduction of a derivative (D) component to the controller. The D parameter, which represents the rate of change of the error signal, is known to improve control system stability and reduce overshoot and oscillations. With the addition of the D component, we transitioned from a PI controller to a PID (Proportional-Integral-Derivative) controller with $t_{set} = 40.8ms$.

   The impact of introducing the D component was profound. The PID controller exhibited remarkable performance, providing a much smoother response with significantly reduced ripples in the final velocity value.

In Conclusion, our motor control simulations revealed that a PI controller works well with no load but needs to be returned for heavy loads. Adding a derivative (D) term to the PI controller creates a PID controller, which greatly improves response time but still has some ripples. This shows that control strategies need to be adaptable to changing conditions. We recommend using a scheduled PID controller to achieve the best motor control, which can adjust its parameters in real-time based on the load conditions. This ensures consistent and precise motor performance.

5.4.2 Voice Coil Motor Simulation and Control

A linear voice coil assembly consists of a frame housing a permanent magnet, with a slender cylinder containing a copper coil (solenoid) that can move within it. Depending on the electric current flowing through the coil windings, this linear actuator demonstrates the capability to swiftly push or pull a load, thanks to the low inertia of the slender cylinder. It can achieve remarkably rapid response times when appropriately sized for the specific load, making it an excellent choice for the robotics application under consideration.

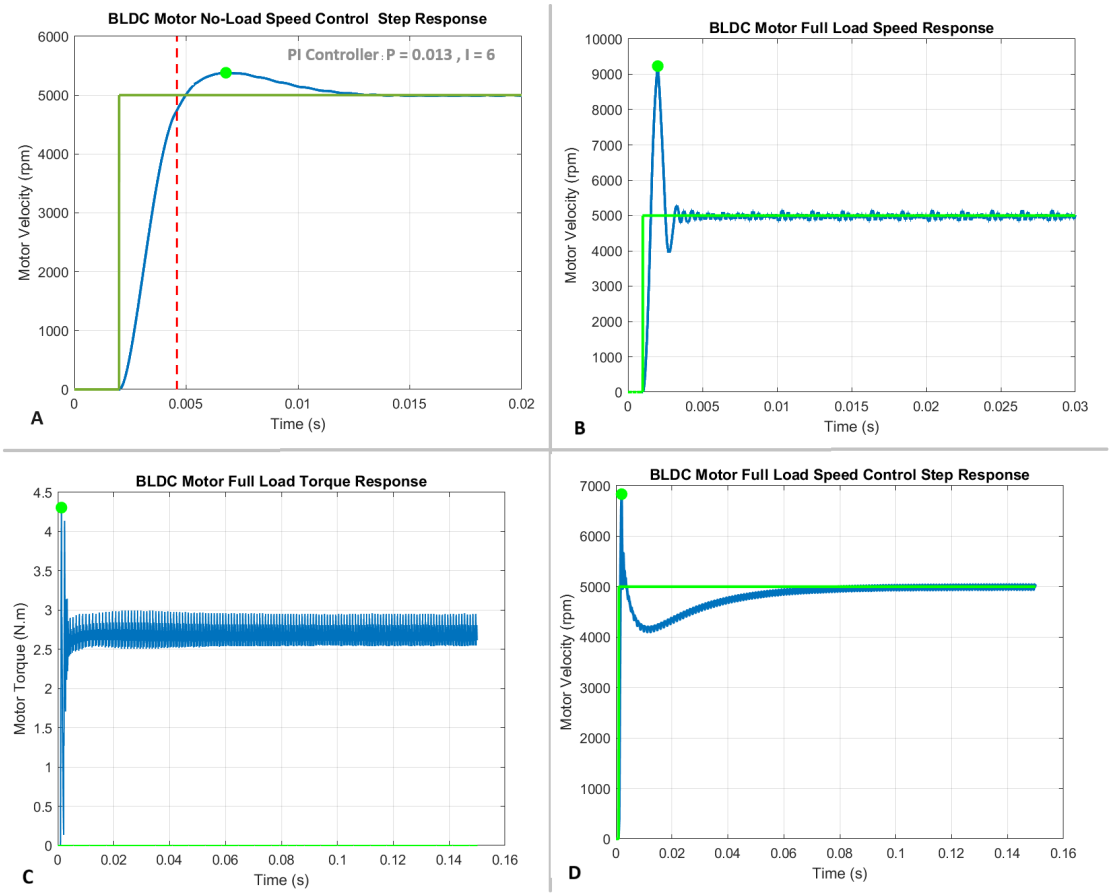

Figure 5.7 BLDC Motor with Driver Simulation Results: A- Step Response of motor_driver system in no-load condition, B- Step Response of motor_driver system in full-load condition with PI controller, C- Mechanical Load Torque and motor Torque, D- Step Response of motor_driver system in full-load condition with PID controller

Table 5.2 Voice Coil Motor Parameters

Description	Value	Unit
Copper coil Resistance (R)	1.3	Ω
Copper coil Inductance (L)	0.19	mH
Maximum Voltage	12	V
Maximum Current	1.8	A
Force sensitivity KF	0.506	N/A
Back-Electro-Motive Force Constant K	0.506	V-s/m

Dynamic Model

The fundamental operational principle of voice coil actuators is governed by the Lorentz force. This force, denoted as F_{vca} and expressed in equation 5.13, is generated by the current I passing through the coil. Notably, the actuator's force sensitivity, denoted as KF, is contingent upon the position x of the cylinder along its axis.

$$F_{\text{vca}} = k_f(x)I \tag{5.13}$$

Electric Equation Regarding its electrical characteristics, a voice coil actuator can be depicted using the equivalent circuit shown in Figure 4a. Within this circuit, we have E representing the external power supply R and L, symbolizing the coil's resistance and inductance, respectively. Additionally, there's KB·v, which signifies the back-electromotive force (BEMF) generated by the cylinder's displacement. Here, v stands for the rate of change of cylinder position (dx/dt), and KB represents the BEMF constant. The following equation describes the circuit:

$$E = RI + K\frac{dx}{dt} + L\frac{dI}{dt} \tag{5.14}$$

This equation encapsulates the interplay of these electrical components within the voice coil actuator.

Mechanic Equation By applying Newton's second law to the cylinder, it becomes possible to describe the motion of the actuator and derive its dynamic

model, which manufacturers typically do not provide. Let's denote "m" as the mass of the cylinder and F_{ext} as the external force acting along the x-axis due to the mechanical load connected to it (e.g., the clutch spring or gear lever). The relationship is as follows:

$$m\frac{d^2x}{dt^2} = F_{\text{vca}} - F_{\text{ext}} \tag{5.15}$$

$$k_f(x)I - F_{\text{EXT}} = m\frac{d^2x}{dt^2} \tag{5.16}$$

building the electrical and the mechanical equations 5.14 and 5.16 in Matlab-Simulink and make the simulation for the voice coil in open-loop, results the motor response shown in Figure 5.8 Noting that this simulation takes the worst case for

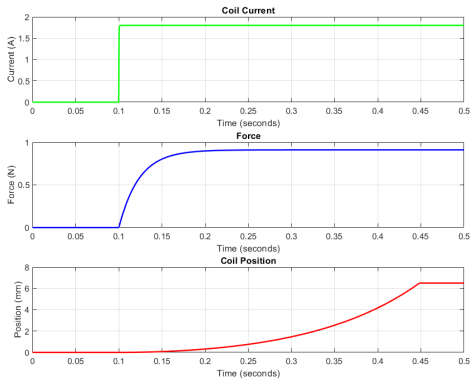

Figure 5.8 Open loop response for the voice coil motor model. The position is shown in blue, the force is shown in green, and the current is shown in red.

the voice motor movement (from 0 to 6.5 mm) and with the full load force $0.91N$, we find that response time for the force is$T_{rforce} = 170ms$and for the current(Figure 5.9 is $T_{rcurrent} = 100ms$ and concerning the position we found the time for such extreme movement takes $T_{rpos} = 450ms$ as response time, which could be improved later using power driver and control. In conclusion, the position response time for our voice coil motor for extreme movement is a little bit high and needs to be reduced, for our study, we will develop the current driver for this motor and the control enhancement may be considered a recommended future work for SEHA.

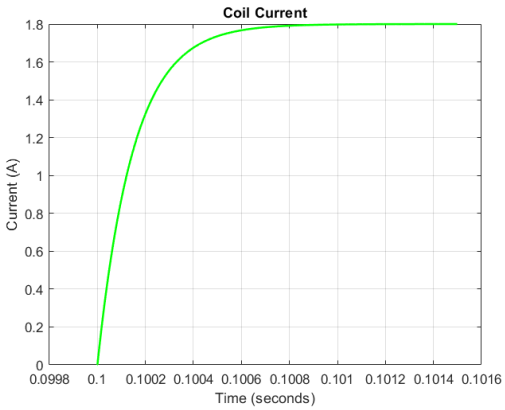

Figure 5.9 Coil Current Dynamic Response

5.5 Conclusion

In conclusion, SEHA's complex nature requires advanced modeling and simulation techniques to understand its behavior and performance characteristics. Simulations of hydraulic, BLDC, and voice coil systems have provided valuable insights. The study recommends further control enhancements for the voice coil motor and emphasizes the adaptability of control strategies to varying conditions for precise motor performance. The findings contribute to the development and optimization of SEHA for robotics applications. In the next chapters, we will discuss the electronic and control layer for SEHA.

Chapter 6

SEHA Electronics and Control Layer

Contents

6.1 Introduction

The design of the electronic layer for a Servo Electro-Hydraulic Actuator plays a crucial role in ensuring its efficient operation and optimal performance. The

electronic layer encompasses various components such as control systems, sensors, and power electronics that are responsible for controlling the actuator's movement and facilitating communication between the actuator and other systems in the overall control architecture. The design procedure entails careful selection and dimensioning of individual components following the precise needs of our SEHA actuator, ensuring seamless integration within the humanoid robot. Modular design is of utmost importance in the design of the Servo Electro-Hydraulic Actuator. A modular design approach involves dividing the SEHA system into smaller, independent modules that can be easily configured, maintained and upgraded. This allows for greater flexibility and scalability, as well as the ability to replace or upgrade individual modules without affecting the entire system. By implement-

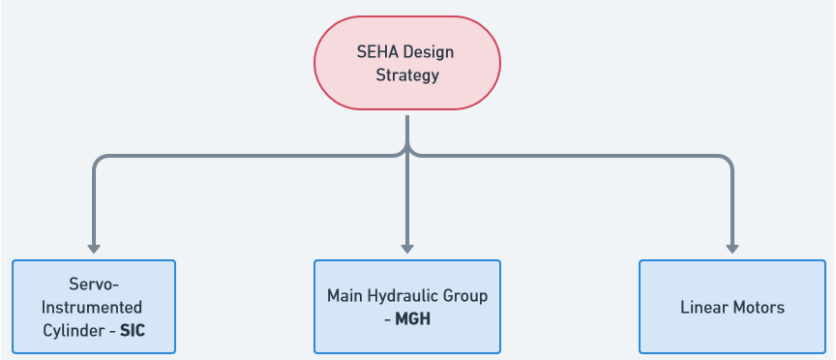

Figure 6.1 SEHA Modular Design

ing a modular design, the SEHA actuator can be easily customized to meet the specific needs of different robotic applications, which is very important since we are targeting humanoid robots with different sizes and exoskeletons with different sizes.

6.2 Servo-Instrumented Cylinder- SIC

The SIC is the output cylinder of SEHA. Therefore, our main strategy for SIC development is to create and develop the most efficient electronic and sensory layer to ensure that the output cylinder meets SEHA specifications. A highly

Figure 6.2 Servo-Instrumented Cylinder- SIC

instrumented hydraulic cylinder has been developed to meet the requirements of hydraulic and electronic integration. The cylinder is structurally integrated with the main hydraulic components (barrel, piston, rod, and caps). The instrumented hydraulic cylinder is driven by the hydraulic circuit of the global SEHA. Despite being developed with the modular design strategy in mind, SIC can also be used as a standalone product. All it needs is a control valve to be integrated into it. So the cylinder can be used in two ways: it can be integrated into SEHA and driven by its hydraulic circuit, or it can be a standalone product that integrates a control valve.

6.2.1 Sensory Envelope System

Developing a sensory system for a hydraulic cylinder involves integrating various sensors that can replicate the functionality of human muscles. The primary sensors chosen for this purpose should be sensitive to parameters such as force, position, and speed, which are crucial for accurate feedback and control of the hydraulic cylinder's movement and functionality.

Position Sensor

Notwithstanding various endeavors and studies like the work presented in [56] by Tom SOURANDER et al., wherein they devise sensor-less control algorithms, integrating a well-calibrated sensor remains a superior design choice for the actuator. We regard the cylinder's position as the pivotal state in effectively governing the cylinder actuator. Broadly, two methodologies exist for detecting the position of

linear actuators. The initial approach involves sensing the commencement of stroke (SOS) and the culmination of stroke (EOS), then formulating a control response based on these two piston states. This methodology finds extensive employment in the industrial sector, particularly in the realm of production line machinery. However, for actuators like the SIC, slated for application in robotics to ensure safety, we must adopt the second approach. This alternative hinges on continuous sensing throughout the cylinder's stroke.

Various position sensor technologies can be considered for use in a linear electro-hydraulic actuator. These include potentiometers, linear variable differential transformers LVDT, magnetostrictive sensors, optical encoders, and Hall effect sensors. Each of these position sensor technologies has its own advantages and limitations. Potentiometers are a commonly used position sensor for linear electro-hydraulic actuators. They are relatively low-cost and provide good resolution. However, they are susceptible to wear and tear, which can affect their accuracy over time. Linear variable differential transformers are another option for position sensing in linear electro-hydraulic actuators. These sensors are capable of providing highly accurate and reliable position measurements. Magnetostrictive sensors utilize the magnetostrictive effect, where changes in the magnetic field cause elongation or contraction of a magnetostrictive material such as Terfenol-D. They offer excellent linearity, high precision, and long-term stability. On the other hand, optical encoders use light to detect position changes and can provide high resolution and precision. However, they may be more expensive and susceptible to environmental factors such as dust or vibration. Table 6.3 provides an overview of the leading technologies employed in position sensing, accompanied by a succinct juxtaposition of the key considerations we hold.

Regarding the difficulties we face in integrating the position sensor, vibration, and shock are the most challenging. Tight mounting and integration of the position sensor can improve the position control loop because shock and vibration can affect position sensing. Besides the precise mounting, applying a soft start and stop control algorithm can protect the sensor from connector damage. Additionally, minimizing the additional mass on both the sensor and actuator and

	Resolution	Non-linearity	Dynamic Response	Temperature characteristic	Cost
Potentiometer	++	++	+	+	$
AC-LVDT	++++	++	++	+++	$$
DC-LVDT	++++	++	++	++	$$
LVIT	+++	++	++	++	$$$
Magnetoresistive	++	++	++	+	$$$$
Magnetostrictive	+++	+++	+	++	$$$$$
Hall-Effect Magnetic Encoder	+++	+++	++	++	$$

Figure 6.3 Position Sensor Different Technologies Comparison

keeping cables short can effectively reduce the risk of noise and electromagnetic interference caused by shock. Traditionally, the cylinder manufacturer places a magnet on the piston head. Then, the robot designer attaches a suitable transducer externally to the robot body using bolts or threads on the end cap. Another possible approach in the industry is to encapsulate the whole thing on the inside of the back end of the cylinder. This approach may be more robust, but we still have two pieces of equipment to install, and the vibration problem is still a concern. It may be transferred to the control level and cause many problems in the control of the actuator system. Another important question to answer concerning the position sensor is the way that it will be interfaced with the microcontroller, where we have many communication protocols like PWM, SSI, CAN, and BiSS. When using SIC actuators in robotics, the speed at which sensor information is transmitted is very important. This speed is essential for developing advanced dynamic controllers that can handle both position and speed. Therefore, it is necessary to identify communication protocols that offer the highest bandwidth. Compared to other Communication protocols, BiSS-C is an Open Source digital interface that caters to sensors and actuators. It seamlessly integrates with the industrial standard SSI (Serial Synchronous Interface). Additionally, BiSS functions synchronously, serially, and cyclically through a pair of unidirectional lines. A notable feature of BiSS is its continuous bidirectional communication capability, denoted by "BiSS C," where the "C" signifies Continuous. BiSS is compatible with the standard Serial Synchronous Interface (SSI), and it can dynamically adjust to transmission times for faster clocking, based on the specific line drivers used. This adaptability allows it to reach speeds of up to 10 MHz with RS422 and 100 MHz with LVDS. The protocol's ability to request processing times makes it suitable for safety-critical applications, complemented by its built-in CRC, error reporting, and warning functionalities [57].

In conclusion, there are three key challenges involved in selecting the optimal position sensor for our SIC design:

1. Determining the most suitable technology to employ (refer to table 6.3).

2. Identifying the ideal method for integrating the sensor with the SIC.
3. Defining the optimal communication interface between the sensor and the microcontroller.

The type of position sensor is another important factor to consider. There are two main types of position sensors: absolute and relative. Absolute encoders provide a unique digital code for each position, which allows for accurate and precise position measurement. They typically have a higher resolution and can provide the absolute position of the actuator at any given time. Relative encoders, on the other hand, measure changes in position relative to a reference point. They provide information about the direction and magnitude of movement from the reference point, but they do not give the absolute position at any given time. Taking into consideration all the aforementioned aspects, we conducted thorough market research to identify a sensor that effectively merges advanced technology with seamless integration into the SIC. Our investigation led us to the LinACE Encoder by RLS, a pioneering integration technology backed by several patents [58]. In the LinACE encoder, the piston shaft of the actuator serves as the information carrier, as shown in Figure 6.4. This provides high integration with the SIC and reduces measurement errors caused by collisions and vibrations. Functioning as sensing technology, the LinACE encoder employs a hall effect array to perceive position changes accurately. For communication protocol interfacing with the microcontroller, it provides many options such as CAN, SSI, PWM, Asynchronous serial, and BISS. Consequently, we opted for the BISS protocol. The encoder's read-head exhibits robustness by withstanding strain, vibrations, and temperatures ranging from -40°C to +85°C. Additionally, it showcases resistance against factors like corrosion, liquids, magnetic fields, dirt, and dust, which makes it perfect for the different working environments of robots [58].

Force Sensor

Force sensing is essential for the safe and efficient operation of humanoid robots and exoskeletons especially for the hydraulic actuated. Force sensors measure the

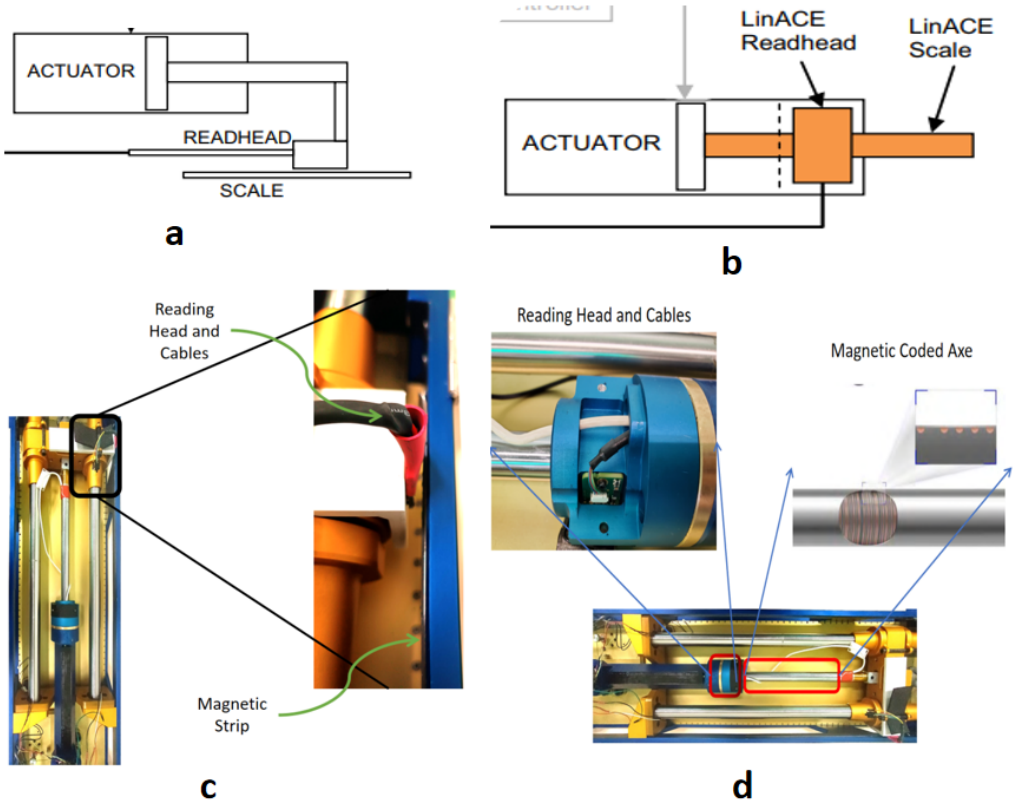

Figure 6.4 Position Sensor Integration : (a) Typical actuator system with linear scale position feedback control.[58],(b) Actuator system with LinACE position feedback control, (c) Typical Integration of the Position Sensor in SIC and Dev-Kit, (d) (b) Integration of Position Sensor on the SIC

force generated by the actuators, which is essential for ensuring that the robots do not apply too much force and damage themselves or their surroundings. This is important for many reasons, such as:

- Safe interaction with humans and objects: Force sensors can help robots avoid collisions and injuries by detecting when they are applying too much force.
- Delicate object manipulation: Force sensors can help robots manipulate objects with care, such as when picking up a fragile object or avoiding dropping it.
- Cooperative activities: Force sensors can help robots work together with humans or other robots, such as when moving a heavy object together [59][60].

While these are the main reasons why force sensing is important globally in robotic devices, the main reason for integrating it into SIC is to create the foundation for developing force control algorithms.

Several types of force sensors are used in humanoid robots and exoskeletons, each with its benefits and adapted applications [61].

- **Load cells** are commonly used in humanoid robots because they are simple and reliable. They work by measuring the deformation or strain caused by an applied force. Load cells can be further categorized into three types: piezoelectric load cells, hydraulic load cells, and pneumatic load cells.
- **Strain gauges** measure the change in resistance when a force is applied to a deformable object. The change in resistance is proportional to the applied force, allowing for accurate force measurement.
- **Six-axis force/moment sensors** (also known as multi-axis force sensors) provide measurements in multiple directions and moments around different axes. These sensors are capable of measuring forces and torques in three orthogonal directions, providing a more comprehensive understanding of the applied force.

- **Optical force sensors** measure the deflection of a beam of light when it is deflected by a force. They are very accurate and can measure very small forces. However, they are also very expensive and can be difficult to use in harsh environments [62].

- **Piezoelectric force sensors** generate an electrical charge when they are deformed by a force. They are very accurate and can measure very small forces. However, they are also very expensive and can be fragile [63].

Strain gauge force sensors are the best choice for force control in humanoid robots and robotic applications due to their high accuracy, sensitivity, compact size, robustness, and cost-effectiveness. Strain gauges offer the advantage of directly measuring strain, which allows them to be highly sensitive to small forces. Additionally, strain gauges can be designed to be small and lightweight, making them suitable for integration into humanoid robots and robotic applications where size and weight are critical considerations. Load cells, which contain strain gauges in a Wheatstone bridge configuration, are another type of force sensor commonly used in robotics. However, load cells tend to be larger and heavier compared to strain gauges, which can limit their integration into compact robotic systems. Furthermore, strain gauge-based force sensors have a wide sensing range, as the measurement range is dependent on the elastic limit range of the flexure elements [64]. This means that strain gauge-based force sensors can accurately measure forces across a wide range, making them suitable for various applications in humanoid robots and robotics, such as force feedback in industrial robots or as tactile sensors in rehabilitation exoskeletons. Another advantage of strain gauge-based force sensors is their versatility in measuring different types of forces. They can measure both normal forces, which are forces applied perpendicular to the surface, as well as shear forces, which are forces applied parallel to the surface. This versatility allows strain gauge-based force sensors to be used in a wide range of robotic applications, such as grasping and manipulation tasks, where both normal and shear forces are involved.

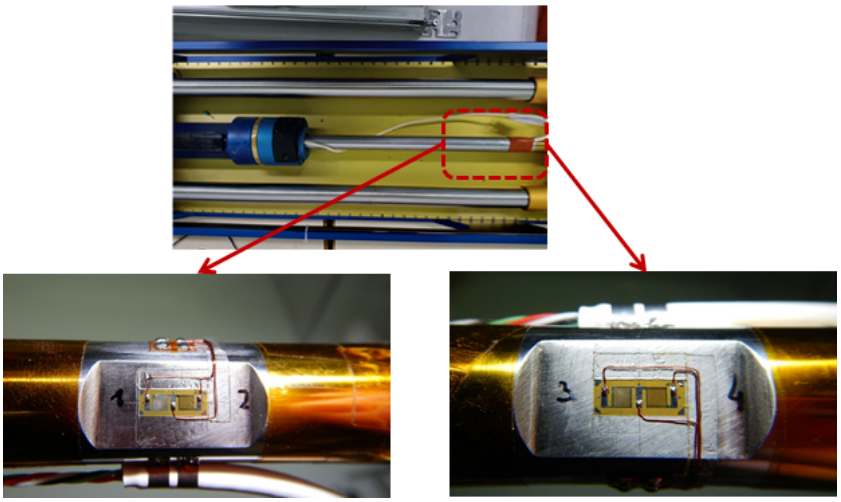

Figure 6.5 Strain Gauge Force Sensor Integration on SIC

Wheatstone bridge

A Wheatstone bridge is a circuit that is used to measure an unknown resistance. It consists of four resistors arranged in a diamond shape. The unknown resistance is connected to one arm of the bridge, and the other three arms are connected to resistors of known resistance. A current is applied to the bridge, and the voltage drop across the unknown resistance is measured.

The three different configurations of the Wheatstone Bridge are:

- Quarter bridge: This configuration has one active strain gauge and three passive resistors. It is the simplest configuration and is used when only one direction of strain is to be measured.
- Half bridge: This configuration has two active strain gauges and two passive resistors. It is more sensitive than the quarter bridge and can be used to measure both directions of strain.
- Full bridge: This configuration has four active strain gauges and no passive resistors. It is the most sensitive configuration and is used for the most accurate measurements.

We will compare the three configurations of the Wheatstone Bridge in terms of their sensitivity, temperature compensation, and complexity.

1. **Sensitivity**: The sensitivity of a Wheatstone bridge is the ability to measure small changes in the unknown resistance. The higher the sensitivity, the smaller the change in the unknown resistance that can be detected. The sensitivity of the quarter bridge is the lowest of the three configurations. This is because the quarter bridge has only one active strain gauge. The half-bridge has two active strain gauges, so it is more sensitive than the quarter bridge. The full bridge has four active strain gauges, so it is the most sensitive configuration.

2. **Temperature Compensation**: Temperature compensation is the ability of a Wheatstone bridge to maintain its accuracy when the temperature changes. The better the temperature compensation, the less the accuracy of the bridge will change when the temperature changes.

   The quarter bridge has the worst temperature compensation of the three configurations. This is because the quarter bridge has three passive resistors, which are susceptible to changes in temperature. The half-bridge has two passive resistors, so it has better temperature compensation than the quarter bridge. The full bridge has no passive resistors, so it has the best temperature compensation.

3. **Complexity**: The complexity of a Wheatstone bridge is the difficulty of constructing and using the bridge. The quarter bridge is the simplest configuration and is the easiest to construct and use. The half-bridge is more complex than the quarter bridge, but it is still relatively easy to construct and use. The full bridge is the most complex configuration and is the most difficult to construct and use.

The full bridge configuration is the most sensitive and has the best temperature compensation. However, it is also the most complex and expensive configuration.

The quarter bridge configuration is the simplest and least expensive configuration, but it is also the least sensitive. The half-bridge configuration is a good compromise between sensitivity and complexity.

Temperature and Pressure Sensor

s Pressure and temperature variations can significantly impact the performance of

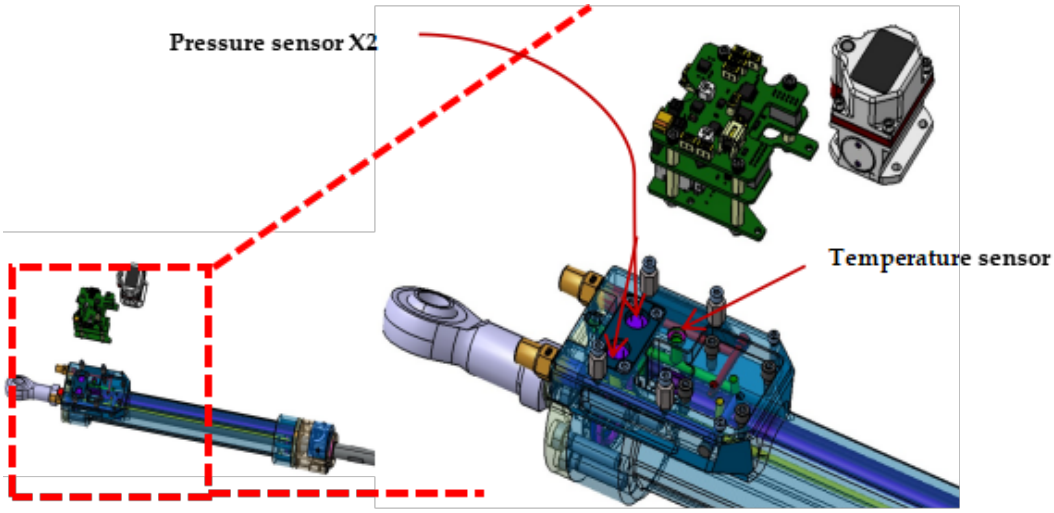

Figure 6.6 The Integration of Temperature and Pressure Sensors in SIC

electro-hydraulic actuators in robotics. Pressure variations can directly affect the force generated by the actuator. Additionally, temperature changes can affect the viscosity of the hydraulic fluid, which can in turn impact the actuator's efficiency and overall performance. To address these challenges, pressure and temperature sensors are crucial in monitoring and regulating the operating conditions of electro-hydraulic actuators. These sensors enable the control system to make real-time adjustments to maintain optimal pressure and temperature levels, ensuring consistent and efficient performance of the actuator. Oh et al [65] reported on the use of Si transistor-based pressure and temperature sensors in a soft robotic hand with multiple sensors and wireless electronic circuits. These sensors were mounted on finger-like soft actuators and allowed real-time monitoring of tactile pressure and

temperature through a mobile phone. The integration of pressure and temperature sensors in electro-hydraulic actuators for robotics offers several benefits. Firstly, it allows for precise control and regulation of the actuator's force output. This ensures that the actuator operates within the desired range, preventing overloading or underperformance. Secondly, it enables early detection of any abnormalities or malfunctions within the actuator system. This is crucial for safety-critical applications such as flight surface actuation in the aerospace industry, where failures can result in catastrophic consequences including loss of lives. Thirdly, pressure and temperature sensors facilitate condition monitoring and predictive maintenance of electro-hydraulic actuators. By continuously monitoring the pressure and temperature levels, any deviations from the normal operating range can be detected. This allows for proactive maintenance and replacement of components before they fail, minimizing downtime and reducing the risk of unexpected failures [66].

6.3 SIC Electronic and Control Board Board

After describing the need for sensors to be integrated into the SIC cylinder we addressed the electronic and control board design challenge with the following constraints: 1- Small and compact size. 2- Real-time firmware Capabilities. 3- Real-time connectivity with other boards and with the Master PC. 4- Sensors conditioning with the best dynamic rate possible.

6.3.1 Sensors Signal conditioning and Power Management

figure 6.7 shows the block diagram with the main feature of the SIC board, while figure 6.9 shows the 3D design of the board.

The board designated as "Board One" in figure 6.8 encompasses essential functionalities, with a primary focus on power management and sensor conditioning to ensure precise measurements and stable operation. Specifically:

1. Power Management: Board One is equipped to handle various voltage supply requirements, catering to the specific needs of different versions of the system. It

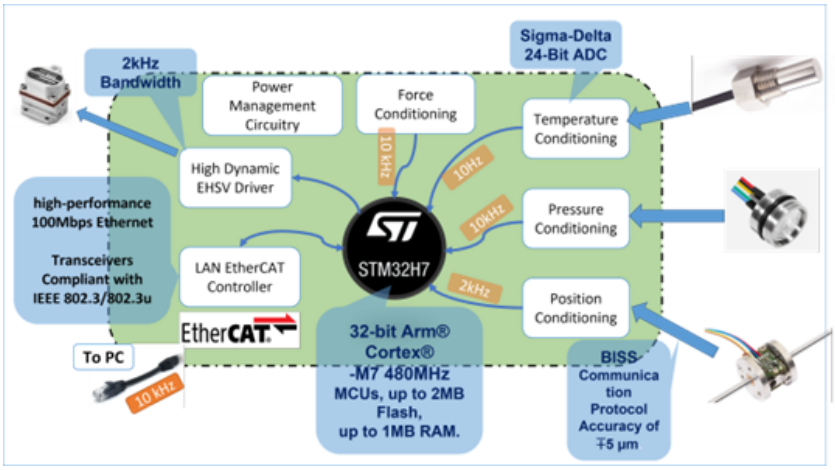

Figure 6.7 Block Diagram of SIC Electronic Board

manages a 24V supply for SICV3 and dual voltage supplies of ±72V and ±12V for SICV4, ensuring consistent and reliable power distribution.

2. Sensor Conditioning: - Pressure Sensor: The board incorporates dedicated circuitry for conditioning the pressure sensor data. We employed Ina188 instrumentation amplifier technology, renowned for its low noise amplification capabilities. This ensures that pressure readings are accurately acquired and maintained within the desired signal-to-noise ratio.

- Force Sensor: Similar attention to detail was given to the conditioning of the force sensor. Leveraging Ina188 instrumentation amplifier technology, we achieve low-noise amplification, facilitating precise and noise-free measurements of applied forces.

- Temperature Sensor: Temperature measurement involves a mixed analog-digital conditioning approach. We utilized a sigma-delta ADC (Analog-to-Digital Converter), a sophisticated technology known for its accuracy and precision in capturing analog signals. This hybrid approach ensures that temperature readings are not only accurate but also effectively digitized for further processing. For more details about the electronic design see appendix B.

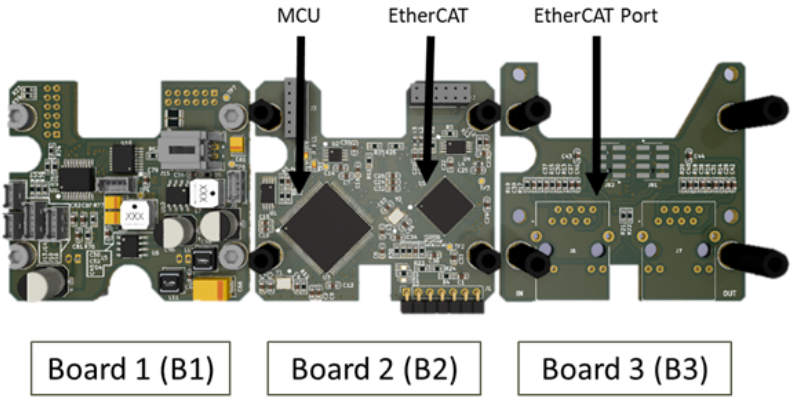

Figure 6.8 SIC Electronic Boards

6.3.2 Slave Communication Interface

In terms of the communication protocol, as outlined by Anas et al and Subhi et al in their work [18], EtherCAT was the chosen protocol. EtherCAT (Ethernet for

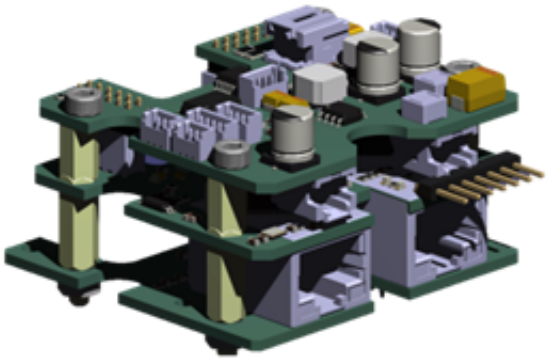

Figure 6.9 SIC Electronic and Control Board Design

Control Automation Technology) is a real-time industrial Ethernet protocol that is used to control and monitor devices in automation systems. It is known for its high speed, low jitter, and flexibility. EtherCAT is a master-slave protocol, with the master device controlling the flow of data on the network. EtherCAT operates at a baud rate of 100 Mbps. However, EtherCAT G, which is a newer version of EtherCAT, operates at a baud rate of 1 Gbps or 10 Gbps.

6.3.3 Embedded Hardware and Firmware Structure

Embedded Hardware

So after optimizing and integrating the sensors in SIC, we need to choose the best-embedded hardware that could be used for developing real-time firmware, has the needed support to interface all the sensors and the drivers, and also can interface with the real-time communication protocol EtherCAT hardware, and also the ability to develop and modify is easy. and here we have two main kinds of technology microcontroller technology and FPGA technology. While both FPGA and microcontrollers possess the capability to handle real-time applications, they exhibit distinctions concerning user-friendliness, implementation, processing speed, and customization potential. A significant divergence between FPGA and microcontrollers lies in their user-friendliness. Generally speaking, microcontrollers are deemed more user-friendly in comparison to FPGAs. Microcontrollers often come equipped with integrated development environments that provide a user-friendly interface for coding and debugging. Conversely, FPGAs demand a deeper comprehension of hardware design and programming languages like VHDL or Verilog. These languages enable the modeling and simulation of intricate systems but may prove more challenging to acquire and master, especially for novices. Additionally, the implementation process differs for FPGA and microcontrollers. Microcontrollers are typically executed using a single chip that combines the CPU, memory, I/O peripherals, and other essential components, rendering them a more compact and straightforward solution for real-time applications. In contrast, FPGAs offer a heightened level of customization. They comprise programmable logic blocks interconnected via electrically programmable switches, enabling the creation and execution of exceedingly tailored and hardware-specific systems.[67][68] So, opting for microcontroller ARM architecture technology appears to be the favorable choice for our specific application. This decision is grounded in several key advantages. Firstly, microcontrollers based on ARM architecture offer a high degree of development potential. Their user-friendly integrated development environments and widespread support make them accessible to a wide range of

developers. Secondly, microcontrollers are generally less complex than FPGAs, making them more manageable and easier to work with, especially for real-time applications. This simplicity can streamline the development process and reduce the learning curve. Furthermore, microcontrollers based on ARM architecture are well-suited for running real-time operating systems (RTOS), providing the necessary real-time capabilities for our application. They can efficiently manage tasks and processes while ensuring the required responsiveness. Lastly, microcontrollers often come equipped with a variety of interfaces, including those essential for sensor integration. This inherent compatibility simplifies the integration of sensors and reduces the need for additional components or complex circuitry [69][70]. So for all SEHA electronic and control boards(SIC, MGH, and Linear motors), we choose the STM32H7 microcontroller from ST-Electronics and we could achieve 480MHz as a main clock for the CPU inside the microcontroller which is higher than many FPGA boards.

Super-Loop or FREE RTOS

The hardware and software components of the SEHA actuator are equally important, as even a small delay in sensor readings or control algorithms could significantly impact safety and performance. For the firmware architecture, we have two main structures for coding, the Super-loop structure *SL* and the Real Time Operating System structure ***RTOS*** [71]. **Superloop firmware** is a simple approach to organizing firmware in embedded systems. It consists of a continuous loop that iterates endlessly, executing various tasks or functions in a predefined order. Superloop firmware is easy to implement and typically used in less complex embedded systems. However, it has limited ability to handle complex multitasking scenarios and can have issues with deterministic timing and responsiveness in real-time applications [72][71].

RTOS-based firmware is a more sophisticated approach to managing tasks and resources in embedded systems. It uses a real-time operating system (RTOS) to provide a robust multitasking environment, deterministic task scheduling, and

efficient hardware resource management. RTOS-based firmware is suitable for complex embedded systems with stringent real-time requirements, such as robotics and safety-critical systems [73][74]. after comparing the two firmware structures as

Characteristic	**Superloop firmware**	**RTOS-based firmware**
Complexity	Simple	More complex
Real-time capabilities	Limited	Excellent
Latency	High	Low
Jitter	High	Low
Multitasking	Limited	Robust
Deterministic timing	Can be an issue	Guaranteed
Hardware resource management	Basic	Efficient

Table 6.1 Comparison of Superloop and RTOS-based Firmware

shown in table 6.1 we found that opting for the RTOS structure was the optimized choice for the SEHA application since the RTOS firmware helps the control developers develop minimum latency algorithms and lets us deal efficiently with the EtherCAT real-time communication protocol. For the RTOS firmware, we have three main firmware available in the market: SafeRTOS, OpenRTOS, and FreeRTOS. We compare these three in table 6.2 and conclude that FreeRTOS would be a good choice for SEHA firmware even though it is not dedicated to safety applications, but it is open-source firmware, which makes it possible to modify for adapting the safety standards such as ISO 26262 for automotive systems and IEC 61508 for industrial applications [75].

Operating System	**Safety Focus**	**Licensing**	**Community Support**
SafeRTOS	High	Commercial	Limited
OpenRTOS	Moderate	Commercial	FreeRTOS Community
FreeRTOS	Moderate	Open Source	Large and Active

Table 6.2 Comparison of SafeRTOS, OpenRTOS, and FreeRTOS

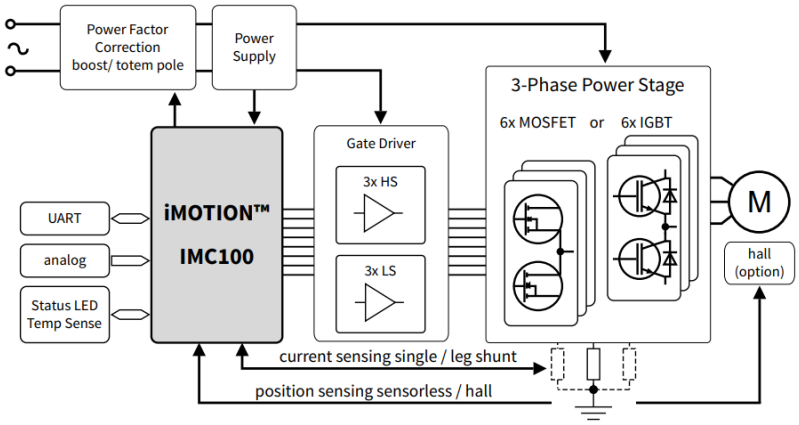

Figure 6.10 BLDC Motor Driver Structure

6.4 MGH Electronics and Control Layer

As demonstrated in the preceding simulation chapter, the driver for the BLDC (Brushless Direct Current) motor comprises two primary components 6.10: the power stage and the controller side. Here's a breakdown of our choices for each of these crucial elements:

1. Power Stage: - IKCM10H60GA Dual In-Line Intelligent Power Module*: Our selection for the power stage centers around the IKCM10H60GA, a Dual In-Line Intelligent Power Module. This module is designed to handle the demanding requirements of our BLDC motor system, offering a 3-phase bridge configuration with a voltage rating of 600V and a current capacity of 10A. Its robust design ensures efficient power delivery and control, making it an ideal choice for driving the motor.

2. Controller Side: - IMC101T - Motion Control Engine (MCE): To govern the operation of our BLDC motor system, we've opted for the IMC101T, a Motion Control Engine (MCE). This component serves as a ready-to-use control solution for variable speed drives, providing a range of essential features: - Integrated Script Engine: Enables customization of application control, allowing for adaptability to specific operational needs. - Integrated Drive and System Protection Features: Ensures the safety and protection of both the drive and the overall system, mit-

igating potential risks. - Field-Oriented Control (FOC): Supports precise control of permanent magnet synchronous motors (PMSM), optimizing efficiency and performance. - Flexible Space Vector PWM: Offers sinusoidal voltage control through space vector pulse-width modulation, facilitating smooth and precise motor control. - Current Sensing Options: Provides the capability for current sensing via single or leg shunt, enhancing control accuracy and enabling effective feedback mechanisms.

By combining the robust power stage with the versatile IMC101T controller, we have established a comprehensive and efficient BLDC motor driver system capable of meeting the demanding requirements of our application. This strategic pairing ensures precise control, high performance, and reliable operation of the BLDC motor within our system.

For more details about the electronic design, see appendix B.

6.5 Linear Electric Motors

SEHA design requires the integration of two linear electric motors: one for the safety unit and the other to control the swatch plate's angle. As discussed earlier, we have opted for voice coil motor technology to control the swatch plate, which directly impacts SEHA's linear speed. We performed open-loop simulations for the voice coil motor in previous chapters, as demonstrated in the simulation section. Now, we will delve into the electronic and control design aspects of the associated electronic boards.

To establish a robust control system for the voice coil motor, our goal is to design electronics capable of supporting both current and position control. For this purpose, we have employed the DRV8874 as shown in figure6.11, an N-channel H-bridge controller. This versatile motor driver serves a variety of purposes, including driving one bidirectional brushed DC motor, two unidirectional brushed DC motors, as well as other resistive and inductive loads. It operates within a broad supply voltage range of 4.5-V to 37-V.

The DRV8874 offers distinct advantages, such as pin-to-pin RDS(on) variants (specifically, the DRV8874 with a 200-m rating for both the high-side and low-side, and the DRV8876 with a 700-m rating for both). It exhibits a high output current capacity, with the DRV8874 providing a 6-A peak and the DRV8876 a 3.5-A peak. Moreover, it features integrated current sensing and regulation, with proportional current output (IPROPI) and selectable current regulation modes (IMODE), which can be either cycle-by-cycle or fixed off time. The DRV8874 also supports selectable input control modes (PMODE), which include PH/EN and PWM H-bridge control modes, as well as an independent half-bridge control mode. .

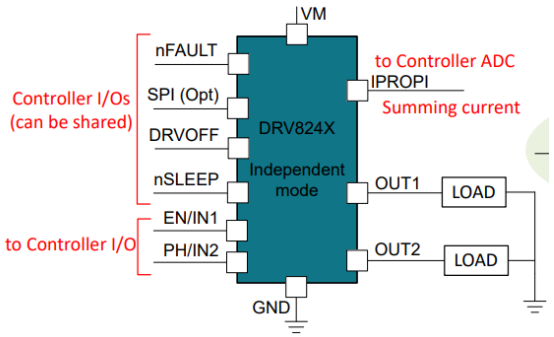

Figure 6.11 Voice Coil Motor Electronic Driver Topolgy

For more details about the electronic design see appendix B

6.6 Conclusion

In conclusion, we have provided a comprehensive overview of the electronics and control layers for SEHA, which have been segmented into three essential modules: SIC, MGH, and Linear Motor. Throughout our discussion, we delved into the sensor envelope, its condition, and the associated interface electronics. We also introduced technologies crucial for establishing a robust control algorithm.

Furthermore, our exploration encompassed the embedded hardware requirements, with the determination that ARM CortexM microcontrollers are optimal

for SEHA's specific applications. We also conducted an in-depth examination of the firmware architecture, drawing comparisons between RTOS firmware and SuperLoop firmware while also assessing various RTOS variations such as FreeRTOS and SafeRTOS.

Additionally, during our discussions, we considered the driver topology for the BLDC motor driver for MGH, and we detailed the topology for the voice coil motor. In the upcoming chapter, we will introduce a novel dynamic driver topology for SIC, further enhancing the control and functionality of SEHA.

Chapter 7

SIC Dynamic Driver

Contents

7.1 Introduction

As we previously mentioned throughout our development of the SIC we used the electro-hydraulic servo valve EHSV to control the flow in the cylinder, in this chapter we propose a high dynamic driver topology to enhance the EHSV performance.

7.2 Electro-Hydraulic Servo-Valve

The servo valve is the key concept that links hydraulics and mechanics on one side and electric and control on the other. Different hydraulic valves are available, like proportional valves, piezo servo valves, pipe-jet, and flapper-nozzle valves.

Proportional valves are more affordable than servo-valves [76]. Some hydraulically actuated robot has used proportional valves, like the lower limb exoskeleton from Virginia Tech [77] and the earlier version of the HyQ robot [78]. Those examples didn't show high dynamic performance due to the limited bandwidth of the proportional valve, which doesn't exceed some tens of Hz [79]. Flapper-nozzle servo-valves and pipe-jet servo-valves are two similar types of valves. They provide fast response and high accuracy in a small size[80]. Both of them are two-stage servo-valves. The first stage is an electrical torque motor. The Piezoelectric valves are direct one-stage valves. It uses Piezoelectric actuators PEAs instead of the torque motor in the flapper-nozzle and pipe-jet servo-valves [76]. The PEAs use the inverse effect of the piezo material: it deforms mechanically when applying excitation voltage to it. The material reacts very quickly, which allows obtaining a very high bandwidth for the servo-valve to achieve the range of 1 kHz [81]. The deformation of the piezoelectric material is relatively small (some micrometers). Therefore, most PEAs adopt complex mechanical amplification to increase the stroke. As a result, the piezoelectric servo-valves need special electronic drivers, and the size of such drivers is quite extensive[81].

7.3 The Rule of the valve in any hydraulic system

The main rule of valves in a hydraulic actuator is to control the flow of hydraulic fluid. Valves play a crucial role in regulating the direction, pressure, and fluid flow rate within the actuator system. They ensure that the hydraulic fluid is directed to the appropriate areas, such as the piston or cylinder, to generate the desired mechanical force and motion. By opening, closing, or adjusting their positions, valves can enable precise control over the actuator's operation, allowing for smooth and accurate movements. Additionally, valves can provide safety features such as pressure relief, preventing damage to the actuator and system components by releasing excess pressure. Overall, valves are vital components in hydraulic actuators, enabling efficient and reliable performance in various applications.

7.4 DYNAMIC MODEL OF MOOG30 SERIES SERVO-VALVE

7.4.1 Principle of Electro-Hydraulic Servo Valve (EHSV)

An electro-hydraulic servo valve is a type of valve used in hydraulic control systems to regulate the flow and pressure of the fluid. There are many servo-valves, but the most common and efficient type is the flapper nozzle servo-valve; the valve uses a flapper and nozzle mechanism, along with a feedback spring, to control the flow of hydraulic fluid and maintain the desired position or velocity of the actuator [81]. Another critical component of the servo valve is the torque motor coupled with the flapper, which causes it to move and change the flow in the nozzle. The workflow of the servo valve is as follows: 1-Electrical input: The electric input of the servo valve is the current flow through the torque motor‘s coils. The current will activate the coils generating a magnetic field. This field acts on a magnetic armature connected to the pivoting arm, causing it to move in a specific direction. 2- Flapper and nozzle mechanism: The nozzle is a small opening through which the fluid flows, and the flapper is a thin, flexible piece of metal attached to a pivoting

arm. The current signal controls the position of a flapper within the servo valve. The position of the flapper determines the size of the opening between the nozzles and, therefore, the flow of hydraulic fluid through the valve(internal flow). 3-Main Spool Movement: The valve has a housing with an inlet and outlet port for hydraulic fluid and a spool mounted inside the housing. This spool has several lands (also called spool positions) that can block or allow fluid flow through the valve (from inlet to outlet and vice versa), depending on its position. The flow from the previous stage(flapper-nozzle) will generate a differential pressure on the main spool and make it move.

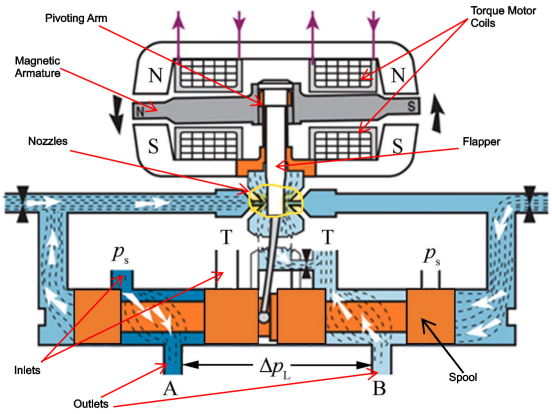

Figure 7.1 EHSV Working Principle

4-Feedback spring: The hydraulic fluid flows through the valve and is directed to the actuator. At the same time, the position of the flapper is also controlled by a feedback spring. The feedback spring provides a force that opposes the force of the electrical input signal and helps to hold the flapper in position. This allows the spool to be precisely positioned and held in place by balancing forces between the electrical signal and the spring. The feedback spring is typically calibrated to provide a specific level of resistance to the movement of the spool. The calibration of the spring is critical for the performance of the servo valve, as it determines the sensitivity and stability of the valve's response to the electrical input signal. 5-Actuator control: The position of the flapper and the size of the opening between the nozzles determine the flow of hydraulic fluid to the actuator, which then moves

to the desired position or velocity. As the actuator moves, it sends a feedback signal back to the control system, which can be used to adjust the electrical input signal and maintain the desired position or velocity. The typical operational parts of the studied servo-valve and the principle of operation are shown in Figure 7.1 [81]. In conclusion, the EHSV consists mainly of two stages; the first stage is a torque motor with a flapper nozzle, and the second stage is a standard four-spool valve [82].

7.4.2 Dynamic model Problem

Despite the simplicity of its working principle (as explained above), the servo valve is considered as a very complex system when we are trying to derive a control model because three domains of science are concerned with this system Mechanics, Hydraulics, and Electrics Many works have been done to have a good model representing the servo valve [83], [84]. Although much work is done for EHSV modeling, they all start with the electric current as input for such a system, as shown in Figure 7.3 [85], which supposes the ideal behavior of the torque motor and ignores the current dynamics caused by the high values of the motor inductance and resistor.

To better explain this problem, let's consider the simplified servo-valve block diagram shown in Figure 7.4 [86], if we keep the torque motor as just a gain, we can write.

$$G_{AF}(p) = \frac{(1/K_f)}{1 + (\frac{2\xi}{\omega_n})p + (\frac{p}{\omega_n})^2} \tag{7.1}$$

$$G_{sp}(p) = \frac{1}{A \cdot p} \tag{7.2}$$

$$\begin{aligned} &(K_1 i - K_w \tfrac{Q}{K_3}) G_{AF}(p).K_2.G_{sp}(p) = \tfrac{Q}{K_3} \\ &\Rightarrow (K_3 K_1 i - K_w Q) G_{AF}(p).K_2.G_{sp}(p) = Q \\ &\Rightarrow \quad \frac{Q}{i} = \frac{K_2.K_3.K_1.G_{sp}(p).G_{AF}(p)}{1 + K_w.K_2.G_{sp}(p).G_{AF}(p)} \end{aligned}$$

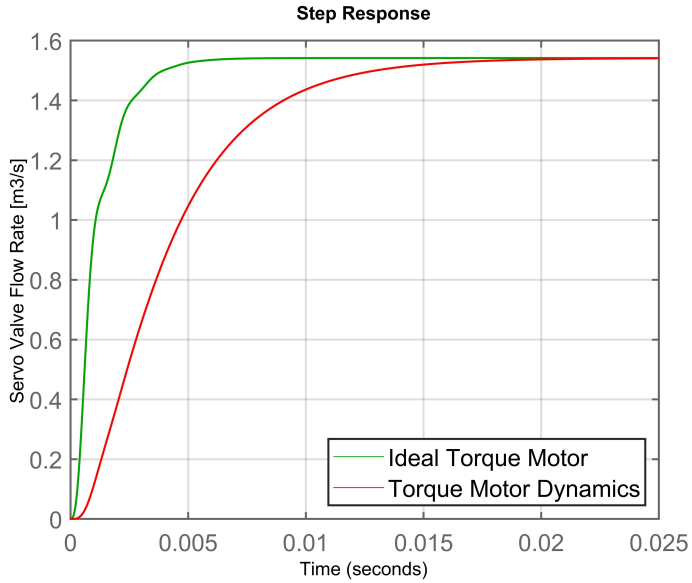

Figure 7.2 Servo Valve Step Response (Green: Ideal Torque Motor, Red: Current Dynamic of the Torque motor is considered)

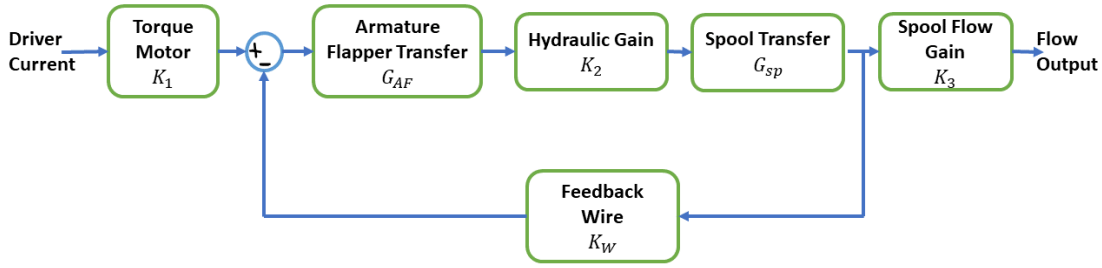

Figure 7.3 Servo Valve Dynamic Model Block Diagram

Considering the control block diagram Figure 7.3 and the equations 7.1 and 7.2, we can express the current (in mA) to flow ((in $m^3/\sec$)) transfer function as in equation (3).

$$\frac{Q_v}{i} = \frac{\alpha}{\frac{A}{\omega_n^2}s^3 + \frac{2A\xi}{\omega_n}s^2 + As + \beta} \tag{7.3}$$

$$where \left\{ \alpha = \frac{K_1 K_2 K_3}{K_f} \quad , \quad \beta = \frac{K_W . K_2}{K_f} \right\}$$

Now, if we consider the current dynamic of the torque motor and add it to the

control block diagram, as shown in Figure 7.4, we can obtain the following transfer function.

$$\frac{Q_v(s)}{I(s)} = \frac{\alpha}{\frac{A}{\omega_n^2}s^3 + \frac{2A\xi}{\omega_n}s^2 + As + \beta} \frac{a_i}{1 + b_i s} \tag{7.4}$$

where $a_i = \frac{1}{R}$ and $b_i = \frac{L}{R}$.

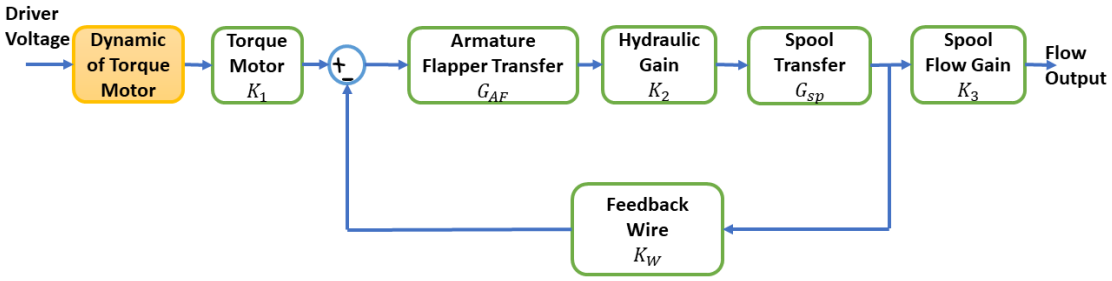

Figure 7.4 Servo Valve Model considering the electric current Dynamic

Simulating the two transfer functions equations 7.4 and 7.3 with the same step input, we get the result shown in Figure 7.2 We notice the high impact the dynamics of the torque motor on the servo-valve dynamic behavior, where the settling time in the ideal torque motor case (the green curve) and for the case where the torque motor dynamic is considered (the red curve) $T_{Torque_s} = 10.8ms$ which is three times greater than the ideal case.

7.5 Proposed solution

Considering the high impact of the current dynamics of the torque motor on the total EHSV system settling time which directly affects the dynamics of the robot's movement, we propose a new dynamic driver topology to overcome this problem and enhance the current dynamics of the torque motor, hence improving the total EHSV system's dynamics.

7.5.1 Proposed high dynamic driver

Figure. 7.5 shows the schematic of our proposed high dynamic driver, with $V_{DD} = 72V$ and $V_{SS} = -72V$.

Linear analysis of the driver

Analyzing the driver circuit linearly, supposing that $R \ll R_f$, we find that the output of the driver can be described by equation 7.5.

$$u = K_i \int (i_{ref} - i)dt + K_p(i_{ref} - i) \tag{7.5}$$

where $K_p = R_s$, $K_i = \frac{R_s}{R_f C_f}$ and $i_{ref} = \frac{v_c}{R_s}$.

Applying Laplace transform to equation 7.5 we got the equation 7.6

$$U(s) = \left(K_p + \frac{K_i}{s}\right) E(s) \tag{7.6}$$

where $E(s) = I_{ref}(s) - I(s)$ is the Laplace transform of the error.

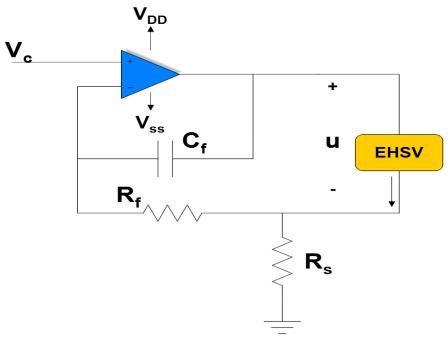

Figure 7.5 High Dynamic Driver Proposed Schematic

Nonlinear analysis of the Driver

Saturation effects occur when any part of a feedback control system reaches a physical limit. This is exactly what happens with an operational amplifier where

the output voltage is limited to a value near the supply voltage. Since our current driver is established using the operational amplifier, then we have the saturation effect, which could be expressed as:

$$V_0 = \begin{cases} +V_{sat} & if \quad V_{in^+} > V_{in^-} \\ -V_{sat} & if \quad V_{in^+} < V_{in^-} \end{cases} \tag{7.7}$$

The saturation effect of our driver will appear in the transient state where the speed change in the current is needed, as we will see in the simulation.

7.6 Simulation results

7.6.1 Current Control Loop – Inner Loop

To validate the dynamic behavior of the proposed driver topology, we build a hydraulic cylinder system with mechanical load and with the proposed servo-valve model in Simscape toolbox (Simhydraulics, Simmechanics) / MATLAB Simulink (Figure. 7.6).

The driver circuit is itself built using the Matlab SimElectrical toolbox and limited bandwidth OP-AMP with ±72 Volt as rail supply Figure 7.7. As shown in (Figure. 7.8), the driver output is the OP-AMP voltage saturation $V_{DD} = 72V$ for the transient phase where the error between the desired current value and actual current is very high, but when the actual current gets close to the desired value we see the linear behavior of the driver.

7.6.2 Double Control Loop – Flow (Outer) and Current (Inner)

To verify the enhancement impact of our driver on the flow control loop, we simulate the flow control loop using a PID controller, as shown in Fig. 7.9.

Our main objective here is to examine the servo-valve flow-settling time, so we did not optimize the PID parameter to obtain the fastest possible response,

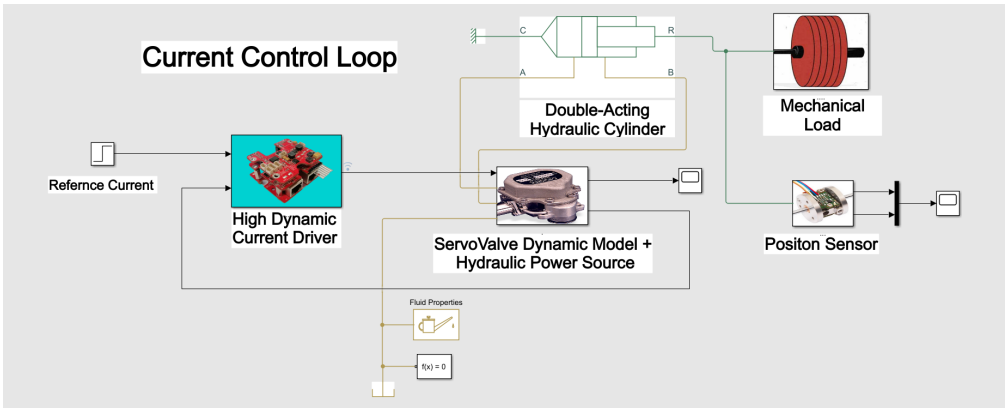

Figure 7.6 Simscape simulation for the Hydraulic System, Servovalve, and Driver

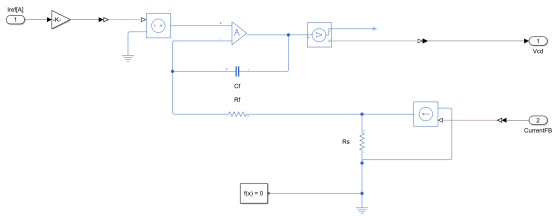

Figure 7.7 Driver Circuit in SimElectrical

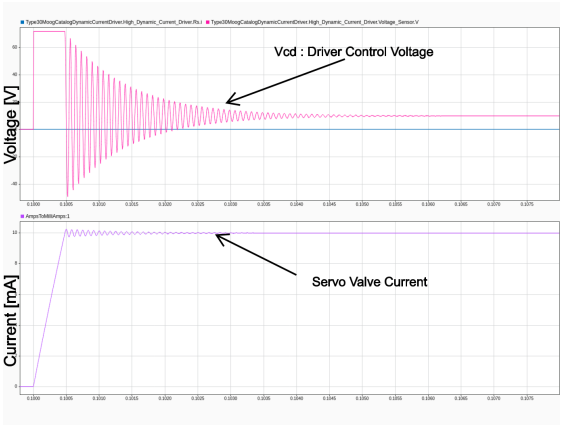

Figure 7.8 Current Dynamic (Down-Orange) and Driver Output Voltage (Up- Blue)

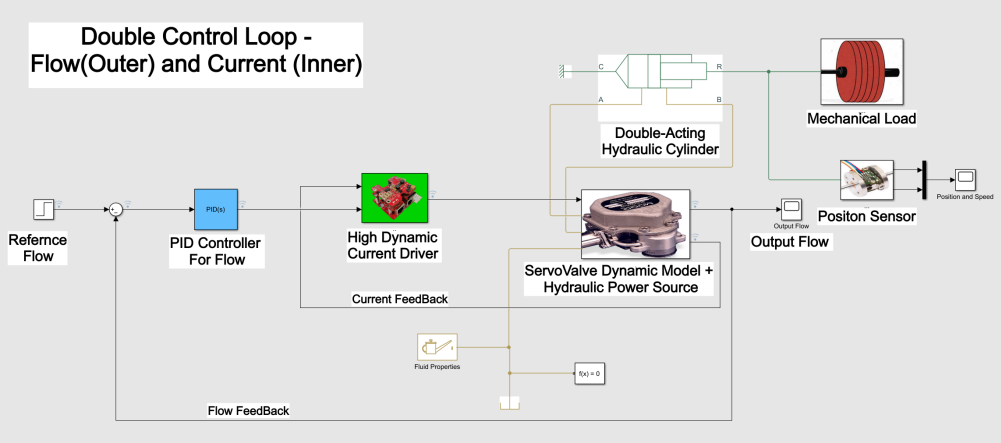

Figure 7.9 Flow Control Loop (Outer) and Current Control Loop (Inner) in Simulink

but we tuned the PID parameter to have acceptable performance in order just to compare the two cases:

1. The settling time of the flow response using the proposed high dynamic high voltage driver.

2. The settling time of the flow response using a low voltage driver.

Fig. 7.10 shows the flow step response of the servo-valve with a step value corresponding to the nominal flow for the Moog30 servo-valve $0.2 \times 10^{-3} m^3/s$, using the proposed high voltage driver, we observe that the settling time is $3.3ms$.

For the sake of better comparison, we placed the flow step response with the same condition just after in Fig. 7.11, where we can observe a $6ms$ of settling time, which means that the high voltage driver enhances the flow control loop speed by 181%.

To illustrate the high impact of the current driver we plotted the reference current (demanded by the PID controller) and the actual servo-valve current to examine the tracking in the current control loop. (Figure 7.12 and 7.13).

We can notice the poor tracking in the case of a low-voltage current driver.

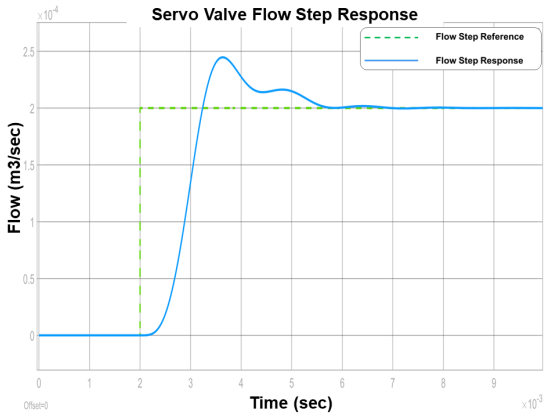

Figure 7.10 Flow Step Response with High Dynamic Current Driver(181 % speed enhancement)

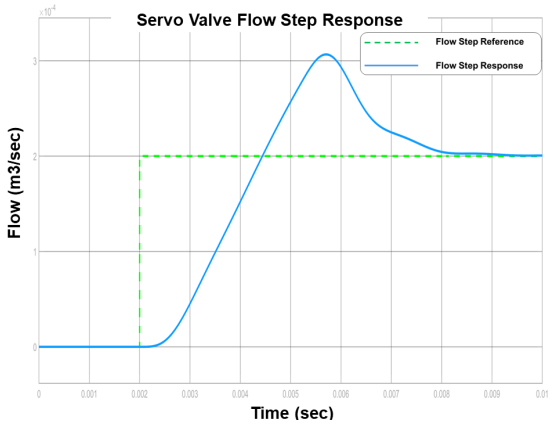

Figure 7.11 Servo-valve Flow Step Response with High Dynamic Current

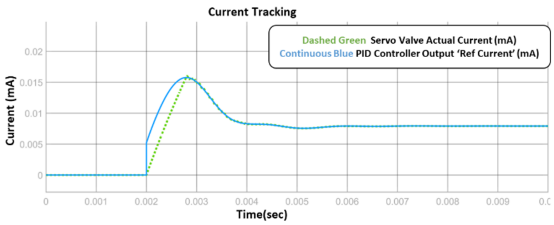

Figure 7.12 Dynamic Driver Current Tracking

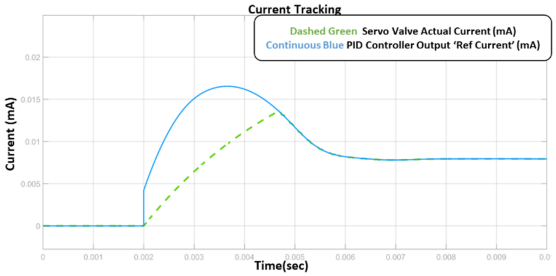

Figure 7.13 Low Voltage Driver Current Tracking

7.7 Conclusion

We discuss in this chapter the development of a driver that enhances the dynamics of the servo-valve system by making the current control faster and even permits controller designers to use whatever model (**??**)-(7.5) because using such driver topology makes the knowledge of the current dynamics unnecessary.

Using the proposed driver in EHSV control system makes the current control loop fifty times faster than the flow outer loop. Moreover, since the servo-valve does not need a high driving current (in the milliamps range), there is no need to use the H-bridge Topology, and the high supply OP-AMPS is a very convenient approach for the driver design. And we will show the practical results that we got in the conclusion chapter.

Chapter 8

Experimental Results

Contents

8.1 Introduction

As we mentioned in the previous chapters of this thesis, our main objective is to contribute to the actuation system for humanoid and assistive devices. In pursuit of

this goal, we chose the Servo-Electro-Hydraulic Actuator SEHA as the cornerstone of our work, aiming to create an actuation system that ensures safety and offers high dynamics and adaptability. For the development of SEHA, we adopted a modular design approach, creating three core products: the Servo Instrumented Cylinder (SIC), the Main Hydraulic Group (MGH), and Linear Motors. These components are designed to synergize and form the foundation of SEHA, offering a versatile and robust solution for actuation needs.

In this chapter, we will discuss the practical results we have obtained through our extensive research and development efforts. We will present the outcomes of our work, highlighting the key performance indicators and metrics achieved by our actuation system components. Furthermore, we will candidly discuss the challenges and obstacles we encountered during this journey, providing insights into the practical constraints that we had to overcome.

With a comprehensive overview of our results and challenges, we will conclude this chapter by offering a glimpse into the future. We will explore the potential applications, advancements, and adaptations that can be made based on our findings. The perspective section will provide a roadmap for the further evolution of our actuation system, and we will identify areas for future work, inviting further research and development to advance the field of humanoid and assistive device actuation.

8.2 SIC Electronics and Control Boards

8.2.1 Development Strategy

To achieve the SEHA product, we are using the modular design discussed in previous chapters and the V-Model (The V-Model, also known as the Validation and Verification Model)[87] [88] shown in Figure 8.1. This model shows that SEHA is currently in the **Unit Test** phase, progressing through the validation phases. Simultaneously, we are moving forward with the SIC Board to **System Test**. Additionally, we are in the **Manufacturing Process** phase for MGH and conducting

unit tests for the voice coil motor.

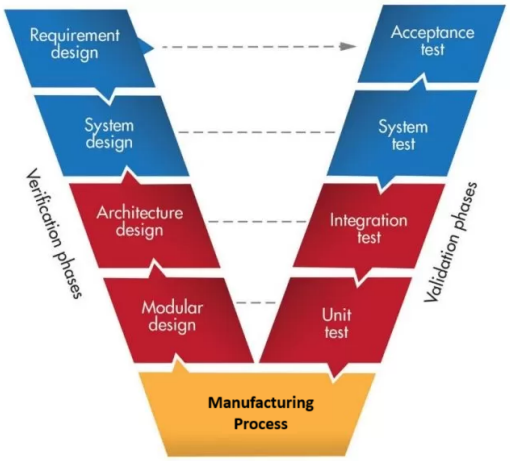

Figure 8.1 V-Model: the Validation and Verification Model

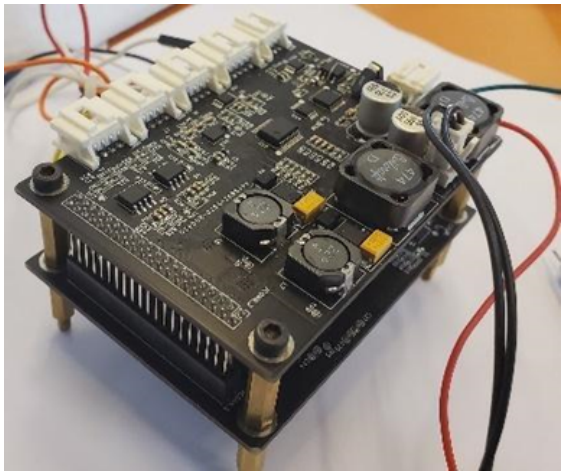

Figure 8.2 SICV1

8.2.2 SIC V1

SIC V1 (shown in figure 8.2) was the first version of the SIC Electronic and Control board. In this initial iteration, we primarily focused on functionality rather than on size constraints. However, this version encountered two significant issues:

Firstly, it suffered from the instability of real-time EtherCAT communication. This problem arose because we generated the required clock signal for the EtherCAT module using the microcontroller. As a result, the synchronization and reliability of real-time communication were compromised.

The second major problem we encountered with SIC V1 was related to the low dynamic current control of the electro-hydraulic servo valve. This issue will be further elaborated on in the subsequent sections.

Furthermore, a third issue stemmed from using a quarter bridge in the strain gauge conditioning circuit. This choice presented limitations and challenges in terms of sensor linearity and temperature compensating, which also needed to be addressed in subsequent versions of the board. Table 8.3 summarizes the test results obtained using the testing procedure outlined in A. The data reveals that the board successfully passed the test, achieving a 63% success rate, despite the challenges discussed earlier.

8.2.3 SIC V3

For the next iteration, SIC V2, our primary objective was to address the strain gauge conditioning problem that had persisted in the previous version. We initiated the design process with a strong emphasis on rectifying this issue. However, due to unforeseen administrative complications, SIC V2 was ultimately canceled. In response to the pressing need for improvements in both strain gauge conditioning and communication stability, we grouped and launched SIC V3. This version was specifically engineered to tackle the communication instability problem while also optimizing the size of the board. Moreover, we made the critical decision to implement a full Wheatstone bridge conditioning circuit for the strain gauge force sensor. These strategic changes allowed us to significantly enhance the overall performance and functionality of the SIC V3 version (figure 8.5, marking a substantial leap forward in our electronic and control board development.

After thoroughly testing SICV3, we embarked on an initiative to streamline and industrialize the manufacturing process. This effort was directed towards the

	N°	Description	Status	Comments	Actions to do
	1-1	Short Circuit Protection	Inconclu	Shifted because destructive	UEVE: Fabricate V3 replica. 1 sep.
	1-2	Static Error	Passed	Tolerated within err. +-0.13 mA	
	1-3	Settling time	failed	2.5 ms instead of 0.5 ms	DFM: V4 using 72V. Date: fin Oct
	1-4	Current Overshot	Passed	Changing PID didn't affect	
	1-5	Electric freq. analysis	failed	500 Hz instead of 2kHz	DFM: V4 using 72V. Date: fin Oct
	1-6	Mechanic freq. analysis	failed	Up to 100 Hz instead of 200 Hz	DFM: V4 using 72V. Date: fin Oct
	2-1	PWR consum. & temp.	Passed	Consumption 2.4 Watts	
	2-2	Internal power supply	Passed	Checked different env. cond (1)	
	2-3	Overvoltage protection	Passed	Tested between 12V and 30V	
	2-4	Reverse Supp. protection	failed	Card is not protected	DFM: V4 using diodes: fin Oct
	3-1	Cycle time test	Passed	Validated at 100us	
	4-1	Prss. Accuracy Test	Passed	Tolerated within err. 0.55%FS	
	4-2	Prss. Resolution Test	Passed	Sensitive	
	5-1	Tmp. Accuracy Test	Passed	Validated at 0.1 °C	
	5-2	Tmp. Resolution Test	Passed	Sensitive	
	6-1	Posi. Accuracy Test	Passed	Validated at 25 um	
	6-2	Posi. Resolution Test	Passed	Sensitive 25 um	
	7-1	Force Accuracy Test	Inconclu	No output signals	UEVE: send force sensor and V3 card to DFM DFM: Prepare test environment. Test the sensor with different conditioning circuits.
	7-2	Force Resolution Test	Inconclu	No output signals	
			63 %		

Figure 8.3 Test Summary of SIC V1

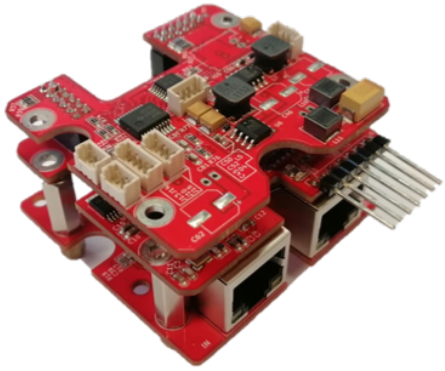

Figure 8.4 SIC V3 Prime

same SIC V3 design, creating a new iteration known as SIC V3 Prime, as depicted in Figure 8.4. During this transition, it became evident that a key challenge we encountered was the frequent stock-outs in electronic component markets. The

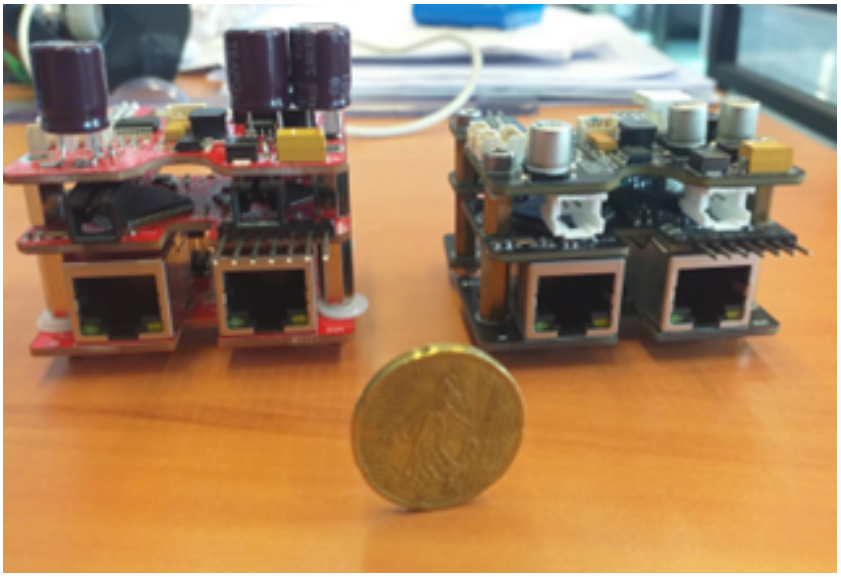

Figure 8.5 SIC Electronic Board V3 (**Right**) and V3Prime (**Left**)

primary accomplishment realized through SICV3 and SICV3 Prime was successfully stabilizing communication between the SIC Board and the PC via EtherCAT. However, further optimization for the servo-valve remained necessary, which prompted us to embark on the development of SICV4.

8.2.4 SIC V4

SIC V4, depicted in Figure 8.6, stands out as the most robust version to date, with an impressive 80% test performance score (see Table 8.8). This version incorporates a highly dynamic driver for the servo-valve, signifying a significant improvement. Nonetheless, it is worth noting that we still encounter certain accuracy issues related to the force sensor, which we plan to address in future developments.

To conclude, the sensor accuracy achieved with SICV4 are listed in Table 8.1.

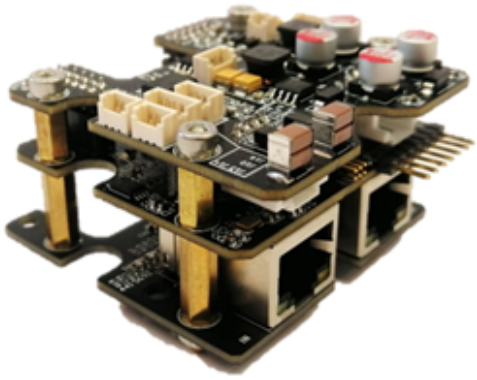

Figure 8.6 SIC V4

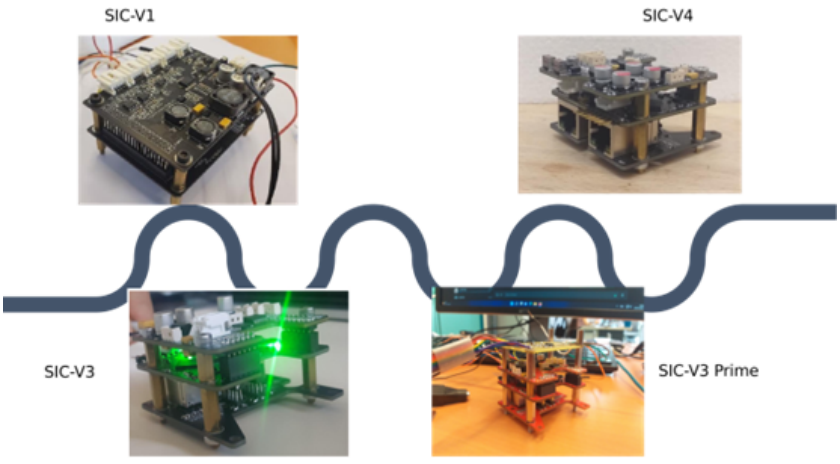

Figure 8.7 SIC Board Development Iterations

	N°	Description	Status	Comments	Actions to do
	1-1	Short Circuit Protection	Passed		
	1-2	Static Error	Passed		
	1-3	Settling time	Passed		
	1-4	Current Overshot	Partially passed	Overshoot less than 10% for a signal step +-100%FS it increases for smaller steps it is 35% for a step +-10%FS	No action to do
	1-5	Electric freq. analysis	Inconclusive	The internal control mode #6 is not fully implemented External sinewave can be used for test purpose.	Using TwinCAT, an External sinewave will be sent. (Subhl, before 16/12)
	1-6	Mechanic freq. analysis	Inconclusive	Dynamic of the mechanical system is ~40 Hz	Long term development
	2-1	PWR consum. & temp.	Partially passed	Temperature of the board achieved 71°C at the normal conditions in the lab.	To be considered during Aging-Test (may need fan)
	2-2	Internal power supply	Passed		
	2-3	Reverse Supp. protection	Passed		
	3-1	Frame test	Passed		
	3-2	Cycle time test	Passed	Passed with 100 us	
	4-1	Prss. Accuracy Test	Passed	+- 2 bar (+-1%FS)	
	4-2	Prss. Resolution Test	Passed		
	5-1	Tmp. Accuracy Test	Passed	Passed within 2°C	
	5-2	Tmp. Resolution Test	Passed		
	6-1	Posi. Accuracy Test	Passed		
	6-2	Posi. Resolution Test	Passed		
	7-1	Force Accuracy Test	failed	Accuracy ~160 N	Plan to be defined in the meeting of Monday 28th Nov
	7-2	Force Resolution Test	failed		
	8-1	Firmware Test	Passed		
			80 %		

Figure 8.8 Test Summary of SIC V4

No	Sensor Types	Measurement Range	Sensor Accuracy	Bandwidth frequency
1	Force sensor	-8.5kN to 8.5kN	170 KN	40 Hz
2	Position sensor	0 to 242 mm	5 µm	2 kHz
3	Oil pressure sensor	1 bar to 210 bar	1 bar	800 Hz
4	Oil temperature sensor	0 to +100 °C	0.5 °C	10 Hz

Table 8.1 Sensor Specifications

8.3 SIC Dynamic Drivers

As we discussed in Chapter 7 concerning high dynamics, we will now present the practical results in this section. Our approach for validating the effectiveness of our proposed driver topology involved a comparative analysis with two alternative drivers:

- An off-the-shelf industrial driver known as My-502.
- A driver utilizing a developed H-bridge-based topology.

As a test bench, we employed the DevKit, a product by Kalysta, which incorporates the SIC actuator along with all the required piping components (refer to Figure 8.9).

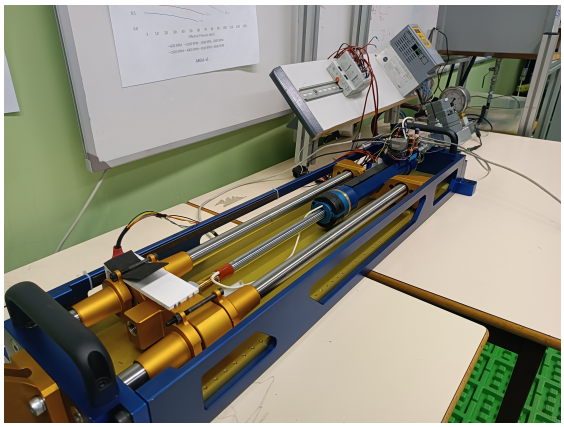

Figure 8.9 DevKit: The Test Environment

8.3.1 Experimental results

First, the current response of the servo-valve is measured using the industrial driver My-502, and it is shown in Fig 8.10 that the response represents $\pm 5mA$. The measured settling time is $T_{My-502_s} = 5ms = 0.5 \times T_{Torque_s}$.

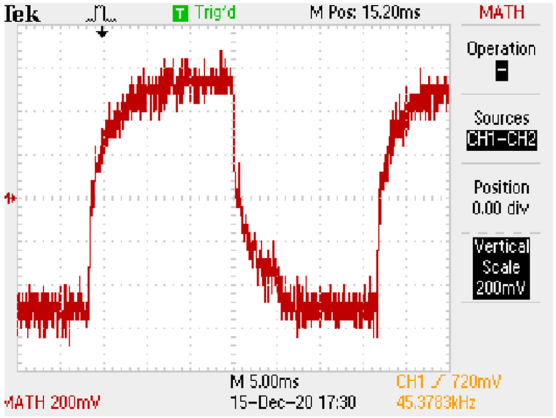

Figure 8.10 Step response of the commercial driver MY-502

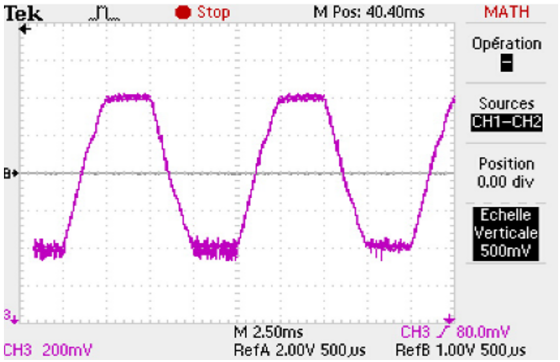

Figure 8.11 Step Response of H-Bridge-based Driver

Second, the H-bridge topology-based driver with digital PID implementation is tested, and we got the current step response shown in Fig. 7.12 (the response represents $\pm 5mA$). The measurement of the current settling time gives $T_{Hbridge_s} = 2ms = 0.18 \times T_{Torque_s}$.

Finally, our proposed driver is tested under the same experimental conditions. The achieved step response is shown in Figure. 8.12.

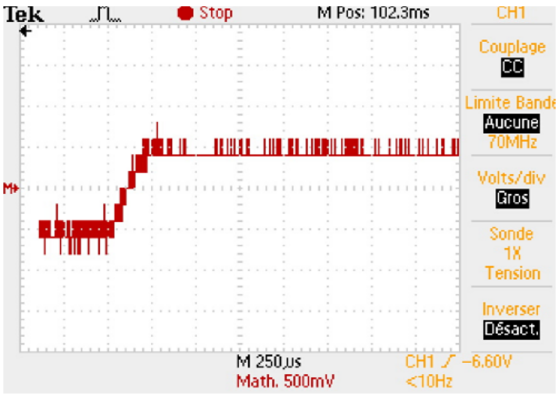

Figure 8.12 Step Response of Proposed Driver

The measured settling time, in this case, is $T_{HighDynamic_s} = 0.25ms = 0.02 \times T_{Torque_s}$. Our control has thus enhanced the settling time.

8.4 MGH Electronic Board

in the appendix B we detailed the electronic design which will be manufactured and tested later for future completion. Figure 8.13 displays the 3D design of our developed BLDC (Brushless DC) motor. In this design, the Control board is divided into two parts:

1. Board 1 - Power Supply Section: - This section of the control board is responsible for managing the power supply for the BLDC motor. It ensures a stable and reliable power source to drive the motor effectively.

2. Board 2 - Three-Phase Inverter and Logic Controller: - Board 2 encompasses the critical components for controlling the BLDC motor. It houses the three-phase inverter, which is essential for converting DC power into the alternating current needed to drive the motor. Additionally, it contains the logic controller, which orchestrates the motor's operation, including commutation and speed control.

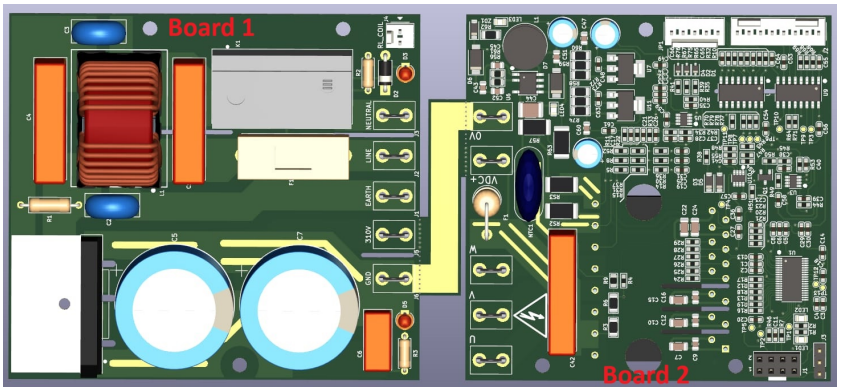

Figure 8.13 Electronic final Layout for MGH Electronic Board

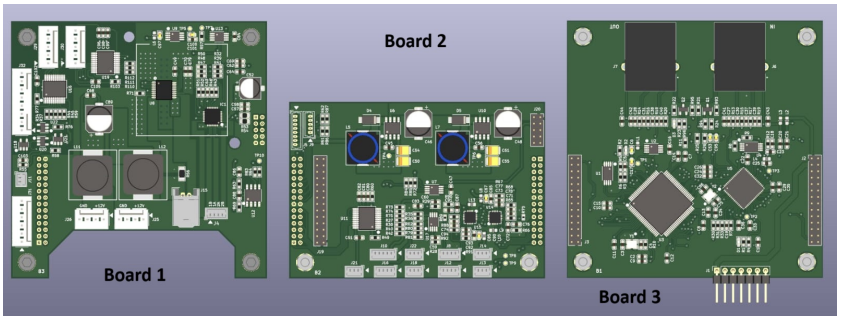

Figure 8.14 Electronic final Layout for Voice Coil Motor Electronic Board

8.5 Voice Coil Controller

Even though we are still in the process of developing the voice coil driver, we have taken a proactive step to verify the performance of the control and electronics board. To achieve this, we implemented the voice coil motor on a 3D printed model of SEHA, as shown in Figure 8.15. We conducted a preliminary position control test with two different steps, one ranging from 0 to 2 mm, depicted in Figure 8.16, and the other from 0 to 5 mm, as shown in Figure 8.17. The results of these tests

Figure 8.15 Voice Coil on 3d Test Bench

indicate that, even at this early stage of development, our design enables primitive position control with some static error. The settling time for these control actions falls within the range of 50ms to 100ms. While we acknowledge that the control system has not been fully optimized, we consider these results a positive hardware validation for the voice coil driver. This validation demonstrates that our control and electronics board is on the right track, and we are making progress toward our goal.

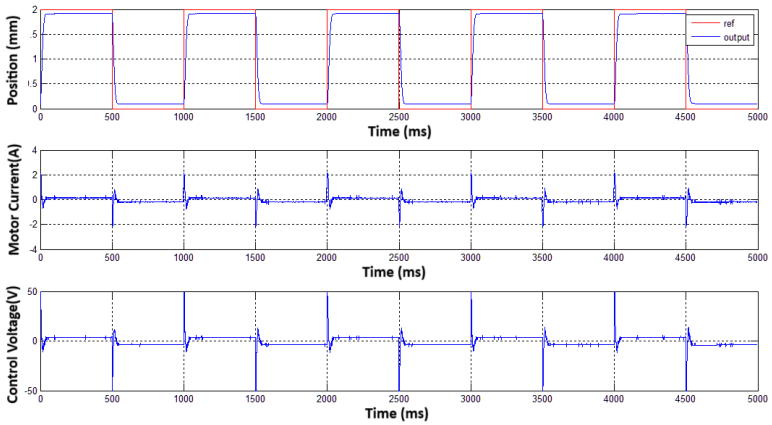

Figure 8.16 Voice Coil Primitive position control 2 mm Step

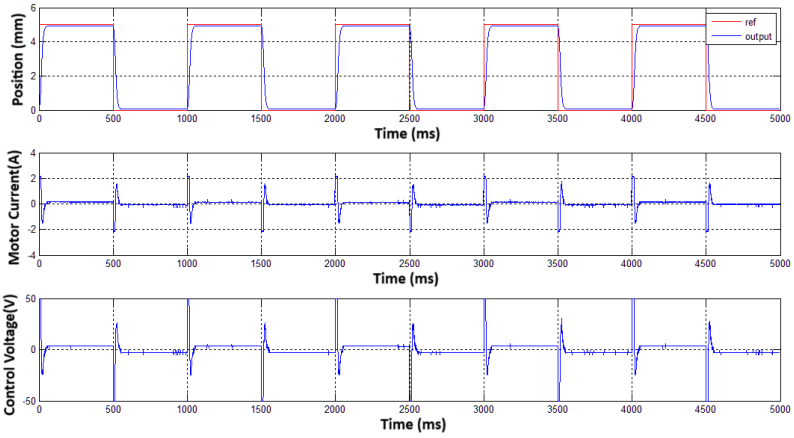

Figure 8.17 Voice Coil Primitive position control 5mm Step

8.6 Conclusion

This chapter presented the experimental results obtained while developing our servo-electro hydraulic actuator (SEHA). These results demonstrate the effectiveness of our modular design approach, highlighting the advancements made in each of the core components: the servo instrumented cylinder (SIC), the main hydraulic group (MGH), and the linear motor.

The SIC Electronic and Control Board has undergone several iterations, culminating in the robust and reliable SIC V4. This version has achieved an impressive 80% test performance score, showcasing its ability to provide accurate and responsive control of the SIC actuator.

The high dynamic driver topology proposed in Chapter 4 has been validated through comparative analysis with two alternative drivers. Our proposed driver has demonstrated a significant improvement in settling time compared to the commercial My-502 driver and the H-bridge-based driver, demonstrating its efficacy in enabling high-speed and responsive actuation.

The electronic board for the Main Hydraulic Group (MGH) is currently under development and will be manufactured and tested shortly. The preliminary design layout in Appendix B indicates a clear and organized approach to the MGH control system.

The voice coil motor controller is still in the development phase, but preliminary tests on a 3D-printed model of SEHA have shown promising results. The control system has demonstrated the ability to achieve primitive position control with some static error, with a settling time within the range of 50-100ms. While optimization is still necessary, these results indicate that the voice coil controller is on the right track.

Overall, the experimental results presented in this chapter provide strong evidence of the progress made in developing SEHA. The modular design approach has enabled efficient development of each component, and the testing results demonstrate the effectiveness of our control systems.

Chapter 9

Conclusions and perspectives

Contents

9.1 General Conclusion

In this thesis, we have addressed the significant challenge of actuation in the context of humanoid robots. Before delving into our novel contributions, we conducted a comprehensive review of existing actuation technologies and conducted a biomedical study to understand the critical safety requirements for such systems. Building upon this foundation, we introduced SEHA, a groundbreaking patented solution for an electro-hydraulic actuator that incorporates essential safety features.

Our research then focused on the electronic and control layer for SEHA, with a deliberate choice of employing a modular design approach. This approach led to the development of three distinct products: SIC, MGH, and DevKit. For SIC, we meticulously designed the sensory layer, crafted the necessary conditioning circuits, selected an optimal firmware structure with FreeRTOS, and fine-tuned the communication layer using EtherCAT at a blazing 100Mbps baud rate. To facili-

tate industrialization, we meticulously documented tests, resulting in the creation of successive versions: SICV1, SICV2, SICV3, SICV3Prime, and SICV4Prime.

Furthermore, we conducted an in-depth study and simulation of the SIC cylinder, incorporating an innovative EHSV driver and developing a dynamic driver to enhance its performance. In the case of the hydraulic pump, we optimized the motor technology by adopting BLDC technology, simulating the driver's behavior using MATLAB Simulink, and proposing the requisite electronic driver.

As we look towards the future, our work is far from complete. The next steps involve manufacturing, testing, and industrializing the BLDC motor driver, mirroring the successful path we have taken with the SIC electronic board. Additionally, our aspirations include integrating all components into the Dev-Kit and conducting comprehensive global tests to ensure seamless functionality. Ultimately, our goal is to integrate SEHA into the Hydroid humanoid robot, marking the culmination of our efforts in revolutionizing humanoid robot actuation.

9.2 Perspectives

As we look ahead, several avenues for future development and refinement emerge. Addressing challenges related to electronic component market stock-outs is essential for seamless progress. Ongoing efforts to enhance sensor accuracy and optimize control systems remain at the forefront of our agenda.

The modular design approach employed in SEHA's development enables flexibility and scalability. Future iterations can leverage this modularity to cater to diverse robotic applications, considering humanoid robots of varying sizes and exoskeletons with distinct requirements.

Exploration of potential applications, advancements, and adaptations based on the findings provides a roadmap for the continued evolution of actuation systems. The identified areas for future work invite further research and development, contributing to the broader field of humanoid and assistive device actuation.

In conclusion, our journey with SEHA has not only yielded tangible outcomes but also paved the way for continuous innovation, pushing the boundaries of what is achievable in the realm of advanced actuation systems. The future holds exciting possibilities as we navigate the dynamic landscape of robotics and contribute to shaping the future of human-machine interactions.

Bibliography

1. Uzun, A. & Vatansever, F. ISMAIL AL JAZARI MACHINES AND NEW TECHNOLOGIES. en. *acta mechanica et automatica* (2008).
2. Moran, M. E. The da Vinci Robot. en. *Journal of Endourology* **20,** 986–990. ISSN: 0892-7790, 1557-900X. http://www.liebertpub.com/doi/10.1089/end.2006.20.986 (2023) (Dec. 2006).
3. *Springer handbook of robotics* en (eds Siciliano, B. & Khatib, O.) OCLC: ocn153562054. ISBN: 978-3-540-23957-4 (Springer International, Berlin, 2008).
4. *Springer Handbook of Robotics* en (eds Siciliano, B. & Khatib, O.) ISBN: 978-3-319-32550-7 978-3-319-32552-1. https://link.springer.com/10.1007/978-3-319-32552-1 (2023) (Springer International Publishing, Cham, 2016).
5. Haynes, G. C. *et al.* in *The DARPA Robotics Challenge Finals: Humanoid Robots To The Rescue* (eds Spenko, M., Buerger, S. & Iagnemma, K.) Series Title: Springer Tracts in Advanced Robotics, 103–144 (Springer International Publishing, Cham, 2018). ISBN: 978-3-319-74665-4 978-3-319-74666-1. http://link.springer.com/10.1007/978-3-319-74666-1_4 (2023).
6. Tadokoro, S. en. in *Encyclopedia of Systems and Control* (eds Baillieul, J. & Samad, T.) 1–7 (Springer London, London, 2013). ISBN: 978-1-4471-5102-9. https://link.springer.com/10.1007/978-1-4471-5102-9_181-1 (2023).
7. Stentz, A. *et al.* CHIMP, the CMU Highly Intelligent Mobile Platform: The CHIMP Robot. en. *Journal of Field Robotics* **32,** 209–228. ISSN: 15564959. https://onlinelibrary.wiley.com/doi/10.1002/rob.21569 (2023) (Mar. 2015).

8. Venture, G., Indurkhya, B. & Izui, T. en. in *Social Robotics* (eds Kheddar, A. *et al.*) Series Title: Lecture Notes in Computer Science, 375–382 (Springer International Publishing, Cham, 2017). ISBN: 978-3-319-70021-2 978-3-319-70022-9. http://link.springer.com/10.1007/978-3-319-70022-9_37 (2023).

9. Wood, L. J. *et al.* en. in *Social Robotics* (eds Kheddar, A. *et al.*) Series Title: Lecture Notes in Computer Science, 53–63 (Springer International Publishing, Cham, 2017). ISBN: 978-3-319-70021-2 978-3-319-70022-9. http://link.springer.com/10.1007/978-3-319-70022-9_6 (2023).

10. Edsinger, A. & Kemp, C. *Manipulation in Human Environments* en. in *2006 6th IEEE-RAS International Conference on Humanoid Robots* (IEEE, University of Genova, Genova, Italy, Dec. 2006), 102–109. ISBN: 978-1-4244-0199-4 978-1-4244-0200-7. http://ieeexplore.ieee.org/document/4115587/ (2023).

11. Hashemi-Petroodi, S. E., Thevenin, S., Kovalev, S. & Dolgui, A. Operations management issues in design and control of hybrid human-robot collaborative manufacturing systems: a survey. en. *Annual Reviews in Control* **49,** 264–276. ISSN: 13675788. https://linkinghub.elsevier.com/retrieve/pii/S136757882030016X (2023) (2020).

12. Hirose, M. & Ogawa, K. Honda humanoid robots development. en. *Philosophical Transactions of the Royal Society A: Mathematical, Physical and Engineering Sciences* **365,** 11–19. ISSN: 1364-503X, 1471-2962. https://royalsocietypublishing.org/doi/10.1098/rsta.2006.1917 (2023) (Jan. 2007).

13. *Digit* en. https://robotsguide.com/robots/digit/ (2023).

14. Radosavovic, I. *et al. Learning Humanoid Locomotion with Transformers* en. arXiv:2303.03381 [cs]. Mar. 2023. http://arxiv.org/abs/2303.03381 (2023).

15. Tesla. *Tesla AI Day 2022* Oct. 2022. https://www.tesla.com/en_eu/AI.

16. Focchi, M. *et al. Water/air performance analysis of a fluidic muscle* en. in *2010 IEEE/RSJ International Conference on Intelligent Robots and Systems* (IEEE, Taipei, Oct. 2010), 2194–2199. ISBN: 978-1-4244-6674-0. http://ieeexplore.ieee.org/document/5650432/ (2023).

17. Sardellitti, I., Park, J., Shin, D. & Khatib, O. *Air Muscle Controller Design in the Distributed Macro-Mini (DM ^{2}) Actuation Approach* en. in *2007 IEEE/RSJ International Conference on Intelligent Robots and Systems* (IEEE, San Diego, CA, Oct. 2007), 1822–1827. ISBN: 978-1-4244-0911-2. https://ieeexplore.ieee.org/document/4399073/ (2023).

18. Ammounah, A. *Architecture de Control pour un robot humanoid à actionnement hydraulique* PhD thesis (Paris-Saclay, 2021).

19. Gordon Cheng *et al. CB: Exploring neuroscience with a humanoid research platform* en. in *2008 IEEE International Conference on Robotics and Automation* (IEEE, Pasadena, CA, USA, May 2008), 1772–1773. ISBN: 978-1-4244-1646-2. http://ieeexplore.ieee.org/document/4543459/ (2023).

20. Stasse, O. & Flayols, T. en. in *Biomechanics of Anthropomorphic Systems* (eds Venture, G., Laumond, J.-P. & Watier, B.) Series Title: Springer Tracts in Advanced Robotics, 281–310 (Springer International Publishing, Cham, 2019). ISBN: 978-3-319-93869-1 978-3-319-93870-7. http://link.springer.com/10.1007/978-3-319-93870-7_13 (2023).

21. *Humanoid Robotics: A Reference* en (eds Goswami, A. & Vadakkepat, P.) ISBN: 978-94-007-6045-5 978-94-007-6046-2. http://link.springer.com/10.1007/978-94-007-6046-2 (2023) (Springer Netherlands, Dordrecht, 2019).

22. Zoss, A., Kazerooni, H. & Chu, A. Biomechanical design of the Berkeley lower extremity exoskeleton (BLEEX). en. *IEEE/ASME Transactions on Mechatronics* **11,** 128–138. ISSN: 1083-4435. http://ieeexplore.ieee.org/document/1618670/ (2023) (Apr. 2006).

23. Sleiman, M. *New Actuation Technologies for humanoid robotics and assistive devices* English. PhD thesis (Paris-Saclay, 2022).

24. Wang, S. *et al.* Design and Control of the MINDWALKER Exoskeleton. en. *IEEE Transactions on Neural Systems and Rehabilitation Engineering* **23,** 277–286. ISSN: 1534-4320, 1558-0210. https://ieeexplore.ieee.org/document/6940308/ (2023) (Mar. 2015).

25. TABTI, N. *Contribution to the design of the scalable exoskeleton SOL3* PhD thesis (Université Paris-Saclay, Vélizy, Fr, Feb. 2021).

26. Mavroidis, C. Development of Advanced Actuators Using Shape Memory Alloys and Electrorheological Fluids. en. *Research in Nondestructive Evaluation* **14,** 1–32. ISSN: 0934-9847, 1432-2110. http://www.tandfonline.com/doi/abs/10.1080/09349840209409701 (2023) (Mar. 2002).

27. Mori, S., Tanaka, K., Nishikawa, S., Niiyama, R. & Kuniyoshi, Y. High-Speed Humanoid Robot Arm for Badminton Using Pneumatic-Electric Hybrid Actuators. en. *IEEE Robotics and Automation Letters* **4,** 3601–3608. ISSN: 2377-3766, 2377-3774. https://ieeexplore.ieee.org/document/8764002/ (2023) (Oct. 2019).

28. Alfayad, S., Ouezdou, F. B., Namoun, F. & Gheng, G. High performance integrated electro-hydraulic actuator for robotics – Part I: Principle, prototype design and first experiments. en. *Sensors and Actuators A: Physical* **169,** 115–123. ISSN: 09244247. https://linkinghub.elsevier.com/retrieve/pii/S0924424711001154 (2023) (Sept. 2011).

29. Ko, T., Yamamoto, K., Murotani, K. & Nakamura, Y. *Compliant Biped Locomotion of Hydra, an Electro-Hydrostatically Driven Humanoid* en. in *2018 IEEE-RAS 18th International Conference on Humanoid Robots (Humanoids)* (IEEE, Beijing, China, Nov. 2018), 280–283. ISBN: 978-1-5386-7283-9. https://ieeexplore.ieee.org/document/8624973/ (2023).

30. Komagata, M., Ko, T. & Nakamura, Y. *Small Size Hydraulic Pumps with Low Heat Generation for Electro Hydrostatic Actuation of Humanoid Robots* en. in *2018 IEEE-RAS 18th International Conference on Humanoid Robots (Humanoids)* (IEEE, Beijing, China, Nov. 2018), 1–6. ISBN: 978-1-5386-7283-9. https://ieeexplore.ieee.org/document/8625055/ (2023).

31. Gomis-Bellmunt, O. & Campanile, L. F. *Design Rules for Actuators in Active Mechanical Systems* en. ISBN: 978-1-84882-613-7 978-1-84882-614-4. http://link.springer.com/10.1007/978-1-84882-614-4 (2023) (Springer London, London, 2010).

32. Dongjun Shin, Khatib, O. & Cutkosky, M. *Design methodologies of a hybrid actuation approach for a human-friendly robot* en. in *2009 IEEE International Conference on Robotics and Automation* (IEEE, Kobe, May 2009), 4369–4374. ISBN: 978-1-4244-2788-8. http://ieeexplore.ieee.org/document/5152744/ (2023).

33. KAWASAKI. *n181en.pdf* https://global.kawasaki.com/en/corp/rd/magazine/181/%20index.html..

34. *Vérin linéaire H-Track | Thomson* https://www.thomsonlinear.com/fr/produits/actionneurs-lineaires/h-track#h-track-literature (2023).

35. Kardo, M. (72) Inventors: Samer ALFAYAD , CACHAN (FR); en.

36. Azahari, A., Siswanto, W., Ngali, M., Salleh, S. M. & Yusup, E. M. Dynamic Simulation and Analysis of Human Walking Mechanism. en. *IOP Conference Series: Materials Science and Engineering* **165,** 012027. ISSN: 1757-8981, 1757-899X. https://iopscience.iop.org/article/10.1088/1757-899X/165/1/012027 (2023) (Jan. 2017).

37. Akay, T. & Murray, A. J. Relative Contribution of Proprioceptive and Vestibular Sensory Systems to Locomotion: Opportunities for Discovery in the Age of Molecular Science. en. *International Journal of Molecular Sciences* **22,** 1467. ISSN: 1422-0067. https://www.mdpi.com/1422-0067/22/3/1467 (2023) (Feb. 2021).

38. Frontera, W. R. & Ochala, J. Skeletal Muscle: A Brief Review of Structure and Function. en. *Calcified Tissue International* **96,** 183–195. ISSN: 0171-967X, 1432-0827. http://link.springer.com/10.1007/s00223-014-9915-y (2023) (Mar. 2015).

39. Pinnell, J., Turner, S. & Howell, S. Cardiac muscle physiology. en. *Continuing Education in Anaesthesia Critical Care & Pain* **7,** 85–88. ISSN: 17431816. https://linkinghub.elsevier.com/retrieve/pii/S1743181617304900 (2023) (June 2007).

40. Severs, N. J. The cardiac muscle cell. en. *BioEssays* **22,** 188–199. ISSN: 02659247. https://onlinelibrary.wiley.com/doi/10.1002/(SICI)1521-1878(200002)22:2%3C188::AID-BIES10%3E3.0.CO;2-T (2023) (Jan. 2000).

41. Muscolino, J. E. Muscular System Manual. en.

42. Hunter, P., McCulloch, A. & Ter Keurs, H. Modelling the mechanical properties of cardiac muscle. en. *Progress in Biophysics and Molecular Biology* **69,** 289–331. ISSN: 00796107. https://linkinghub.elsevier.com/retrieve/pii/S0079610798000133 (2023) (Mar. 1998).

43. Heckman, C. & Enoka, R. M. en. in *Comprehensive Physiology* (ed Prakash, Y. S.) 1st ed., 2629–2682 (Wiley, Oct. 2012). ISBN: 978-0-470-65071-4. https://onlinelibrary.wiley.com/doi/10.1002/cphy.c100087 (2023).

44. Filatov, M. A., Poluhin, V. V. & Shakirova, L. S. IDENTIFYING OBJECTIVE DIFFERENCES BETWEEN VOLUNTARY AND INVOLUNTARY MOTION IN BIOMECHANICS. en. *Human. Sport. Medicine* **21** (2021).

45. Redekar, A., Deb, D. & Ozana, S. Functionality Analysis of Electric Actuators in Renewable Energy Systems—A Review. en. *Sensors* **22,** 4273. ISSN: 1424-8220. https://www.mdpi.com/1424-8220/22/11/4273 (2023) (June 2022).

46. Ehsan, M., Rampen, W. H. S. & Salter, S. H. Modeling of Digital-Displacement Pump-Motors and Their Application as Hydraulic Drives for Nonuniform Loads. en. *Journal of Dynamic Systems, Measurement, and Control* **122,** 210–215. ISSN: 0022-0434, 1528-9028. https://asmedigitalcollection.asme.org/dynamicsystems/article/122/1/210/460194/Modeling-of-DigitalDisplacement-PumpMotors-and (2023) (Mar. 2000).

47. Hamilton, R. DC motor brush life. *IEEE Transactions on Industry Applications* **36,** 1682–1687 (2000).

48. Hwang, C., Li, P., Liu, C. & Chen, C. Design and analysis of a brushless DC motor for applications in robotics. en. *IET Electric Power Applications* **6,** 385. ISSN: 17518660. https://digital-library.theiet.org/content/journals/10.1049/iet-epa.2011.0267 (2023) (2012).

49. Visconti, P. & Primiceri, P. AN OVERVIEW ON STATE-OF-ART AND FUTURE APPLICATION FIELDS OF BLDC MOTORS: DESIGN AND CHARACTERIZATION OF A PC-INTERFACED DRIVING AND MOTIONTROL SYSTEM. en. *ARPN Journal of Engineering and Applied Sciences* **12,** 4913–4926. ISSN: 1819-6608 (2017).

50. Alfayad, S., Ouezdou, F. B., Namoun, F. & Cheng, G. *Lightweight high performance integrated actuator for humanoid robotic applications: Modeling, design & realization* en. in *2009 IEEE International Conference on Robotics and Automation* (IEEE, Kobe, May 2009), 562–567. ISBN: 978-1-4244-2788-8. http://ieeexplore.ieee.org/document/5152286/ (2023).

51. Irwin, J. D. Academic Press Series in Engineering. en.

52. Totten, G. E. *Handbook of Hydraulic Fluid Technology* 0th ed. en (eds Totten, G. E. & De Negri, V. J.) ISBN: 978-0-429-09284-8. https://www.taylorfrancis.com/books/9781420085273 (2023) (CRC Press, Oct. 2011).

53. Esposito, A. *Fluid power with applications* Seventh Edition, Pearson new international edition. en. ISBN: 978-1-292-02387-8 (Pearson, Harlow, 2014).

54. Chen, S.-Y. & Yang, M.-C. Nonlinear Contour Tracking of a Voice Coil Motors-Driven Dual-Axis Positioning Stage Using Fuzzy Fractional PID Control with Variable Orders. en. *Mathematical Problems in Engineering* **2021** (ed Wang, G.) 1–14. ISSN: 1563-5147, 1024-123X. https://www.hindawi.com/journals/mpe/2021/6697942/ (2023) (Mar. 2021).

55. Ruiz-Díez, V. *et al.* Piezoelectric MEMS Linear Motor for Nanopositioning Applications. en. *Actuators* **10,** 36. ISSN: 2076-0825. https://www.mdpi.com/2076-0825/10/2/36 (2023) (Feb. 2021).

56. Sourander, T., Minav, T., Pietola, M. & Hänninen, H. Sensorless position control of direct driven hydraulic actuators. en. *JFPS International Journal of Fluid Power System* **11,** 26–35. ISSN: 1881-5286. https://www.jstage.jst.go.jp/article/jfpsij/11/3/11_1103-001/_article (2023) (2019).

57. BiSS Interface BiSS C Protocol Description. en.

58. Sivec, M. LinACE in-axis absolute linear encoder. en.

59. Meng, Q., Yue, Y., Li, S. & Yu, H. Electromyogram-based motion compensation control for the upper limb rehabilitation robot in active training. en. *Mechanical Sciences* **13,** 675–685. ISSN: 2191-916X. https://ms.copernicus.org/articles/13/675/2022/ (2023) (Aug. 2022).

60. Ohmukai, M. & Kami, Y. Recognition of Force Magnitude Applied to Pressure-Sensitive Conducting Rubber Sensors on the Basis of Frequency Table. en. *Journal of Sensor Technology* **08,** 88–95. ISSN: 2161-122X, 2161-1238. http://www.scirp.org/journal/doi.aspx?DOI=10.4236/jst.2018.84007 (2023) (2018).

61. Saboor, A. *et al.* Latest Research Trends in Gait Analysis Using Wearable Sensors and Machine Learning: A Systematic Review. en. *IEEE Access* **8,** 167830–167864. ISSN: 2169-3536. https://ieeexplore.ieee.org/document/9187883/ (2023) (2020).

62. Díez, J. *et al.* Customizable Optical Force Sensor for Fast Prototyping and Cost-Effective Applications. en. *Sensors* **18,** 493. ISSN: 1424-8220. http://www.mdpi.com/1424-8220/18/2/493 (2023) (Feb. 2018).

63. Liu, J. *et al.* Principle Research on a Novel Piezoelectric 12-DOF Force/Acceleration Sensor. *Journal of Sensors* **2017** (ed Stassi, S.) Publisher: Hindawi, 2836365. ISSN: 1687-725X. https://doi.org/10.1155/2017/2836365 (Dec. 2017).

64. Jeong, H. *et al.* Rugged and Compact Three-Axis Force/Torque Sensor for Wearable Robots. en. *Sensors* **21,** 2770. ISSN: 1424-8220. https://www.mdpi.com/1424-8220/21/8/2770 (2023) (Apr. 2021).

65. Oh, B. *et al.* Untethered Soft Robotics with Fully Integrated Wireless Sensing and Actuating Systems for Somatosensory and Respiratory Functions. en. *Soft Robotics* **7,** 564–573. ISSN: 2169-5172, 2169-5180. https://www.liebertpub.com/doi/10.1089/soro.2019.0066 (2023) (Oct. 2020).

66. Dao, H. V., Tran, D. T. & Ahn, K. K. Active Fault Tolerant Control System Design for Hydraulic Manipulator With Internal Leakage Faults Based on Disturbance Observer and Online Adaptive Identification. en. *IEEE Access* **9,** 23850–23862. ISSN: 2169-3536. https://ieeexplore.ieee.org/document/9333569/ (2023) (2021).

67. Ledin, J. *Architecting high-performance embedded systems: design and build high-performance real-time digital systems based on FGPAs and custom circuits* en. ISBN: 978-1-78995-596-5 (Packt, Birmingham Mumbai, 2021).

68. Bruno, F. *FPGA Programming for Beginners* 1st edition. en. OCLC: 1246197093. ISBN: 978-1-78980-541-3 (Packt Publishing, 2021).

69. Vasil'ev, A. E. & Kolodeznikov, I. V. The Development and Use of Data Acquisition and Control Systems Based on Arm Microcontrollers. en. *Measurement Techniques* **58,** 245–249. ISSN: 0543-1972, 1573-8906. http://link.springer.com/10.1007/s11018-015-0693-3 (2023) (June 2015).

70. Ünsalan, C., Gürhan, H. D. & Yücel, M. E. *Embedded System Design with ARM Cortex-M Microcontrollers: Applications with C, C++ and MicroPython* en. ISBN: 978-3-030-88438-3 978-3-030-88439-0. https://link.springer.com/10.1007/978-3-030-88439-0 (2023) (Springer International Publishing, Cham, 2022).

71. Amos, B. *Hands-on RTOS with microcontrollers: building real-time embedded systems using FreeRTOS, STM32 MCUs, and SEGGER debug tools* en. OCLC: 1197980473. ISBN: 978-1-83882-928-5 (Packt Publishing, Birmingham, UK, 2020).

72. Baynes, K. *et al.* The performance and energy consumption of embedded real-time operating systems. en. *IEEE Transactions on Computers* **52,** 1454–1469. ISSN: 0018-9340. http://ieeexplore.ieee.org/document/1244943/ (2023) (Nov. 2003).

73. Anh, T. N. B. & Tan, S.-L. Real-Time Operating Systems for Small Microcontrollers. en. *IEEE Micro* **29,** 30–45. ISSN: 0272-1732. http://ieeexplore.ieee.org/document/5325154/ (2023) (Sept. 2009).

74. Hamblen, J. Using a Low-Cost SoC Computer and a Commercial RTOS in an Embedded Systems Design Course. en. *IEEE Transactions on Education* **51,** 356–363. ISSN: 0018-9359. http://ieeexplore.ieee.org/document/4589060/ (2023) (Aug. 2008).

75. Barry, R. Using the FreeRTOS™ Real Time Kernel. en.

76. Plummer, P. A. Electrohydraulic servovalves – past, present, and future. en.

77. Yang, J. *Design and experiment of the lower extremity exoskeleton* en. in *2017 IEEE 2nd Advanced Information Technology, Electronic and Automation Control Conference (IAEAC)* (IEEE, Chongqing, China, Mar. 2017), 1380–1383. ISBN: 978-1-4673-8979-2. http://ieeexplore.ieee.org/document/8054240/ (2023).

78. Semini, C. HyQ - Design and Development of a Hydraulically Actuated Quadruped Robot. en.

79. Sarkar, B. K., Das, J., Saha, R., Mookherjee, S. & Sanyal, D. Approaching Servoclass Tracking Performance by a Proportional Valve-Controlled System. en. *IEEE/ASME Transactions on Mechatronics* **18,** 1425–1430. ISSN: 1083-4435, 1941-014X. http://ieeexplore.ieee.org/document/6494307/ (2023) (Aug. 2013).

80. Xuan Hong Son, P. & Thien Phuc, T. Comparison of jet pipe servo valve with flapper nozzle servo valve. en. *Science and Technology Development Journal* **20,** 78–83. ISSN: 1859-0128, 1859-0128. http://stdj.scienceandtechnology.com.vn/index.php/stdj/article/view/418 (2023) (Mar. 2017).

81. Tamburrano, P. *et al.* A Review of Novel Architectures of Servovalves Driven by Piezoelectric Actuators. en. *Energies* **14,** 4858. ISSN: 1996-1073. https://www.mdpi.com/1996-1073/14/16/4858 (2023) (Aug. 2021).

82. Manring, N. D. Hydraulic Control Systems.

83. Xu, Y. Modelling and Control of a High Performance Electro-hydraulic Test Bench. fr.

84. Xu, Y., Bideaux, E., Sesmat, S., Sidhom, L. & Brun, X. Hydro-Mechanical Model of Electro-Hydraulic Servovalve Based on Bond Graph. en.

85. *Type 30 nozzle-flapper flow control servo valves* Available online. https://www.moog.com/content/dam/moog/literature/sdg/defense/Moog-Type30-Servo-Valve-Catalog.pdf.

86. *30 series micro servo valves* Available online. https://www.moog.com/content/dam/moog/literature/products/servovalves/industrial/flow-control/analog/Moog-ServoValves-30Series-Datasheet-en.pdf.

87. Shi, H., Zhang, B., Mei, X. & Song, Q. Realization of Force Detection and Feedback Control for Slave Manipulator of Master/Slave Surgical Robot. en. *Sensors* **21,** 7489. ISSN: 1424-8220. https://www.mdpi.com/1424-8220/21/22/7489 (2023) (Nov. 2021).

88. *A guide to the project management body of knowledge: PMBOK® guide* 5. ed. en (ed Institute, P. M.) ISBN: 978-1-935589-67-9 (PMI, Newtown Square, Pa, 2013).

Publications

Journaux

- G. Abdulmalek, A. Ammounah, N. A. Oufroukh, S. Alfayad and S. Mammar, "Design and Implementation of High Dynamics Servo-Valve Driver for Electro-hydraulic Actuator in Legged Robot's Applications," 2023 3rd International Conference on Electrical, Computer, Communications and Mechatronics Engineering (ICECCME), Tenerife, Canary Islands, Spain, 2023, pp. 1-7, doi: 10.1109/ICECCME57830.2023.10253324.
- G. Abdulmalek, A. Ammounah, N. Ait Oukfroukh, S. Alfayad, and S. Mammar *, "Electronic Implementation of High Bandwidth Linear Hydraulic Actuator for Legged Robot's Applications," International Journal of Modeling and Optimization vol. 13, no. 3, pp. 100-106, 2023.

Conférences internationales avec comité de relecture

- ICECCME 2023 : International Conference on Electrical, Computer, Communications and Mechatronics Engineering. Online 19th-21th, July 2023

Conférence nationale avec comité de relecture

- JNRH'2023 : Journées Nationales de la Robotique Humanoïde 5th - 7th,Bordeaux July 2023.

- JJJCR 2022 : Journée des Jeunes Chercheurs et Jeunes Chercheuses en Robotique 2022. Paris 7th, Nov 2022

Appendix A

Developed Test Document For SIC Electronics Board

Contents

A.1 Introduction

A servo-instrumented cylinder (SIC) is developed that integrates the hydraulic and electronic components in one device. Besides to the main hydraulic components (piston, rod, barrel), the SIC integrates a servo valve that controls the fluid flow to the actuator, a position sensor measuring the position of the rod, two pressure sensors measuring the pressure of the oil in the two chambers A and B, a force sensor measuring the force on the rod, temperature sensor measuring the oil temperature, and an electronic board that contains sensors conditioning circuits, servo valve driver, power circuit, EtherCAT communication port, and a microcontroller STM32H7 to monitor and control the system.

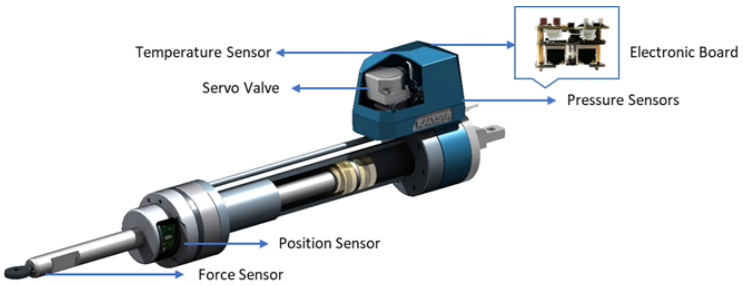

Figure A-1 Servo Intelligent Cylinder (SIC)

A.2 Objective and Prerequisties

The objective of this document is to describe the tests required to validate the performance of the developed electronic board that is responsible for the monitoring and control of the actuator Servo- Instrumented Cylinder (SIC). 1. In order to perform the test, the following requirements should be provided: 2. The SIC actuation system, including: a. The hydraulic cylinder of the actuator SIC, b. The mechanical installation base of the hydraulic cylinder with the load, c. Position sensor AMS, d. SPI sender device, e. Pair of pressure sensors Keller 4LC or equivalent, f. Temperature sensor PT1000, g. Force sensor based on strain gauge,

h. Servo valve Moog 30 or equivalent. 3. Referential measurement systems, recently calibrated, including: a. An Oscilloscope, typically Tektronix TBS 1022, b. Referential pressure measurements, typically Dspace DS1104, c. Referential temperature measurements, typically Precision GP 02 TSGP02, d. Referential position measurements, typically RLS referential measurement kit, e. Referential force measurements, typically ClipX BM40IE, f. Data acquisition system with sufficient channels, typically Dspace DS1104, g. Precise Ammeter, typically Fluke 117 portable 10A AC 600 AC, h. Accurate Voltmeter, typically Fluke 365 true RMS clamp meter, i. Thermometer, typically Fluke 62 MAX IR THERMOMETER, j. Flowmeter, typically Nauder VS02GB012V-. 4. Power supply unit up to 30V 5A. Variable-voltage, typically EL302RD DUAL Power Supply. 5. Power supply unit up to 400V 5A. Variable-voltage, typically Voltage Adjustable Power Supply SMPS 1500W. 6. Industrial PC or equivalent, typically C6025. 7. Real-time operating system, typically Windows IoT. 8. Real-time evaluation software, typically TwinCAT. 9. PC with SOEM installed on it. 10. Hydraulic group with variable pressure regulation, flow up to 4 l/min at least, typically MGH V1.0. 11. Temperature controller, typically Precision GP 02 TSGP02. 12. Sufficient pipes, manifolds, and hydraulic components to construct the hydraulic circuits. 13. Sufficient wires, connectors, and electronic components to construct the electronic circuits. 14. BLDC test bench with driver to run up to 5000 rpm. 15. Source of hot air.

A.3 Test Procedure

The test described in this document is divided into eight tests examining the performance of the different parts of the SIC electronic board including the driving circuit of the servo valve, the power circuit, the circuit responsible for EtherCAT communication protocol, the conditioning circuit of the pressure sensors, the temperature sensor, the position sensor, the force sensor, and the firmware of the board as shown in Figure A-2.

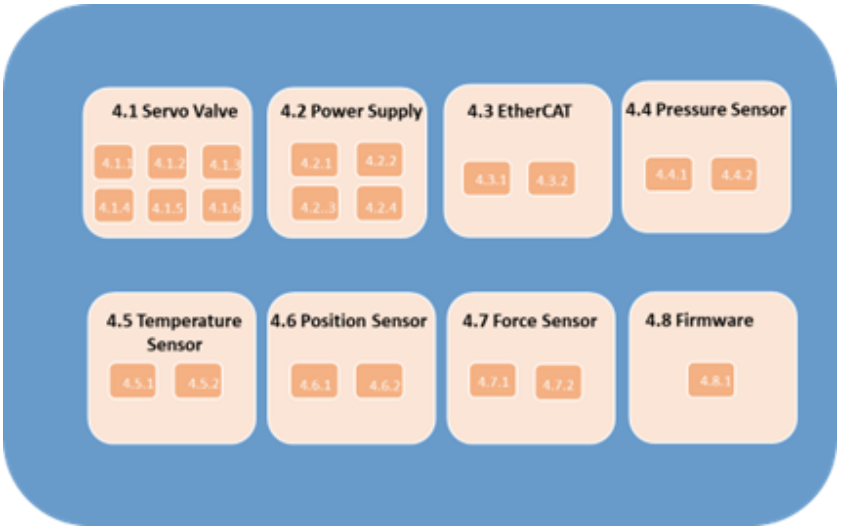

Figure A-2 Blocks of Tests for SIC Electronics Board

A.3.1 Servo Valve Diving Circuit Test

This section presents the different tests that are needed to validate the performance of the driving circuit of the servo valve. For the tests to be accomplished, the connections of connections shown in Figure A-4 should be established. The current is measured by measuring the voltage drop V0, on the measurement resistance Rsh. The measurement of the current is shown on the oscilloscope. The flow rate meter will measure the hydraulic flow rate, and the flow signal will be shown on the oscilloscope.

Short Circuit Protection Test (Destructive Test)

To perform this test, the following should be done:

1. Short-circuit the two terminals of the output of the servo valve driver (on the SIC board) via a small resistance (10 Ohm).
2. Add an ammeter in series (or scope in parallel), and measure the current.
3. Set on the software (TwinCAT) the desired current and measure it on the output to verify if the driver is still functional.

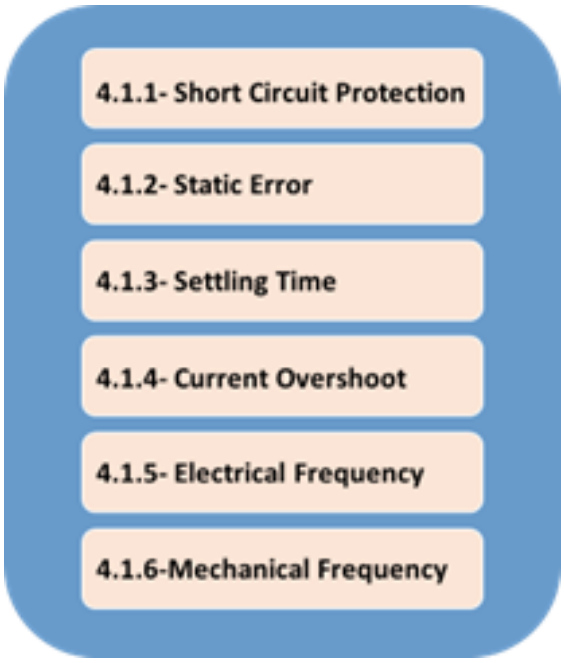

Figure A-3 Servo Valve Driver Tests

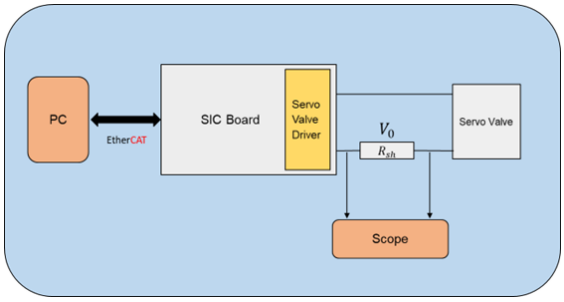

Figure A-4 Servo Valve Driver Test Implementation

The test is successful if the measured current did not exceed 60 mA and if the electronics are still functional and not burnt.

Static Error Test

To perform this test, the following should be done:

1. On TwinCAT, set a constant desired value for the servo valve current (rated current is between +-10mA).
2. Measure the voltage V0 on Rsh (or the DC current on an ammeter) and monitor it on the accurate meter.
3. Repeat the test for different samples of the ordered value. (+-10%, +-25%, +-50%, +-75% and +-100% of rated current)

The test is successful if the static error (real current/desired current) is less than 0.5%FS (0.1mA)

Settling Time Test

To perform this test, the following should be done:

1. Apply a square signal with an amplitude +-100%FS to the servo valve driver as the desired value using TwinCAT.
2. Set a large Frequency to see all the transient periods, for example, 10Hz.
3. Measure the voltage V0 on Rsh and monitor it on the oscilloscope. Step response characteristics should be observed.
4. Measure the settling time at 95%.

The test is successful if the settling time is less than 0.6 ms (in the worst case).

Current Overshoot Test

To perform this test, the following should be done:

1. Apply a square signal with an amplitude +-100%FS to the servo valve driver as the desired value using TwinCAT.
2. Set a large Frequency to see all the transient periods, for example, 100Hz.
3. Measure the voltage V0 and monitor it on the oscilloscope. Step response characteristics should be observed.
4. Measure the maximum overshoot if it exists.

The test is successful if the maximum overshoot is less than 10%.

Electrical Frequency Test (Cut off & Phase Shift)

To perform this test, the following should be done: 1. Apply a sinewave signal with an amplitude +-100%FS to the servo valve driver as desired value using TwinCAT entry fields. 2. Measure the signal of the flow rate meter Vflow and monitor it on the oscilloscope besides to the desired signal. 3. Vary the frequency of the sine wave on TwinCAT from 1 Hz up to 200 Hz 4. Measure the amplitude and the phase shift of the Vflow signal. The test is successful if at all frequencies, the amplitude of the Vflow signal is higher than 50% of the amplitude of the static signal (signal at 1 Hz). And if at all frequencies, the phase shift of the Vflow signal is less than 90° of the static signal (signal at 1 Hz).

Mechanical Frequency Test (Cut off & Phase Margin)

To perform this test, the following should be done:

1. Apply a sinewave signal with an amplitude +-100%FS to the servo valve driver as the desired value by using TwinCAT.

2. Measure the signal of the flow rate meter Vflow and monitor it on the oscilloscope beside the desired signal

3. Vary the frequency of the entry sine wave on TwinCAT from 1 Hz up to 200 Hz

4. Measure the amplitude and the phase shift of the Vflow signal. The test is successful if at all frequencies, the measured Vflow amplitude is higher than 50% of the amplitude of the static signal (signal at 1 Hz). And if at all frequencies, the phase shift of Vflow signal is less than 90° of the static signal (signal at 1 Hz).

A.3.2 Power Supply Circuit Test

This section presents the necessary tests to evaluate the performance of the power supply circuit on the SIC board. Four tests are to be performed. These tests mainly consider the measurements of the input voltage and input current besides to the internal temperatures of different Integrated Circuits (ICs), and monitoring of the internal voltages (5V, 3.3V, and 2.5V).

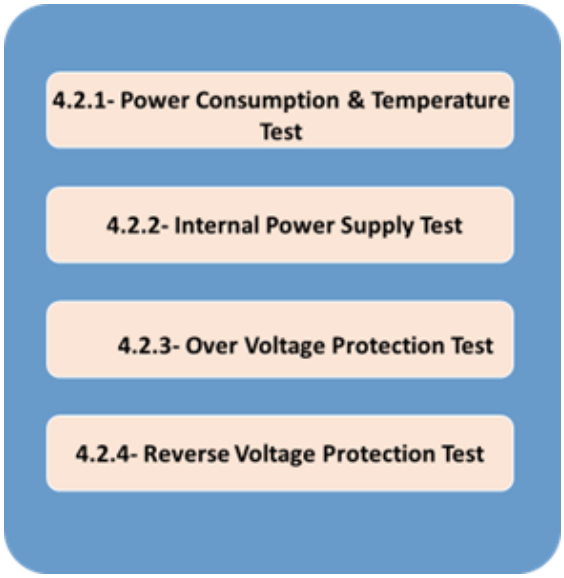

Figure A-5 Power Supply Block Test

Power Consumption and Temperature Test

To perform this test, the following should be done:

1. Connect the board to the power supply and to the PC.
2. Measure the temperature T on the IC's of the electronic board, the voltage V, and the current "I" consumed by the board every 5 minutes for 1 hour during the operation of the different functionalities of the board.

The test is successful if consumed energy V*I did not exceed 5W, during the testing period and if the temperature did not exceed 85 °C.

Internal Power Supply Test

To perform this test, the following should be done:

1. Connect the board to the power supply and to the PC.
2. Vary the environmental conditions (1) and operate different functionalities of the card.
3. Measure the internal supply voltages on the test points available on the card.

The test is successful if, during an hour (or more) of operation, the internal supply voltages did not vary more than 1%.

Reverse Voltage Protection Test

To perform this test, the following should be done:

1. Connect the board to the power supply BUT reverse the polarity of the supply voltage.
2. Reconnect the power properly again.

The test is successful if after reversing the polarity and reconnecting properly the board is functioning normally.

A.3.3 EtherCAT Test

This section presents the tests needed to evaluate the performance of the EtherCAT communication protocol on the SIC electronic board. Two tests are to be performed. These test aims to verify if the board is detected by different master PCs and to evaluate the cyclic time of the EtherCAT communication which is the time the EtherCAT frame takes to start from the host and return to the host after traveling all the EtherCAT device nodes.

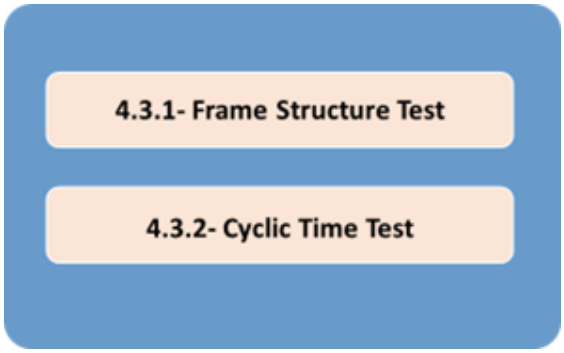

Figure A-6 EtherCAT Block Test

Frame Structure Test

To perform this test, the following should be done:

1. Connect the SIC board to the master PC equipped with TwinCAT software through the EtherCAT network.
2. Verify that the SIC board is detected through “scan” on TwinCAT.
3. Start communication using TwinCAT. Check the variables of input and output in the frame.
4. Disconnect the TwinCAT.
5. Start communication using SOEM. We check the variables of input and output in the frame.

For the test to be successful, the frame detected by SOEM and the frame detected by TwinCAT should be identical and the same as the frame defined in the requirements. The aim is to ensure that the board is detected by different slaves. Note: Insure that the input and output in SOEM are not reversed.

Cyclic Time

To perform this test, the following should be done:

1. Connect the SIC board to the EtherCAT network with the master PC equipped with TwinCAT software. Verify the detection of the card.
2. Start the communication using TwinCAT and set the cycle time to 100 us.
3. Operate the test for one minute and observe the counter variable ***Cycle Counter***. The value of this variable indicates the number of cycles of transmission with the slave.

The test is successful if the evolution of the ***Cycle Counter*** variable is linear and the counter increases by 1 each 100 us. The test fails if the counter step is detected with a delay of 200 us or more.

A.3.4 Pressure Sensor Test

This section presents the tests needed to evaluate the performance of the pressure sensor and its conditioning circuit integrated with the SIC board. Two tests are to be performed with the aim of measuring the accuracy and the resolution of the two pressure sensors in the actuator.

Accuracy Test

To perform this test, the following should be done:

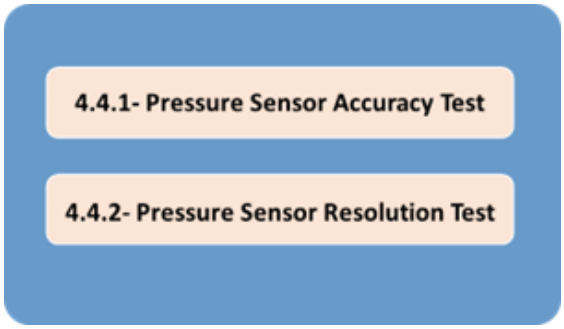

Figure A-7 Pressure Sensor Block Test

1. Set a value of the pressure in the hydraulic pump using the integrated pressure limiting valve in the pump. Vary the pressure between 10 and 210 bar.
2. Wait until the pressure stabilizes
3. Measure the pressure using the SIC board by the software TwinCAT.
4. Measure the pressure using the pressure referential measurement system (Beckhoff and the gauge). The referential measurement can be done by measuring using the Analog inputs of the Beckhoff unit. The real pressure is defined in the datasheet of Keller 4LC by the following equation Pressure = 300 *((Vp - 0.1Vcc)/(0.8 Vcc)) and is related to Vp/Vcc (ratiometric).
5. Repeat the test by varying the environmental conditions (1) of the card.
6. Compare the SIC board readings to the referential reading.

For the test to be successful, the difference between the two readings should not exceed 0.25%FS. The repeatability of the reading should be less than 0.1 %FS.

Resolution Test

To perform this test, the following should be done:

1. Vary the pressure slightly on the pressure limiting valve.

2. Determine the resolution of measurements.

For the test to be successful, the resolution should be sensible to 0.1%FS.

A.3.5 Temperature Sensor Test

This section presents the tests needed to evaluate the performance of the temperature sensor and its conditioning circuit integrated in the SIC board. Two tests are to be performed in the aim of measuring the accuracy and the resolution of the oil temperature sensors in the actuator.

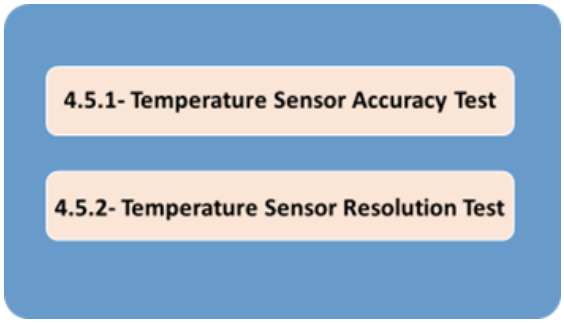

Figure A-8 Enter Caption

Accuracy Test

To perform this test, the following should be done:

1. Set a value of the temperature of the (oil or water) between 0 and 100 °C and wait until the temperature stabilizes.
2. Read the temperature on the SIC board using TwinCAT.
3. Measure the temperature using the referential device.
4. Compare the two readings and repeat the test by varying the environmental conditions (1) of the card.

For the test to be successful, the difference between the two readings should not exceed 0.5 °C and the repeatability of the reading should be less than 0.1 °C.

Resolution Test

To perform this test, the following should be done:

1. Vary the temperature slightly in the oven.
2. Determine the resolution of measurements.

For the test to be successful, the resolution should be sensible to 0.5°C.

A.3.6 Position Sensor Test

This section presents the tests needed to evaluate the performance of the position sensor and its conditioning circuit integrated in the SIC board. Two tests are to be performed in the aim of measuring the accuracy and the resolution the rod position sensor in the actuator. Note: If the position sensor of the cylinder is unavailable, perform the test on an external test bench equipped with an AMS sensor and use the RLS sensor as a reference for measurement.

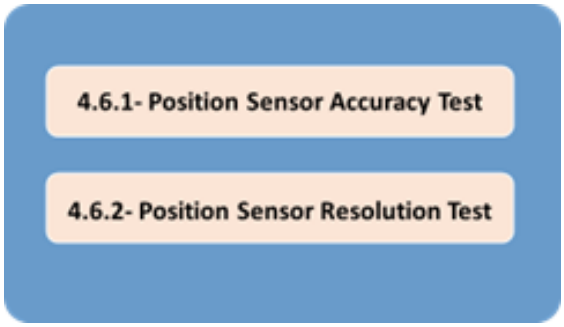

Figure A-9 Position Sensor Block Test

Accuracy Test

To perform this test, the following should be done:

1. Use RLS referential measurement kit, and set the position to a desired value.

2. Measure the position read on the SIC board using the software TwinCAT.
3. Measure the position using the RLS referential measurement.
4. Compare the two readings and repeat the test by varying the environmental conditions (1).

For the test to be successful, the difference between the two readings should not exceed 50 um. And the repeatability of the reading should be less than 50 um.

Resolution Test

To perform this test, the following should be done:

1. Vary the position slightly on the RLS referential measurement kit.
2. Determine the resolution of measurements.

For the test to be successful, the resolution of the sensor should be sensible to 50 um.

A.3.7 Force Sensor Test

This section presents the tests needed to evaluate the performance of the pressure sensor and its conditioning circuit integrated in the SIC board. Two tests are to be performed in the aim of measuring the accuracy and the resolution of the two pressure sensors in the actuator.

Accuracy Test

To perform this test, the following should be done:

1. Set direct current to the servo valve on TwinCAT, so that the cylinder moves until it hits the kit wall.

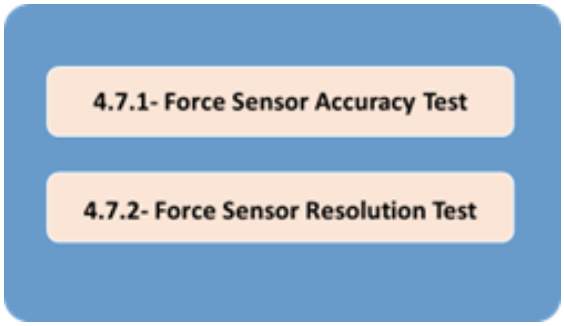

Figure A-10 Force Sensor Block Test

2. Augment the applied pressure using the relief valve, starting from 10 bar to 180 bar.
3. Measure the differential output voltage from the force sensor (Vsm) using a Tektronix volt meter.
4. Measure the differential output voltage read by the by the SIC board (Using TwinCAT).
5. Compare the two readings and repeat the test by varying the environmental conditions (1) of the card.

For the test to be successful, the difference between the readings should not exceed 0.002mV and the repeatability of the reading should not exceed 0.002mV.

Resolution Test

To perform this test, the following should be done: 1. Va0ry the force slightly on the test bench. 2. Determine the resolution of measurements. For the test to be successful, the resolution should be sensitive to 0.0020mV.

A.3.8 Firmware Test

The aim of this test is to check the ability to develop and reconfigure the firmware easily using the IDE (CubeIDE) that is already used in creating the firmware.

Configuring Additional SPI

Using CubeIDE latest version do the following:

1. Open the firmware project and build the project. Warnings Numbers: Errors Numbers:
2. Open the .ioc file in the firmware and configure the SPI port.
3. Save and generate the code.
4. Build the Modified firmware Warnings Numbers: Errors Numbers:

The test is successful if 0 errors occur

A.4 Conclusion

This test document aims to describe the test procedure for evaluating the performance of the SIC board developed to control and monitor the Servo Instrumented Cylinder. Eight tests were presented that covered the test of the board communication, the power supply circuit, the conditioning circuits of the different sensors, and the firmware of the SIC board.

Appendix B

SEHA Hardware Design

B.1 SIC Hardware

B.1.1 EtherCAT and MCU Connection Block

B.1.2 Sensor Block

B.2 SEHA Electric Motors

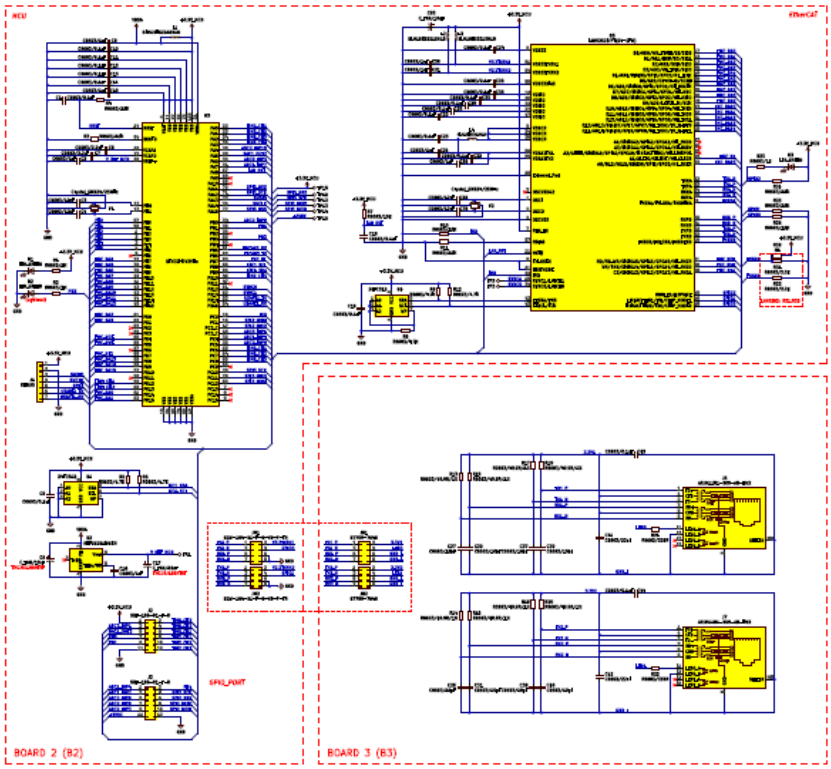

Figure A-1 Schematic of EtherCAT and MCU

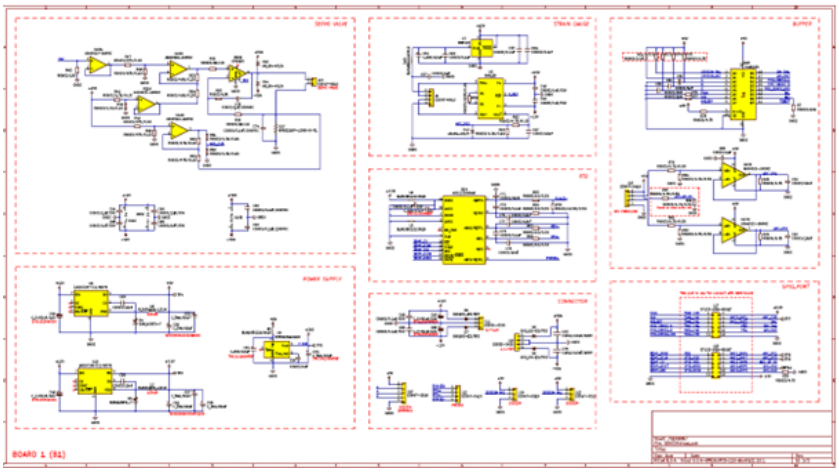

Figure A-2 Schematic of Sensors Conditioning and Servo-Valve Driver

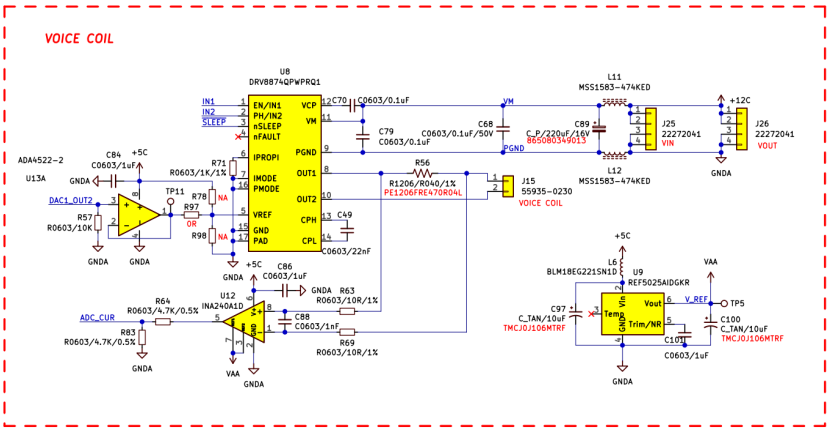

Figure A-3 Voice Coil Motor Electronic Driver

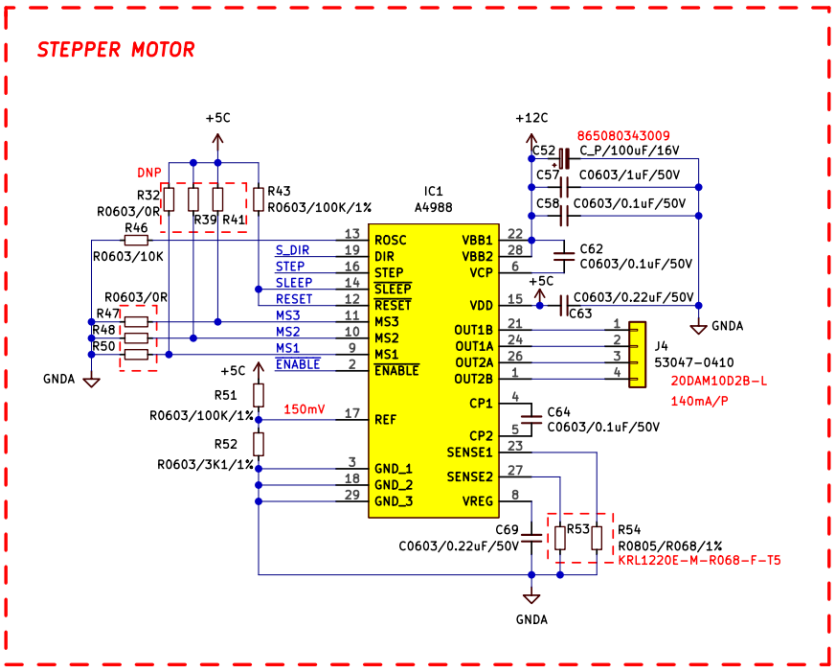

Figure A-4 Stepper Motor Electronic Driver

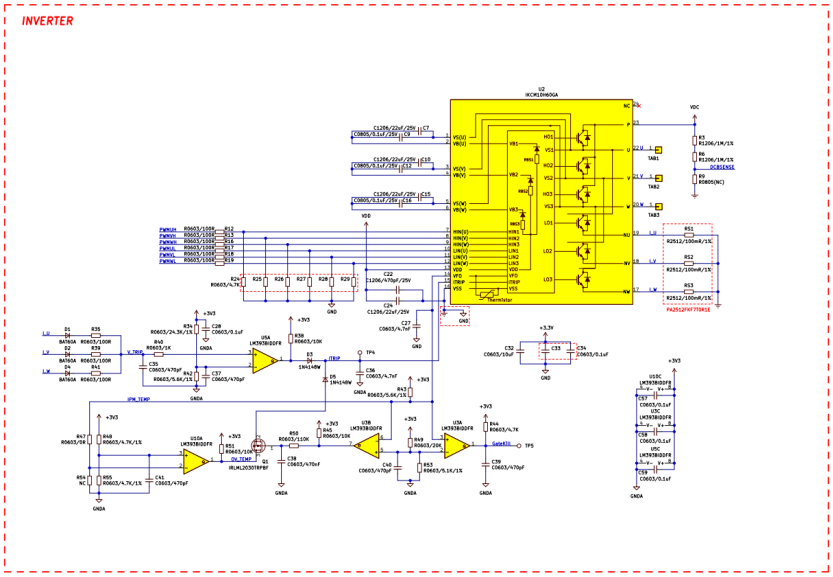

Figure A-5 BLDC Motor Driver Power Stage

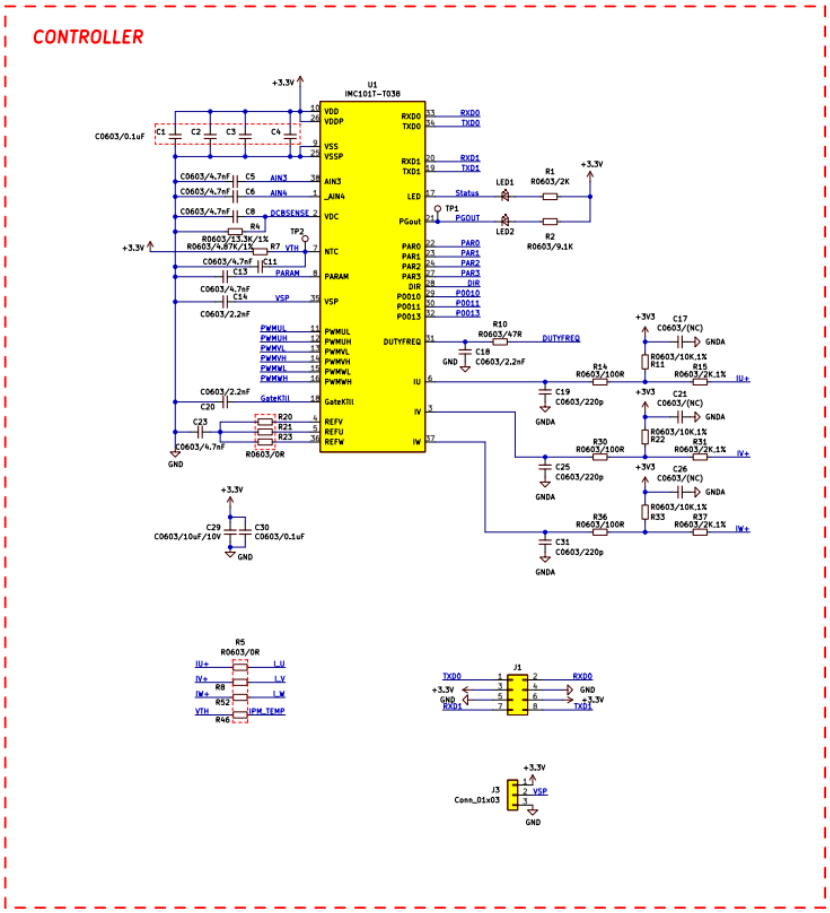

Figure A-6 BLDC Motor Driver Control Stage